University of Nevada, Reno

Blunt Force Trauma to the Ribs: Creating Predictive Models

A dissertation submitted in partial fulfillment of the requirements for the degree of Doctor of Philosophy in Anthropology

By

Cortney Nell Hulse

Kyra E. Stull/Dissertation Advisor

December, 2021

THE GRADUATE SCHOOL

We recommend that the dissertation
prepared under our supervision by

Cortney Nell Hulse

entitled

Blunt Force Trauma to the Ribs: Creating Predictive Models

be accepted in partial fulfillment of the
requirements for the degree of

Doctor of Philosophy

Kyra E. Stull, PhD
Advisor

Marin Pilloud, PhD
Committee Member

Christopher Jazwa, PhD
Committee Member

Ericka L'Abbe, PhD
Committee Member

David Raymond, PhD
Committee Member

Yurean E. Yang, PhD
Graduate School Representative

David W. Zeh, Ph.D., Dean
Graduate School

December, 2021

Abstract

Forensic anthropologists receive more requests for trauma analysis than any other aspect of the biological profile. Blunt force trauma to the ribs is some of the most common trauma recorded in a medical examiner's setting, however the structural complexity of ribs make it difficult to move beyond descriptive documentation of injuries. The purpose of this study is to identify common rib fracture patterns, influential variables, and provide probabilistic statements to guide rib fracture interpretations.

A sample of 1,415 deceased individuals with known blunt force trauma to the torso were collected from four geographically diverse medical examiner offices. Demographic data and fracture variables were recorded per individual. Frequency distributions, chi-squared tests, Kruskal-Wallis tests of independence, Dunn's tests, and multiple correspondence analysis were employed to understand variable relationships. Conditional probabilities were calculated to provide probabilistic statements. Additionally, random forest analysis was conducted to classify location and type of fracture based on covariates.

A total of 24, 853 fractures were recorded. The most common fractures were displaced and simple fractures on ribs three through seven in the anterolateral and posterolateral locations. The less common fracture patterns revealed significant relationships with demographic data and provided empirical evidence for previously untested statements. BMI had a significant relationship with location, such that fractures were more frequently recorded in lower ribs in individuals with a BMI category of obese.

Age had a significant relationship with fracture type and fracture location in all analyses; younger individuals were more likely to have incomplete fractures and incur fractures anteriorly, and older individuals were more likely to have multi-fragmentary fractures.

The current study indicates that rib fracture types and location are dependent on the demographics of the individual. Demographics, such as age and health of the individual inform the material properties and structural geometry of bone, which is how bone biomechanics are recommended to be incorporated into trauma analysis. Furthermore, the results from this research can be applied to motor vehicle safety research, experimental research avenues, and bioarcheological trauma analysis. Future rib fracture research should focus on including a more holistic view of an individual during the interpretation of fracture patterns.

Dedication

Dedicated to Richard and Kim Hulse,
and Garret Sluder. I love you.

Acknowledgements

This dissertation was only accomplished with the help and support of so many great people. First, I want to thank my advisor, Dr. Kyra Stull, for not just being my mentor but a great friend who always believed in my skills long before I did. Thank you for looking at the countless edits, the many drafts, and hundreds of R scripts I've sent you for every project I've attempted, while remaining so encouraging and enthusiastic about my work. You allowed me to experience so much and do research across the world. I will never forget all our adventures. I appreciate our years together so much, and all the wonderful people you've brought into my life. You've taught me so much. You've changed the course of my life forever, and I couldn't be more grateful. I want to thank the other members of my committee as well, for taking the time to teach me and provide such great feedback to make this project what it is. Dr. Marin Pilloud and Dr. Chris Jazwa for providing departmental support. Dr. Yurean Yang for being willing to talk statistics with me, even if it was all above my head. Dr. David Raymond for encouraging me to peruse classes and research deeper into biomechanics. A special thanks to Dr. Ericka L'Abbé, for taking me under your wing and teaching me so much about trauma and continually inspiring and encouraging me in the years I've known you.

I want to thank the staff at every location I collected data. I want to thank Dr. Knight from the WCRMEO for being so kind and encouraging of my research ideas, and always having an open desk ready for my next project. Dr. Edgar from the University of New Mexico for supporting my ideas and allowing me full access to the data I needed.

From the HCIF Dr. Wiersema, Dr. Pinto, Dr. Soto-Martinez, and Dr. Fleishman, thank you for being so kind and welcoming to me. You all took time out of your days to talk with me and teach me so much during my visit. I will always appreciate my time spent with you. I'd like to thank Dr. Adams, and the staff at NY OCME for your continued interest in my work over the years and letting me continue research with you for so long. Particularly, Chris Rainwater, your support, troubleshooting, and guidance during my time there and ever since has meant so much. I can't thank you enough.

Financial support was provided for this research by the National Institute of Justice, Graduate Research Fellowship in Science, Technology, Engineering, and Mathematics. This funding has provided all the travel, technology, and man hours needed to accomplish this work. I am so humbled and grateful for this opportunity.

I am so unbelievably grateful for the huge amount of moral support and friendship I received from my UNR cohort. Elaine Chu, thank you so much for all the hours of hard work you put in to making my GUI dreams a reality. And your delicious baked treats. You're such a sweet presence in my life. Chris Wolfe (and Rachel) thank you for always offering a smile, a great beer, and wonderful homemade biscotti. Stephanie Cole, I appreciate your support and kind words through our time working together so much. Louise Corron you have become such a dear friend and I appreciate your sense of humor, your straight talk, and constant support. I love every minute of our adventures together. And Laura Cirillo, we've definitely had some crazy times through the years, but under it all you were such a great support for me. Thank you for always providing the best Korean skin care, video game nights, and baked goods to cope with the stress of it all.

Thank you for always letting me into your home and being the listening ear when I needed it most. Most of all, thank you for being my friend.

To all my friends who listened to me complain and struggle, and always were there to make me laugh and remind me to see the light, thank you. To Emily Moes and Michael Chapman, thank you for always being so interested in my life and my work. Our monthly meet ups make me so happy. I can feel you cheering for me every day. Emily, thank you for all those writing days and reminding me to be a positive influence in our world. To Kota Terrace and Steven Conway, thank you for being my breath of fresh air, reminding me of my passions, and keeping my spirit alive. Emily Taft, it doesn't matter how much time has passed you are still one of the people who knows me best and still loves me for it. I cannot thank you enough. To Carina Muir, who often times served as the only anchor to my sanity, thank you for always being willing to go to bat for me, to call it how it is, and to make me laugh until I cry. You are my confidant, my lifeline, my best friend. I can't wait until we live next door to one another and get to grow into grumpy old ladies on our rockers like we've always planned.

To my mommy and daddy, the biggest thanks of all. I could not be more grateful to be your daughter, or to have your continued unconditional love and support. You are truly the most incredible examples of love and strength; I hope to one day have a fraction of your temperance. You have been my steadfast rocks through my whole life, and without the amazing family you created I know I would be lost at sea. Thank you for always being interested in my work, and open for tearful video chats whenever I faltered. You are both so brave and smart, I admire you so much. I truly love you so much. To my

wonderful siblings and sibling-in-laws, thank you for being there for big hugs, late night chats at Bear Lake, and with all the love I could ever ask for. And to my nieces and nephews who drew me so many pictures and wrote me so many notes to remind me how loved I am, and to always make me feel like the cool aunt, thank you so much. I love you so much.

To my sweet husband, the man who kept me together every time I was so close to shattering, I cannot thank you enough. You have worked so hard to learn how to take care of everything so I could bury myself in work, day after day. I wouldn't have made it without you. You have the sweetest heart, and every day I am grateful you decided to give it to me. Thank you for taking such good care of our little family and providing more support and kindness during all my days of weakness than I ever knew was possible.

Table of Contents

List of Tables

List of Figures

Chapter 1. Introduction

Forensic anthropologists regularly perform trauma analysis in conjunction with the biological profile when analyzing human remains. Notably, when a forensic anthropologist is requested to provide expert witness testimony, they are asked to testify on trauma analysis more often than any component of the biological profile (Galloway, Wedel, and Zephro 2013). Not only is expert testimony most often requested for trauma analysis, but there is an increasing trend in the number of requests for expert witness testimonies on skeletal trauma and a decreasing trend in the requests for testimonies on the biological profile (Crowder et al. 2016). Lesciotto (2015) specifically states the proportion of requests relating to trauma increased from 24% to 53% from 1980 to 2013 whereas the proportion of requests relating to the biological profile decreased from 25% to 11% from 1990 to 2013. Trauma analysis can aid pathologists in their determination of manner and cause of death and therefore plays a large role in the multidisciplinary death investigation process. Furthermore, the increasing presence of forensic anthropologists working in medical examiner's offices has likely contributed to the increase in requests for expert witness testimonies involving trauma analysis (Harden, Kang, and Agnew 2019; Crowder et al. 2016).

While it is essential for a practicing forensic anthropologist to be competent in trauma interpretation, advanced methods in trauma analysis are not often taught in graduate coursework, and acquiring this skillset often requires further training through

internships, short courses, and/or hands-on experience. Ultimately, this leads to practitioners with varying skillsets. Many practitioners have limited experience evaluating trauma, which could hinder their ability to perform a proper trauma interpretation or be called upon as an expert witness. Consequently, trauma interpretations in forensic anthropological casework usually consist of broad categorizations into blunt, ballistic, or sharp trauma and generalized fracture descriptions. Ultimately, this all contributes to a subjective analysis and one that may not be much use in a death investigation (Symes et al. 2012; Harden, Kang, and Agnew 2019; Marinho and Cardoso 2016).

While the literature on fracture characteristics and identifying trauma types exists (*e.g.*, Wedel 2013; Passalacqua and Rainwater 2015; Love and Wiersema 2016; Smith and Symes 2003), more detailed methodologies with statistical substantiation is required to meet best practices outlined by the Scientific Working Group for Forensic Anthropology (SWGANTH). SWGANTH states that all trauma interpretations should be "based on scientifically valid methods and principles, beyond observation and documentation" (SWGANTH Trauma 2011). Specifically, the *Daubert* criteria requires a known error rate for a scientific or technical expert testimony to be admissible in federal cases (Christensen et al. 2014). While identifying presence of perimortem trauma is common practice, there is little guidance in the literature for what 'beyond observation' means and in general how to *interpret* fractures. The lack of guidance on interpretation is likely linked to the variability of fracture patterns and wide range of intrinsic and

extrinsic variables that one needs to account for in skeletal trauma analyses. Unfortunately, it is difficult to create scientifically valid methods for trauma analysis when acquiring sufficient data requires either a sample with documented trauma, incident information, and known demographic and health variables or, if conducting experimental trauma, expensive equipment and likely a multidisciplinary team. No matter the research situation, trauma research requires knowledge of biomechanics, material engineering, taphonomy, anatomy, osteology, and a grasp of intrinsic and extrinsic variables that may influence fracture (SWGANTH Trauma 2011; Daegling et al. 2008; Crowder and Rosella 2007; L'Abbé et al. 2019).

When considering the major classifications of trauma (*e.g.*, sharp, gunshot, *etc.*), blunt force trauma is the most observed type of trauma in a medical examiner's setting (Prahlow and Byard 2012) and it is common in all manners of death (homicide, suicide, and accidental) (Hulse et al. 2018). In forensic anthropology, blunt force trauma literature focuses on bone's reaction to the relatively slow load of force and the identifiable characteristics associated with blunt trauma (*i.e.*, plastic deformation) (SWGANTH Trauma 2011; Symes et al. 2012; Love and Wiersema 2016). However, these characteristics are normally described on features of the cranium and/or long bones, and relatively little attention is given to the thorax. In most literature, rib fractures are not thoroughly addressed, even when discussing trauma to the axial skeleton (Loe 2016). In *Broken Bones,* Wedel and Galloway discuss common fracture locations, and they advise readers that the rib cage is an important area to pay attention to, even emphasizing the

torso be carefully cleaned to observe the ribs closely (Galloway, Wedel, and Zephro 2013). Beyond this advice, they offer no guidance for determining trauma type, recording fracture type, or fracture location. When addressing other skeletal elements, such as long bones, the authors provide detailed information regarding fracture types, common injury locations, and possible interpretations using concepts, such as tension and compression to interpret direction of impact (Galloway and Wedel 2013). This is reflective of the way most practitioners deal with rib fractures: the presence or absence of rib fractures is recorded, but with no further detail on location, severity, or possible interpretation (Love et al. 2013).

Rib trauma is difficult to analyze for several reasons; some of which include: the ability to study the rib cage as a unit in forensic anthropological contexts. Therefore conceptualizing the rib cage as an enclosed unit with a single response to applied forces is difficult (Galloway and Wedel 2013; Love and Symes 2004). For this reason, among others, rib fractures are difficult to assess, record and describe in an anthropological report. Yet research suggests that ribs are one of the most fractured elements in blunt force trauma scenarios in both clinical and medicolegal contexts (Hulse et al. 2018; Prahlow and Byard 2012).

While trauma research is difficult because of the necessary research design components, and rib trauma is especially difficult for the reasons mentioned above, there are also some notable advancements in rib trauma research. Rib trauma is most well known as an indicator of systemic child abuse (Kleinman and Schlesinger 1997;

Leventhal 1993). Researchers have standardized documentation of fracture type and location, and developed scientifically sound methods which have led to the ability to identify fracture patterns that distinguish between accidental injuries from instances of child abuse (Kriss et al. 2020; Leventhal 1993; Ross and Juarez 2014). Love et al (2014) created a classification system to document the location and type of rib fracture to identify abuse-related patterns. Since then, many studies have substantiated these relationships and continue this type of casework-driven research (Ross and Juarez 2014; Soto Martinez et al. 2019; Kriss et al. 2020). The research design and conceptualizations implemented to initiate the advancements of rib trauma interpretations in relation to child abuse cases should be used as a guide for other components of trauma research.

Using experimental research, Harden et al. (2019) have taken steps to create a hierarchical classification system for rib fractures on mature bone that can be used across multiple disciplines. Common rib fracture morphologies observed in clinical literature (*e.g.*, Meinberg et al. 2018) were used to record and validate experimental trauma impactions. This research was undertaken to create a standardized way to record rib fractures, which will provide guidelines for practitioners and researchers in the future, and ultimately improve understanding of rib fractures and facilitate comparisons across projects and case studies.

Experimental research is aimed at understanding the biomechanics of rib fracture in a controlled environment. Individual bones, cadavers, or animal proxies are placed into a controlled impact scenario with sensors attached to the bones to directly measure the

stress and strain experienced by the bone and more broadly to observe its response to the applied force. Such studies have made headway in understanding the structural and material properties that ribs possess that cause them to react differently to loading than long bones (Schafman et al. 2016; Kang et al. 2021; Kemper et al. 2007; Kemper et al. 2005). The parameters and extrinsic variables are usually kept constant and multiple ribs, or individuals, are impacted to observe the consistency or variation in fracture location and type (Daegling et al. 2008). Multiple impact studies on ribs have shown that the location of fracture is usually consistent, which is thought to be directly related to the structural and geometric properties of bone (Daegling et al. 2008; Agnew 2015; Schafman et al. 2016).

An extension of experimental research but outside of biological and forensic anthropology is the technological approach in traffic safety research. Rib fractures have been extensively studied in the vehicle safety industry because of their high prevalence in motor vehicle accidents (MVAs), and the strong relationship between morbidity and mortality rates associated with chest wall fractures (Poole and Myers 1981; Jentzsch et al. 2020; Sharma et al. 2008). Much of the vehicle safety research focuses on creating computer generated models that simulate bone fractures to understand fundamental failure mechanics and fracture tolerance and identify location and severity of predicted fractures. These predictions are then validated through experimental testing (either full torso sled impacts, or single rib experimental impact testing, like those in forensic anthropology) (Shi et al. 2014; Kang et al. 2021; Vavalle et al. 2015). However, the

samples for these experiments frequently lack diversity (Kang et al. 2021). For example, impacted ribs will originate from a single individual, or the few cadavers used in full torso impact tests are not diverse in age, sex, or population (*i.e.*, two to three white males around the same age) (Jingwen, Rupp, and Reed, 2012) and therefore these experiments cannot identify different patterns or trends related to age, sex, or other demographic variables. As such, the computer models and the validation tests are difficult to apply to real world scenarios as they do not reflect a realistic population in their sample.

While there is current progress in rib trauma research, there are residual gaps in our knowledge that are fundamentally problematic. Rib trauma analysis in forensic anthropology requires further standardization of documentation of injuries, elucidation of injury patterns and/or trends, statistically substantiated patterns, and probabilistic statements, as well as guidelines and directions for future research. The current study proposes a retrospective design that includes a large, diverse sample of individuals from medical examiner's offices that have all incurred rib trauma (n = 1415). This type of sample allows for broad patterns to be revealed and conclusions to be drawn about the normal and abnormal behavior of rib fractures in real world scenarios. The objective of this research is to identify injury patterns in the ribs, identify influential variables in the prediction of rib failure, and develop predictive insight into rib failure characteristics. Ultimately, this approach provides foundational knowledge and substantiation of injury patterns that will fundamentally impact practitioners and inform researchers.

Chapter 2. Literature Review

Mechanics of Materials/Basic Biomechanics

To understand the mechanisms of fracture, a basic understanding of biomechanics is required. Biomechanics is the quantification of forces applied to a body, the forces developed in a body, and the resulting movement or failure of the structures. The term "body" in this section is not meant to depict the entire human body, but rather an arbitrary object being observed. When a force is applied to a body (*i.e.*, a beam, a rod, or a bone) it will have a specific response dictated by its internal structure, structural geometry, and material properties, which when understood could aid in understanding the circumstance(s) of fracture.

A force is defined as a push or pull on a body. Force is a vector quantity, which means is has both magnitude and direction. Magnitude is how large or small the force is and direction is the way the push or pull is going. A Mathematically, force is always denoted with a known magnitude, and often direction is expressed through a free-body diagram when analyzing the effect of forces on bodies (Gere and Goodno 2013). The free-body diagram is a simplified sketch used in mechanics to represent a body and its applied forces acting on, and within, the body (Figure 2.1). Diagrammatically, the magnitude of a force is indicated by the length of the force vector and the direction of a force is indicated by the angle it makes relative to a given coordinate axis, along with the sense (arrowhead). There are two types of forces to be aware of: internal forces and

external forces. Internal forces develop within a body in response to external loading and act to keep the object together. Importantly, internal forces will not cause a change in motion. External forces are applied to a body by external contacting objects and/or connections to adjacent objects and can result in a change of motion of the body, depending on the magnitude and direction of applied forces. External forces can be further divided into two types: applied and reaction forces. Applied forces develop on the body because of direct contact from an external object. Reaction forces develop at points of constraint on the body when an external or body force/weight is applied. For example, reactionary forces develop in joints. Applied external forces are transmitted from one bone to another through joints. The transmitted forces are dictated by the constraint provided by particular joint types and develop in response to Newton's third law.

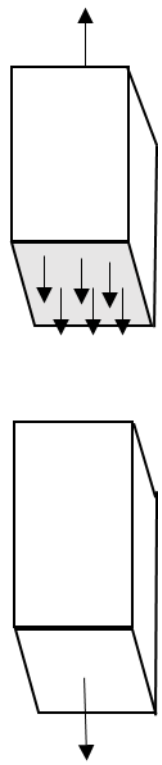

Figure 2.1. Example of a free body diagram. Body is under normal tensile loading (i.e., pulling apart along the longitudinal axis, with the stress evenly distributed through the material).

When forces are applied to a body, this is called “loading”. There are several modes of loading a body but only the two most common will be defined. Axial loading is when a force is applied along the object’s axis, typically the long axis. Transverse loading is perpendicular to axial loading. Applied loads create internal forces within the body, which in turn develops stress within the material comprising the body. The mathematical definition of stress is force divided by the cross-sectional area. Stress is directly proportional to the magnitude of the force and inversely proportional to the cross-

sectional area. If the area over which the internal force acts is small, then the resulting stress will increase. If the area is increased for same internal force then the stress is decreased (Gere and Goodno 2013).

Normal stress developed when an internal force acts perpendicular to a cross sectional area, which is denoted with a lowercase sigma (σ). Shear stress is when a force is applied parallel to the given cross-sectional surface and is denoted by a lowercase tau (τ). Shear stress occurs when loading is parallel to the cross section or perpendicular to the body and essentially works to slide two parts of the body across one another.

$$Normal\ Stress\ (\sigma) = \frac{Normal\ Force\ (F)}{Cross\ Sectional\ Area\ (A)}$$

$$Shear\ Stress\ (\tau) = \frac{Shear\ Force\ (V)}{Cross\ Sectional\ Area\ (A)}$$

There are two types of normal stress: tensile and compressive stress. Tensile stress occurs as the ends of a body are *pulled* further away from one another, and compressive stress occurs as the ends of a body are *pushed* closer together. Bending of a body result in the development of both tensile and compressive stress within the material (Gere and Goodno 2013). In the idealized free body diagram shown below, the body is exposed to a distributed load which results in bending (Figure 2.2). The side of the body closer to the applied loading experiences compressive stress, while the side of the body further away from the loading experiences tensile stress. The shape of the body will play a significant role in the stress distribution within the material (i.e., distribution of tensile

versus compressive stress). In the idealized condition below, internal stress varies linearly from the inner surface to the outer surface of the body. The neutral axis represents the axis of zero stress within the material and the point of transition between compressive and tensile stress (Figure 2.3). Assuming the body is symmetric, the neutral axis lies at the centroid where one side will be under compressive stress (negative) and the other side

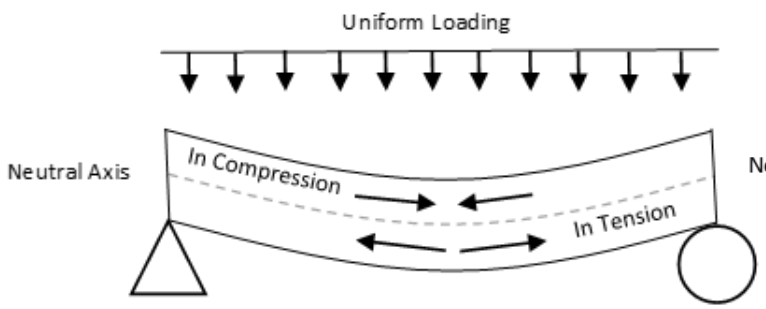

Figure 2.2. Diagram depicting a body's response under bending stress. The part of the object closer to the force is in compression, while the surface further away is in tension. The neutral axis is under no stress.

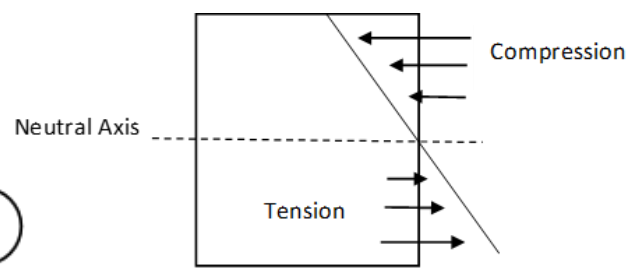

Figure 2.3. This diagram depicts the magnitude of stress of a body under bending stress. The stress is higher at the outer surfaces of the body, while at the neutral axis remains zero

will be under tensile stress (positive). The maximum expression of these stresses will be on the outer most surface of the body, and in a material that tends to fail first in tension, like cortical bone, a crack will first propagate from that point (the outer surface) (Roylance 2000).

As stress develops within a body it causes the material of that body to deform, and this deformation is called strain. The definition of strain is the relative change in shape or size of an object. Like stress, there are two types of strain, normal and shear. Normal strain causes an object to change in size/length, where shear strain causes a change in a body's shape. Normal strain results from normal tensile and compressive stresses. A body under tensile stress causes strain to make the body longer and narrower, and a body under compressive stress causes strain resulting in the body getting shorter and wider. Assuming the material is isotropic, or the material reacts uniformly regardless of direction of applied stress, and only experiencing elastic stress/strain, the ratio of

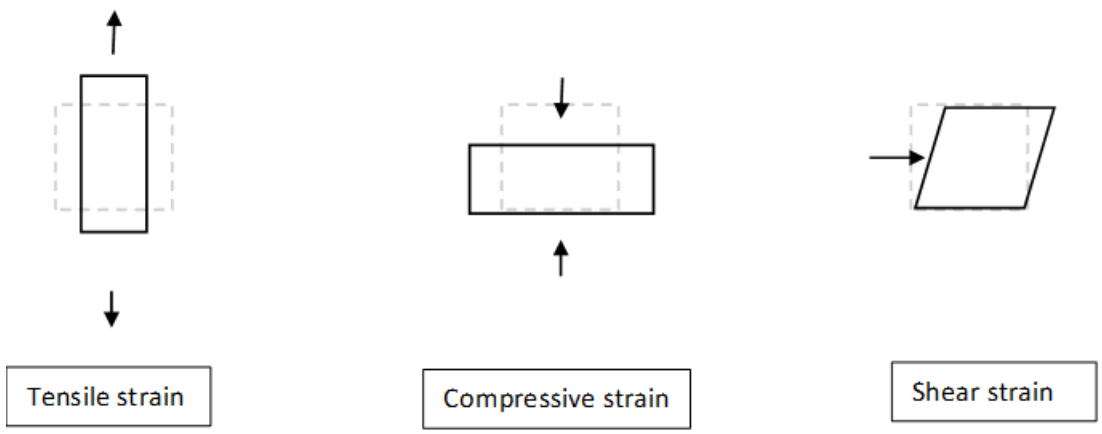

Figure 2.4. These images depict the deformation that occurs to a body under each strain type. Note that Poisson's ratio is only applicable to tensile strain and compressive strain.

longitudinal to transverse deformation a body goes through when under a force will always remain constant, which is known as Poisson's ratio (Yamada and Evans 1970). For example, a body under tensile strain will be pulled by that loading longitudinally, as that occurs it will also constrict laterally becoming thinner as well as longer. The amount

the body deforms laterally (becomes thinner) is directly proportional to how the body is being deformed longitudinally (getting longer). However, Poisson's ratio is only relevant under normal strain as the material resists losing volume, and does not work on shear strain, because shear stresses cause change in shape rather than volume.

Mathematically, normal strains (lowercase epsilon ε) are determined by observing the change in the object's length (Δl) over the original length of the object. Shear strain is always defined in terms of an angle and is denoted with the lowercase gamma symbol (γ). The mathematical formula for shear strain is τ (shear stress) divided by the modulus of rigidity of the object (G) which is the ratio of shear stress over shear strain (Gere and Goodno 2013).

$$Normal\ Strain\ (\varepsilon) = \frac{Change\ in\ Length\ (\Delta l)}{Original\ Length\ (l_o)}$$

$$Shear\ Strain\ (\gamma) = \frac{Shear\ Stress\ (\tau)}{Modulus\ of\ Rigidity\ (G)}$$

Stress and strain are mathematically related; the equations used to measure both are known as constitutive equations, which are specific to a material. This can be visualized on an engineering stress-strain curve, which depicts the relationship between the internal stress resulting from that load being applied to the body. The stress-strain plots commonly referenced in forensic anthropology texts only depict the tensile stress and strain characteristics of bone (Dirkmaat 2012).

In a stress-strain plot the y axis represents the amount of stress being developed within the object in response to the external loading. The x axis depicts the amount of strain that the object is experiencing. At coordinate position 0,0 there is no stress or strain being experienced. Young's modulus, or the modulus of elasticity (E), is the slope of the stress-strain curve within the initial linear region. The elastic modulus is measure of a material's stiffness, which is a material's ability to resist deformation under a given amount of stress. A material with a higher modulus indicates the material is stiffer, and more resistant to deformation under a given stress. The relationship between normal stress and normal strain within the elastic region is known as Hooke's law, which mathematically is defined as: a) normal stress is equal to the elastic modulus times normal strain ($\sigma = E\epsilon$), and b) sheer strain equals the modulus of rigidity times shear strain ($\tau = G\gamma$).

The prior equations apply while the body is behaving elastically and is depicted in the stress-strain curve within the linear region. If the applied force is removed from the body while loading in the elastic region of the material, the resulting unloading stress-strain curve will following the loading curve back to 0 and the body will return to its original form without any permanent deformation (i.e., purely elastic response). The elastic region of a stress-strain curve begins at the origin point (0,0) and extends until it reaches the material's elastic limit, or yield point. The elastic limit is the maximum amount of stress and strain a material can withstand before experiencing permanent

deformation. Following the yield point the material undergoes permanent deformation and the relationship between stress and strain changes.

The plastic region extends from the elastic limit to the failure point. When the elastic limit is exceeded the internal structure of the material is damaged; once the body's material has been compromised/altered, the material is incapable of returning to its original shape if the loading is removed. After this point, the modulus from the elastic region no longer applies, and the relationship between stress and strain will change based on the material and load-rate. The maximum amount of stress the body can withstand is defined as the body's ultimate strength. Once the ultimate strength is reached, strain will decrease until the body fails. The failure point of the material is when the body physically separates, or fractures.

Figure 2.5 demonstrates an example of a mild-steel stress-strain curve. It is a general representation, only depicting normal tensile stress and strain and a generalized material response. The steepness, depth, and length of the curve are determined by the properties of the body's material. For example, a body made of a brittle material will have a steeper elastic module with a shorter distance between the yield point and the elastic limit, and a ductile material will have a short rounder curve between the elastic limit and the failure point. A body made of a more pliant material will possess a curve that is shorter along the y axis and longer along the x axis as it can endure more strain before it becomes compromised and reaches its elastic limit. The stress-strain curve for every object will vary widely as the curve depends on the unique properties of that object (Gere and Goodno 2013).

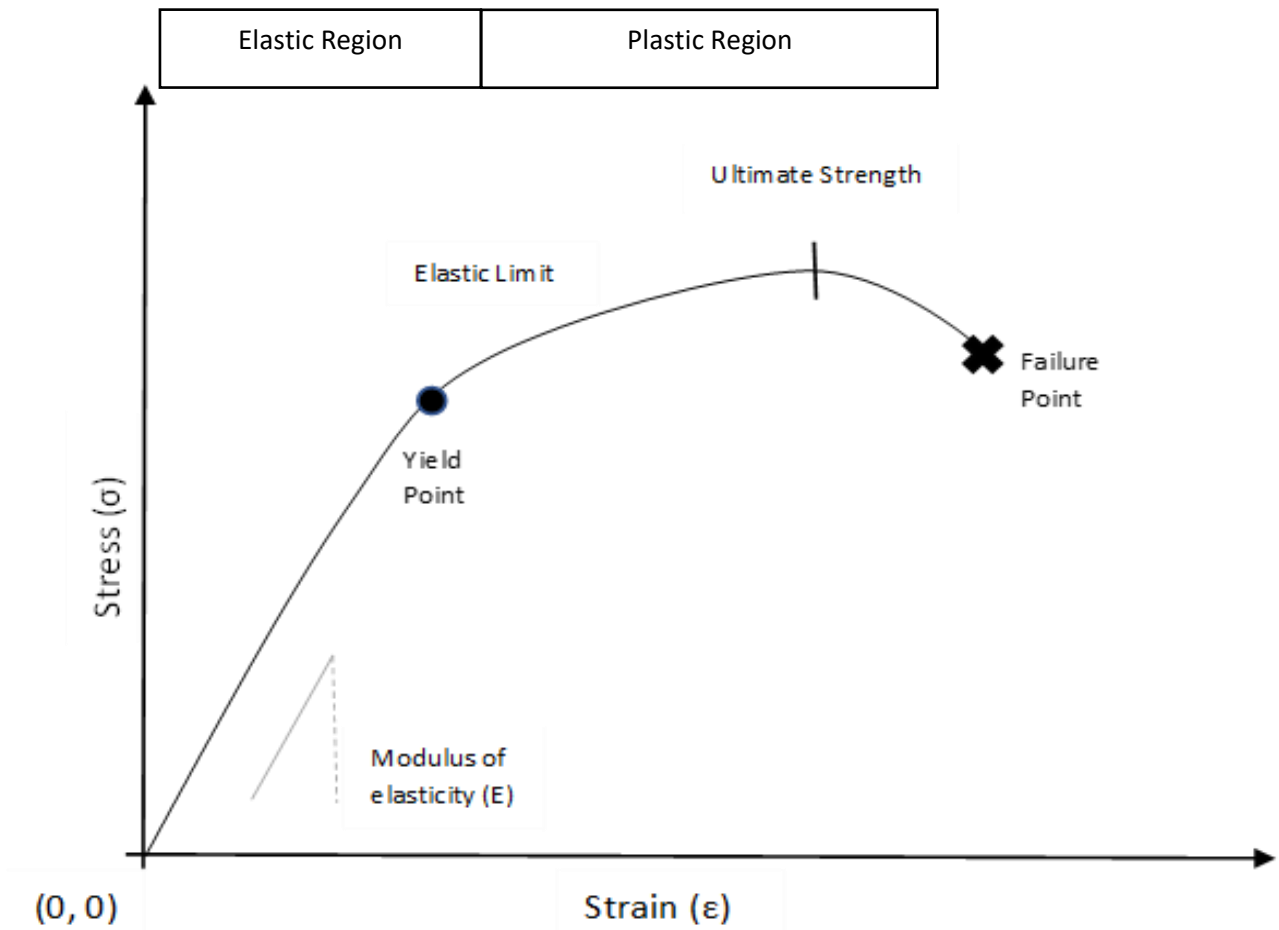

Figure 2.5. A generalized stress-strain curve depicting positive, tensile loading, on a regular material. The initial linear increase of stress/strain is the Modulus of elasticity (E) and will indicate the required stress for a given strain. The yield point indicates the point where strain begins to exceed the stress as the material begins to deform elastically, and then plastically. The Ultimate strength is the amount of stress the material can undergo, and the failure point is the separation of the material.

Material and Structural Properties of Bone

Bone is a composite material made up of calcium hydroxyapatite, collagen, water, blood vessels, and a small number of other polysaccharides and cells. Hydroxyapatite takes the form of a solid crystalline structure, which embeds itself within long fiber-like strands of elastic collagen. This combination is the basis for the basic material of bone. The rigid structure of the hydroxyapatite provides strength, as the multifaceted crystalline shape is resistant to compressive loads, which makes it a stiffer material. However, it is also brittle, and possesses little ability to deform elastically before failure. Contrary to this, the structure of collagen is pliant and has a high elastic threshold (Herman et al. 2007). The interaction of the hydroxyapatite and collagen within the material of bone provides resistance to both regular tensile and compressive stresses. In healthy adult bone, the ratio of hydroxyapatite to collagen is skewed slightly toward hydroxyapatite, the inorganic compound (L'Abbé et al. 2019). Because of this, bone is less able to withstand tensile force and will subsequently fail quicker when under tensile stress than when under compressive stress (Yamada and Evans 1970).

The hydroxyapatite embedded collagen fibers are arranged in thin sheets of bone called lamellae that are stacked to form layers. The shape, size, and overall orientation of the lamellae layers are dependent on the type of bone. There are two major types of bone: cortical and trabecular. In cortical bone layers of lamellae are wrapped in concentric circles around a central canal, called a Haversian canal, through which nerves, veins, and arteries run. Each canal has approximately 30 rings/layers of lamellae that surround it.

The orientation of the hydroxyapatite imbedded collagen fibrils differs between lamellas as a function of external stresses on the bone. They are adapted to specific functions, which provides strength to the material properties of bone in a similar way that plywood is strong in multiple directions (Rubin and Rubin 2006).

Other structures and cells, such as osteoclasts, osteocytes, and Volkmann's canals (which connect Haversian canals), also reside in the layers of lamellae. The total of these structures constitutes an osteon, which is the most basic unit of compact bone. Within cortical bone, the overall structure of osteons constitute small cylinders that run longitudinally along the length of the bone at varying lengths from a few millimeters to 1 centimeter (Maggiano, Maggiano, and Cooper 2021). Within trabecular bone, the lamellae are arranged in plates, or rods, and do not have a central canal. These rods and plates are made of "packets" of lamellar bone and create thin struts resulting in a porous sponge-like structure (Keaveny et al. 2001).

As mentioned earlier, the stress-strain curve of the composite structure of bone is dependent on the makeup of the material (e.g., cortical versus trabecular bone). The same is true for each bone, location of impact, and the ratio of bone type in a specific location. Cortical bone is tightly packed with osteons and has little vascularity. In contrast to cortical bone, trabecular bone is highly vascularized, and its structure consists of open spaces and bony struts that allow for better absorption and distribution of applied force. Cortical and trabecular bone have different responses to applied forces. Cortical bone can withstand a high amount of stress with little strain before failure, where trabecular bone

can withstand large amounts of strain under small amounts of stress due to its apparent density (Figure 2.6) (Keaveny et al. 2001).

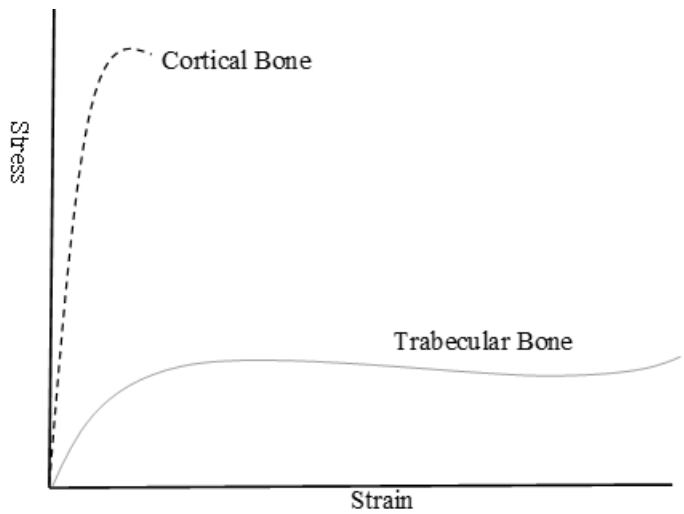

Figure 2.6. This graph indicates the differences in stress and strain between bone type. Cortical bone is much stiffer, and therefore has a much higher peak yield, and then can withstand little deformation under strain before failure. In contrast, trabecular bone yields at a low strain point but can undergo high amounts of plastic deformation before ultimate failure. Adapted from Herman, 2007, based on Frankel and Burnstein, 1970

Material Properties and Health

The material properties of an individual's bones are biologically dependent and change with age, hormone level, and health of an individual (Turner 2002). These health-related changes will influence a bone's material properties and its subsequent reaction to force. For example, as an individual ages, cortical bone becomes thinner and porosity

increases, and bony struts in trabecular bone lose connectivity. These age-related changes influence a bone's elastic properties, causing it to be less tough, which in turn causes the bone to become more brittle with age (Lynch 2015). Similarly, the amount of remodeling a rib has undergone, due to injury or age, can cause changes in yield strength (Agnew 2015; Mccreadie and Goldstein 2000). The presence of other factors, such as diseases like osteoporosis, can cause changes to composition or density of a bone that will similarly affect bone's toughness and elasticity (Osterhoff et al. 2016).

As material properties of bone are directly related to the health of that bone, it becomes imperative to understand how to determine bone health, and therefore likely material properties. Bone mineral density (BMD) is the measurement of a bone's mineral content and is often used as an indicator of bone toughness (Agnew et al. 2015). However, recent studies have shown that BMD is a good indication of health, but it is not useful in predicting fracture, particularly in the ribs (Agnew et al. 2015; Mccreadie and Goldstein 2000). The majority of BMD in an individual is genetically controlled and may help indicate if an individual is at higher risk of fracture, or likelihood of osteoporosis, but it does not provide information on fracture. Specifically, Shultz *et al.* (2017) indicated a lack of any correlation between BMD and rib fractures. As BMD is an indication of health, but not of fracture, this indicates other health related variables that cause more substantial changes to the material properties may be influencing presence of fracture.

When assessing bone health, the morphological and physiological properties of ribs should be considered. For example, differences in material properties, such as bone

weight, reduction in rib angle, and ossification, have been noted as good indicators of overall rib health and may influence fracture (Jingwen, Rupp, and Reed 2012). Therefore, the general health of the individual, such as age and weight, are directly associated with changes in the overall geometry of ribs and shape of the rib cage. Geometry and shape of bone are regarded in the literature as having an influence on presence of fracture, and therefore the health-related variables that influence these changes to the material properties should be assessed when observing rib fractures.

Structural Properties

A bone's response to loading does not solely rely on the material properties, but also on its structural properties. Material and structural properties of bone interact to dictate its behavior under applied loading. The size and cross-sectional shape of the bone will influence its response when placed under different types or directions of loading. For example, if one were to take a yard stick, orient it so it was flat, with the numbers and ticks facing upwards, and attempt to break it over their knee, the stiffness of that object and the force needed to break it would be much different than if the yardstick was turned perpendicular, so the numbers were now facing outward, rather than up. The material properties of the wood did not change, but the structural properties would differ based on the direction of applied force. Generally, thicker cross sections will have greater resilience to applied forces, and therefore, larger bones demonstrate higher resistance to force (Radasch 1999). Mechanically, objects with a cylindrical shape are best suited to resist torsional forces, and those with square shapes are best at resisting bending forces.

The geometry of bone, and specifically long bones, are generally considered to be the combination of these shapes, essentially a “rounded square”, which allows for a better resistance to torsion, and bending (Radasch 1999). Furthermore, tubular shapes, such as a long bone, rather than a solid cylinder have greater resistance to both torsional and bending loads. Mechanically, a tube has a further distance to the neutral axis, which allows for more room to incur bending or torsion forces without fracture. Therefore, the shape of long bones is well adapted to resist loading associated with everyday forces.

The material properties of bone are heterogenous, meaning the bone is comprised of multiple material structures. As such, the bone will respond differently to force depending on where the load is being applied on a bone because bone’s internal structure, or cross-sectional geometry, contributes to its ability to resist force (Galloway, Wedel, and Zephro 2013; Wescott 2013). While cortical bone constitutes the outer most layer and trabecular bone is the internal layer, the ratio of cortical to trabecular bone varies within each bone and along the length of each bone. For example, in the epiphyses of a long bone, there is a higher amount of trabecular bone than cortical bone to allow the joints an amount of “shock absorption” in axial loads. At the midway point of a diaphysis, the cross section consists of mostly cortical bone, which provides more stiffness and rigid strength. Additionally, the direction of force also determines how the bone responds. Because of its material properties, cortical bone is transversely isotropic, which means that the material will react differently when loaded axially versus transversely(Rubin and Rubin 2006). When loaded axially, the bone can resist

compressive forces because of the longitudinal structure of cortical bone. In contrast, if a bone is loaded perpendicular to the length of the bone, it is more susceptible to bending, and eventually failure. However, bone is a heterogenous material and therefore, cortical bone works in concert with trabecular bone, which is anisotropic (Figure 2.7). The collaboration between cortical and trabecular bone make the entire structure anisotropic as well, meaning the response to force is dependent on the direction of applied load (Gozna 1982).

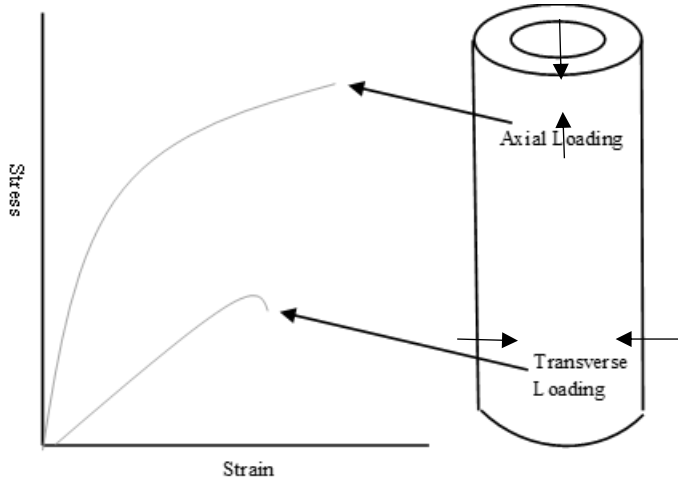

Figure 2.7. This diagram depicts the anisotropic nature of bone, and the resulting differences in stress-strain curves based on the direction of applied loads. From Hart et al. 2017, which was adapted from Keaventy et al 1993, and Nordin & Frankel 2012

Blunt Force Trauma

Skeletal trauma exists as a continuum as bone's reaction to force is constrained by its material and structural characteristics (described in previous sections), therefore

distinguishing trauma type is based off the impacting forces and not solely the characteristics of bone fracture (Kroman and Symes 2013). Blunt force trauma is defined by the general characteristics of being a slow-loaded trauma, and having an unfocused area of impact (Symes et al. 2012; Galloway, Wedel, and Zephro 2013; Berryman, Kutyla, and Russell Davis 2010). These distinctions separate it from high-velocity trauma (*i.e.*, gunshot wound), or narrowly focused sharp force trauma (*i.e.*, knife wound).

As blunt force trauma is usually characterized by slow-velocity and a wide enough area of impact that it doesn't penetrate the bone, it can be difficult to assess blunt trauma as there exist a multitude of mechanisms that may cause it, including falls from height, impacts from a blunt implement, MVAs, and many others. Furthermore, blunt force trauma can be caused by a myriad of instruments (*e.g.*, cars, the ground, other humans and their instruments). This contrasts with sharp force trauma and gunshot wounds, as these specifically result from specific mechanisms (*i.e.*, saws, knives, and guns). Finally blunt force trauma often occurs while the body is supported or interacting with another object, which can cause blunt force in multiple directions and impacts (*i.e.*, entrapment, supported by seat/constrained by belt in an MVA, multiple impacts in a pedestrian vehicle accident (PVA)) (Symes et al. 2012; Galloway and Wedel 2013). This illustrates why blunt force trauma is the most common trauma type as it is so varied, however, it makes it difficult to encapsulate blunt force trauma in a clean definition or example. Velocity, and duration of the applied forces, to the bone are important characteristics to understand when investigating blunt force trauma (Wescott 2013).

Slow-loading, or velocity, was discussed above as being a key differentiating feature to other trauma types.

The viscoelastic properties of bone interact with velocity to produce varying responses. Lower velocity is a longer duration of impact, and less viscoelastic response. Therefore, fractures will manifest relatively less quickly than those associated with high-velocity trauma, and subsequently, the response will vary (McElhaney 1966). Under a slow load, the elastic modulus for bone is more gradual, and allows for more strain, and therefore deformation as it progresses first through elastic deformation, then into plastic deformation, until it reaches ultimate failure. When undergoing plastic deformation, bone incurs micro-cracks to mitigate the stress and release kinetic energy prior to ultimate failure. These plastic deformations are the main diagnostic characteristic of blunt force trauma (Galloway, Wedel, and Zephro 2013).

Anatomy of Ribs, and the Rib Cage

Bony Structures

The rib cage is an osseocartilaginous structure that encases the thoracic viscera to provide protection and aid in visceral functions like breathing. The rib cage is composed of twelve sets of paired ribs, one on the right and left side, which articulate posteriorly to the twelve thoracic vertebrae, and anteriorly with the sternum via costal cartilage. Ribs are classified as flat bones, which unlike long bones, consist of a singular flat layer of

trabecular bone, sandwiched between two thin layers of cortical bone. Comparatively to long bones they are thin and lightweight but are highly resilient to applied forces because of their shape, cross-section, and ratio of trabecular to cortical bone.

Ribs are identified numerically from the most superior (1st rib) to the most inferior (12th rib) on their respective sides. The first seven ribs are considered "true" ribs, which indicates their anterior portions articulate directly with the sternum. The next three ribs, eight through ten, are considered "false" ribs because they articulate with costal cartilage that conjoin to form the costal arch, which then articulates with the sternum. The remaining two ribs (11 and 12) are known as "floating" ribs, as they articulate posteriorly with the thoracic vertebrae, but do not articulate anteriorly (Moore, Dalley, and Agur 2014).

General anatomy is similar throughout all the ribs aside from some size and shape differences, however several have unique characteristics. The most posterior section of the rib is the head, which is wide, wedge shaped, and composed of thicker cortical bone. Generally, the head possesses two articular facets, except for the 1st rib and ribs 10-12, which only have a singular facet. Just lateral to the head of the rib is the neck. The neck is an elongated cylindrical section of rib also composed of thicker cortical bone with no articulation points. Laterally and anteriorly, the structure of the neck increases gradually in size until it reaches the tubercle. The tubercle is a slight projection that possesses an articulation point to the transverse process of the thoracic vertebrae. Further anterior to the tubercle is the costal angle that extends down the body of the rib. The body makes up most of the rib and is characteristically long, flat, and curved. Cross-sectionally, the body

is mostly trabecular bone with a thin outer layer of cortical bone. The area of the costal angle curves anterior and laterally relatively sharply. In comparison the body of the rib gently curves along its length to angle the bone more anteriorly and inferiorly. The body makes up the majority of the rib and is largely uniform in cross section. Along the inferior internal surface of the rib is the costal groove, which serves as a protective cove for the costal nerves and vessels. The anterior articulation points on ribs are created from small divots or "cups" at the anterior end of each (articulating) rib where the costal cartilage attaches.

Several ribs are atypical and deviate from the generalized anatomical pattern. The most evident is the first rib. The first rib is shorter than the lower ribs. The cross section of the first rib is broad laterally and much shorter superiorly-inferiorly than it is wide. The first rib has only one facet, large grooves on its superior surface for major vessels, and a ridge for a muscle attachment site. The second rib is also considered an atypical rib and is also cross-sectionally wider and shorter than the mid-level ribs. However, its body possesses general rib anatomy with the exception of a large tuberosity on its body at a muscle attachment point. Ribs ten through twelve are also considered atypical. The tenth rib for the already mentioned singular facet. Ribs eleven and twelve are quite different from other ribs as they are short, possess no neck or tubercle, and end within the muscles of the posterior abdominal wall without anterior articulations.

Posteriorly, each rib articulates with corresponding thoracic vertebrae. The twelve thoracic vertebrae are regular in form but increase in size inferiorly along the spinal column. Each vertebrae possesses two major structures: a body and the vertebral arch.

The body of vertebrae is thick spongy bone with a very thin outer layer of cortical bone. They stack on one another separated by cartilaginous intervertebral disks that contain synovial fluid. At the superior and inferior anterolateral corners of the body are small demi facets, that when paired with the superior or inferior vertebrae make the costal notches where the head of the rib articulates. The arch projects posteriorly from the body of the vertebra and is composed of laminae and pedicles with seven projecting processes. The most posterior projection is the spinous process and serves as an attachment point for muscles of the back. The two most superior projections have facets that articulate with the two most inferior processes of the superior vertebrae, which creates a tight articulation. The transverse processes correspond to the articular facets on the tubercle of the rib.

Anteriorly, the ribs and costal cartilage articulate with the sternum at the costal notches. The sternum is composed of three separate parts, namely the manubrium, the sternal body, and the xiphoid process, superiorly to inferiorly. The manubrium has 7 notches, the most superior is the jugular notch flanked laterally on both sides by paired clavicular notches that articulate with the clavicles. Just inferior are the synchondroses of the first rib, which are tight articulations with the anterior end of the first rib. The manubriosternal joint of the manubrium to the sternal body meets at a slightly projecting angle, called the sternal angle. This is also the location of the articulation point with the anterior end of the second rib. The body of the sternum is longer superior-inferiorly and thinner anterior-posteriorly than the manubrium and has paired costal notches for articulations with the true ribs 2-7 laterally along its body. At the most inferior point on

the sternal body there is the xiphisternal joint with the xipoid process. The articulation point for rib 7 is shared between the end of the sternal body and the xiphoid process. The most inferior articulation is also the attachment point for the costal arch to which all the "false" ribs (8 – 10) are articulated though costal cartilage.

Joints

The joints in the rib cage are smaller and produce more restricted movements in comparison with most other joints in the body. Yet, these movements are enough to aid in respiration and provide flexibility in the thoracic region. The most posterior joint of the rib is with the vertebral bodies. The head of each rib articulates with the superior costal facet of the same numbered thoracic vertebrae, and the inferior costal facet of the thoracic vertebrae is just superior. An intra-articulate ligament of the head of the rib attaches the point between its two facets to the intervertebral disc, which creates a tight connection that separates the two-facet articulations. Over the anterior surface of the head the radiate ligament attaches the rib to the two vertebrae. These ligament attachments ensure a tight joint capsule that allows for only very slight movement between the head of the rib and the vertebral column.

The facet of the rib tubercle articulates with the transverse process of the same numbered thoracic vertebrae. The shape of this articulation varies within the rib cage. In ribs 1 – 7 the surface of the facet is curved and causes a rotational movement at the joint to rise and fall during respiration. This is often described as a "pump handle" type movement (Moore, Dalley, and Agur 2014). In ribs 8, 9, and10, the articular facet is flat,

which permits a gliding movement within the joint. This articulation allows these ribs to have movement described as similar to a bucket handle. The costotransverse ligament attaches the neck of the rib to the transverse process of the vertebrae, while the lateral costotransverse ligament attaches the tubercle of the rib to the top of the transverse process, which supports the joint anteriorly and posteriorly. The superior costotransverse ligament is a broad band with two sections that attach the entire neck of the rib to the transverse process superior to it, which further aids in strength of the joint anteriorly and posteriorly.

The sternocostal joints also vary by function and rib. The first rib has a unique articulation with the manubrium called the synchondrosis of the first rib. This is a fibrocartilaginous joint with a very tight articulation that allows for little movement. The sternocostal joints for ribs 2 – 7 are synovial joints, which allow more flexibility and movement. Over the entire sternum is a thin membranous sheet composed of multiple ligaments called the radiate sternocostal ligaments, which extend from the costal cartilages of each rib to attach to and cover the sternum. Each of these joints allow for movement within the rib cage, but also showcase the strong and stable articulations each component has with the others. These articulations give the rib cage its ability to act as a unit when force is applied(Kang et al. 2021).

Muscles

The internal, or pleural, surface of the ribs lack thick musculature to allow for space for the viscera, whereas the external surface of ribs have many origin and insertion

points for muscles of respiration, movement, and stabilization. Not only do these muscles of the thoracic wall aid in movement of the ribcage but can also serve protective functions. The muscles that are directly related to movement and protection of the rib cage are the scalene muscles, serratus posterior, intercostal muscles, levatores constarum, transversus thoracis, subcostal muscles, and the diaphragm. The scalene muscles aid in forced inhalation and attach the first and second ribs to the cervical vertebrae. The serratus posterior has two parts, the superior and inferior, where they elevate ribs 2-4 and depress ribs 8-12, respectively. The serratus posterior are thought to help in respiration and serve a protective function (Vilensky et al. 2001). Intercostal muscles attach superiorly to the inferior border of the superior rib, and inferiorly to the superior border of the inferior rib. Their major functions are to support the rib cage and contract during forced respiration. There are three types of intercostal muscles, the external which are the most superficial, oriented inferolateral from the tubercle of the rib to the costochondral junction, and are most active during inspiration, the internal intercostals which are angled inferoposteriorly from the costal angle to the sternum and are active during expiration, and the innermost intercostals which are essentially a deeper extension of the internal intercostals and are only present on the lateral-most part of intercostal spaces. The muscle fibers of the intercostals are tightly woven and oriented in different directions which effectively knits the ribs together and allows contractions of the fibers in multiple.

The levatores constarum are twelve small muscles that connect the transverse processes of thoracic vertebrae 7-11 to the inferior associated rib near the costal angle. They are thought to elevate the ribs as the body moves. Transverses thoracis attach the

inferior sternum to the costal cartilages of ribs 2 – 6 and aid in depressing ribs and protection of the area. Subcostal muscles are small muscles on the pleural surface of the posterior ribs that vary in size and shape and run in the same directions as intercostal muscles, but their function is largely unknown, other than to provide a protective function and bind the ribs together. Lastly the diaphragm, which attaches to the most inferior borders of the lower ribs may not have a direct attachment to the ribs, but the movement of this muscle is what largely causes respiration, and therefore the movement of the ribs.

There are other muscle groups that do not directly affect the movement or protection of the ribs, but instead originate on the ribs as anchors for movement or stabilization. Examples would include muscles associated with the shoulder and arm such as the pectoralis major, the pectoralis minor, and the serratus anterior. These muscles have specific attachment points on the ribs which slightly alter the rib's morphology and ratio of cortical bone to provide strength and stabilization to other areas of the body.

Movement

The major movements of the ribcage are related to respiration. As explored in the previous sections, movements of the rib cage are small in comparison to some other areas of the body, and mostly are associated with elevation and depression of the ribs. During inspiration, the intercostal muscles contract, which elevates ribs 2 – 6 due to their joint surfaces at the transverse processes. This causes an increase in size of the overall ribcage anteriorly-posteriorly. The elevation of ribs 2 – 6 and the contraction of associated muscles also causes ribs 7 – 10 to elevate. However, due to their flat joint surfaces, and

muscle attachments, these ribs expand more laterally which increases the dimension of the rib cage in all four directional planes. Unless expiration is forced, the muscles used to elevate the ribs relax, and ribs will return to their resting position. However, if exhalation is forced and muscles such as the obliques are engaged, this can cause the ribcage to compress, forcing more air from the lungs, until the muscles are relaxed.

Biomechanics of Ribs

As detailed in the previous sections, ribs have a unique geometry and cross-section. Ribs possess no open medullary cavity, and therefore are not considered a “tube” structure but instead a solid, which makes them less resilient to bending and torsional stresses. The combination of geometric features constitutes a complex “curved beam” structure, with dramatically different cross-sectional geometry along its length that leads to varying responses under applied forces. While the ribs are buttressed by articulations anteriorly and posteriorly, they still remain quite flexible and resistant to fracture (Kang et al. 2021).

The primary function of the rib cage is to protect the heart and lungs. The primary function of long bones, in comparison, is locomotion. The unique structure of cortical bone in ribs allows it to behave more elastically. In experimental bending tests, generally rib cortical bone deformed plastically for 60% of the stress-strain curve, with a higher peak strain laterally (Kemper et al. 2005; Kemper et al. 2007). The elasticity maintained in the thin cortical bone, in conjunction with the high amount of trabecular bone provides

large amounts of flexibility. Furthermore, the thin cortical bone and flexible trabecular bone allow partial fractures to occur, such as buckle and incomplete fractures, while maintaining the overall structure of the bone, and thereby rib cage, which maintains protection of the viscera after incurring damage (Leport et al. 2011). The cortical bone structure in long bones is thick and provides little flexibility to withstand the necessary stresses of movement. The differences in form follow the differences in function, and therefore their mechanical and material properties are difficult to compare.

The same assumptions used in the analyses of tension and compression in a long bone cannot be applied to a curved bone like a rib (Love and Symes 2004). Biomechanically, the analyses used to calculate the distribution of stresses when applied to a “curved beam” structure differ to those used to in the usual “beam” calculations used for long bones. Use of a normal beam implies it is prismatic, homogenous, and symmetric when undergoing pure bending, which is when a beam undergoes bending with no longitudinal loading or shear loading. In a curved beam the neutral axis does not lie at the same point as the centroid, or axis of symmetry, and “inner” and “outer” portions might not be proportional. Under pure bending a curved beam will distribute stress differently on either side of the neutral axis and the “inner” section of the material relative to the neutral axis endures more stress under the same amount of loading than the “outer” half of the material, as the geometry of the curve influences the distribution of forces (Figure 2.8). Where for a long bone under bending, the neutral axis lies at the centroid and compression and tension are linear (Figure 2.2). Therefore, the assumptions

used to interpret biomechanics of long bones in forensic anthropology do not apply to the ribs due to their structure.

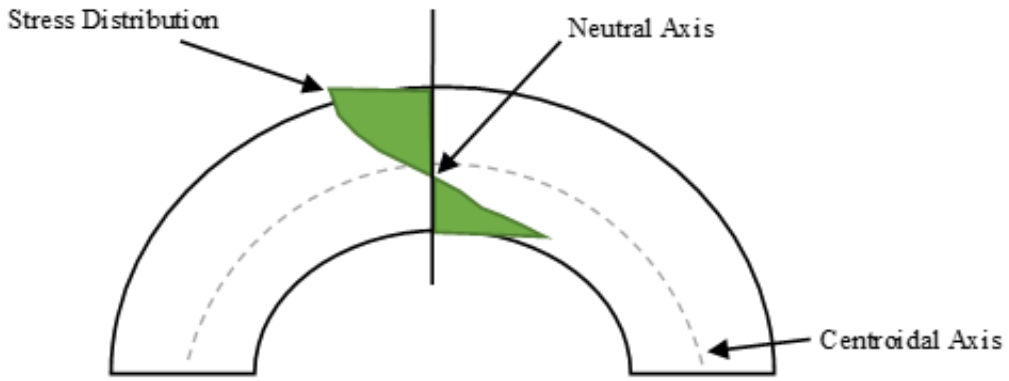

Figure 2.8. Internal normal stress in a curved beam with rectangular cross-section under pure bending. Adapted from Norton, 2010.

The material properties (*i.e.*, the small anatomical structures that constitute cortical and trabecular bone) of ribs have been found to be largely consistent along the bodies of all ribs within an individual, regardless of rib number, side, or anatomical location (anterior v. lateral v. posterior) (Kemper et al. 2007). While each rib has an individual stiffness and peak strain associated with it, which makes it difficult to draw conclusions of rib cage behavior from a single rib, general trends in behavior can be observed between similar ribs (Li et al. 2010). Experimental impact studies have demonstrated that a rib's response to applied forces varies by level (e.g. rib 4 vs rib 10)

primarily because of the geometric differences between the ribs (Kemper et al. 2007). Therefore, ribs that are closer together will have more similar geometry, and will behave/fracture similarly, whereas ribs higher or lower in the rib cage will have different geometry to one another and will behave/fracture differently.

Differences in peak strain at the individual level have been attributed to the geometry and material characteristics of ribs, which are determined by demographic variables (Shi et al. 2014; Kang et al. 2021; Schafman et al. 2016; Agnew et al. 2018). The structural differences that occur with sexual dimorphism have a significant influence on the amount of strain a rib can undergo (Schafman et al. 2016). For example, males have exhibited a higher peak strain than females (Kemper et al. 2005). Age was also seen as an influential factor in the stiffness of ribs; as age increases, so does the bone's brittleness and its ability to withstand strain lessens. Furthermore, the rib cage widens because of a reduction in the rib angle, which can increase likelihood of fracture in older individuals (Agnew et al. 2015; Shi et al. 2014). However age and sex only explains a small portion of the differences in material properties, and resulting reaction to force between individuals (Schafman et al. 2016). Size, measured either by stature or body mass index (BMI), also play a role in biomechanical response of ribs (Compston et al. 2014).

Differences in geometry of the rib are influenced by body size and will directly affect the rib's reaction to applied forces. Research suggests that ribs within those with higher BMI have overall decreased peak yield in comparison to other BMI groups

(Agnew et al. 2018). The widening of the ribcage associated with higher BMI allows less flexibility, and one study showed that younger females with higher BMI will fracture similarly to older women of normal BMI (Abdulrahman et al. 2013). Within a population of individuals, those with generally smaller rib cages and more severe rib angles were mechanically stiffer and more resistant to force, whereas rounder rib cages are more pliable in response to applied loads (Holcombe, Wang, and Grotberg 2016). The interaction of all of these variables (age, sex, and body size), will influence the cross-sectional geometry, material properties, and structural geometry of ribs, and therefore will cause variation in the rib cages reaction to applied forces (Shi et al. 2014; Agnew et al. 2015; Agnew et al. 2018; Kemper et al. 2007).

Chapter 3. Materials

To capture as much variation as possible and negate any biases that might appear in the dataset, such as population specific or location specific trauma patterns (Zabell et al. 2009), the current sample was comprised of four geographically diverse medical examiner's offices. The collaborating institutions include: the Washoe County Regional Medical Examiner's Office in Reno, Nevada (WCRMEO), the New York Office of Chief Medical Examiner in New York City, New York (NY OCME), the New Mexico Decedent Image Database (NMDID) established at the New Mexico Office of the Medical Investigator in Albuquerque, New Mexico (NM OMI), and the Harris County Institute of Forensic Sciences in Houston, Texas (HCIFS). The jurisdictions of the collaborating MEOs range from densely populated metropolitan areas to remote and rural locations with very small populations. Furthermore, the inclusion of MEOs from east coast, central, and west coast locations capture different demographics of the country (Frey 2021).

The National Center for Health Statistics (NCHS) Urban-Rural Classification Scheme is used by the CDC in health studies (Ingram and Franco 2014) to classify counties based on population density and presence of metropolitan areas. The same criteria are used to aid in the descriptions of the MEO samples. The basic NCHS classifications are separated into: 1) Large Central Metro – which contain a population of 1 million or more entirely contained in their principal city; 2) Large Fringe Metro – contain a population of 1 million or more without the population living in a single metro

area; 3) Medium Metro – Counties of populations from 250,000 to 999,999; 4) Small Metro- counties of populations less than 250,000; and 5) Nonmetropolitan, which has two subdivisions a) Micropolitan, which contains a city of 10,000 or more, and b) Noncore. It is also noted if most of the population for that county lives in or near a town/city.

Each medical examiner/institution's local databases were queried for individuals that met the parameters of the study between the years of 2015 and 2020, which were adult males and females with a blunt force related traumatic incident that resulted in death and no pathological conditions. The data collected for every decedent were age, sex, height, weight, ancestry, MOD, and COD. Other variables were collected when available; these included if CPR was performed, any associated health information (*e.g.*, chronic substance abuse, obesity, or illness), and if the individual, if in an MVA, was wearing a seat belt restraint at the time of the incident. Not all locations provided access to medical histories, unless the attending pathologist recorded it as having been a contributing factor to cause of death. In the incidences that medical history information proved important, the information was recorded. Otherwise, those variables were not collected. The number of individuals, and the sample composition in general, varied by location. The specific breakdown per each institution is detailed below.

Collaborating Institutions

Washoe County Regional Medical Examiner's Office (WCRMEO)

The WCRMEO services 14 counties in Nevada, as well as six northern California counties. Of all the counties serviced by the WCRMEO, two classify as Medium Metro, one county classifies as Small Metro, and all other counties (n=17) classify as Nonmetropolitan. Only five counties serviced by the WCRMEO were shown to house most of their populations in a city or town. The NCHS classification breakdown of the WCRMEO sample clearly demonstrates the majority of counties serviced are in rural and sparsely populated areas.

The total number of individuals in the WCRMEO sample was 267 individuals; males (n = 185) comprised a larger portion of the sample than females (n = 82) (Table 3.1). The ages ranged from 18 to 91 years of age with a median age of 52 years (Figure 3.1). The most common MOD was accidental death, which accounted for 252 individuals; there were substantially fewer individuals with a MOD of homicide (n = 7), suicide (n = 7), and undetermined (n = 1) in the sample. Demographic data for the WCRMEO sample was collected from autopsy reports, while fracture information and location were collected from available autopsy photographs and confirmed by x-ray images when available.

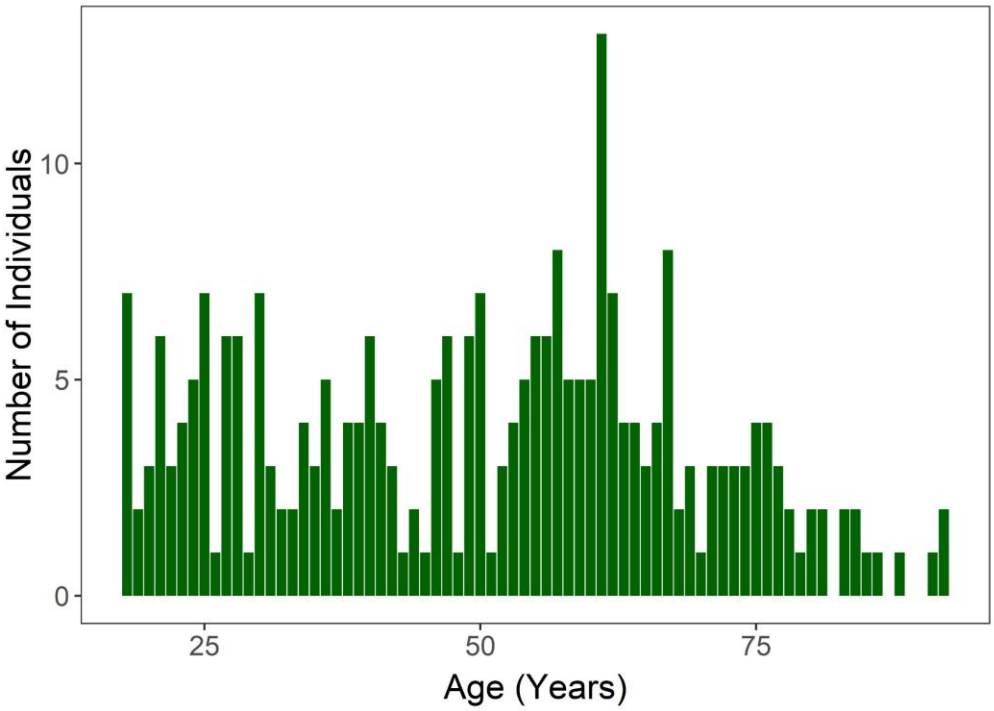

Figure 3.1. Distributions of ages represented in the WCRMEO sample.

New York Office of Chief Medical Examiner (NY OCME)

The NY OCME services five counties in the major metropolitan area of New York City. All five counties classify as Large Metro where most of the population lives in a major city. In stark contrast to the WCRMEO sample, the NY OCME sample is from a geographically small, but densely populated and diverse area.

The sample from the NY OCME included 271 individuals (males = 190, females = 78, 3 unknown) (Table 3.1). The ages ranged between 18 and 88 years of age, with a median age of 46 years (Figure 3.2). The most common MOD was accidental with 146 occurrences, closely followed by suicide with 113 occurrences. Homicides (n = 10) and undetermined (n = 2) MODs comprised a substantially smaller portion of the sample. The records available for data collection were autopsy reports and associated documentation, such as incident reports. Fracture location was documented from pathologist's notes as well as autopsy photographs.

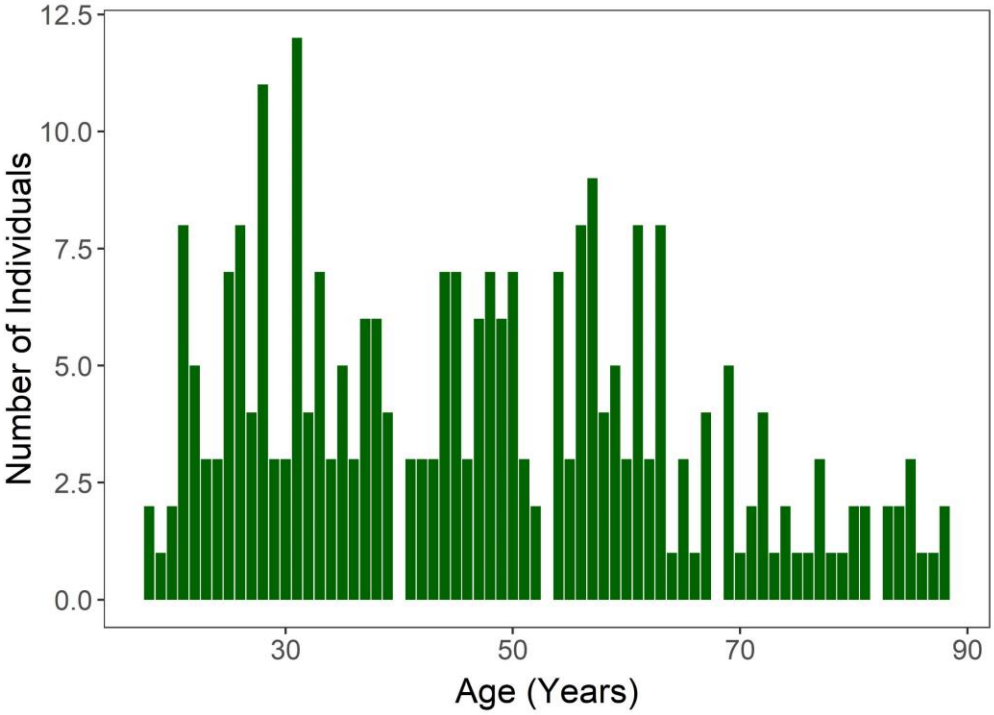

Figure 3.2. Distributions of ages represented in the NY OCME sample.

Harris County Institute of Forensics (HCIF)

The HCIF is in Houston, Texas and services a singular county, Harris County. Consultation work and transfer cases are minimal at HCIF and makes up less than 1% of their annual case load (Harris County Institute of Forensic Sciences 2019 Annual Report 2019). Harris county is classified as Large Central Metro, the most population dense classification. Like NY OCME, this sample all comes from a geographically small, but population dense location.

Data from 496 individuals were collected from the HCIF. Of this sample, 130 are females, 365 are males, and 1 is unknown. Ages range between 18 and 91 years of age, with a median age of 38 years (Figure 3.3). Most individuals had a MOD of accident (n = 462); the rest of the cases included 27 suicides and seven homicides. The records available for this data were mainly autopsy reports and autopsy images.

New Mexico Decedent Image Database (NMDID)

The NMDID is a freely accessible database of full body computed tomography (CT) scans generated at the New Mexico Office of the Medical Investigator (NM OMI). The database includes ~15,000 New Mexicans who died between 2010 and 2017. The New Mexico OMI services every county in the state (n = 33) and will sometimes accrue cases from small counties in Arizona or Texas. Similarly, to the WCRMEO, only two counties serviced by the NM OMI classify as Medium Metro areas, while three counties

are Small Metro areas, and the remaining 28 counties all classify as largely rural populations.

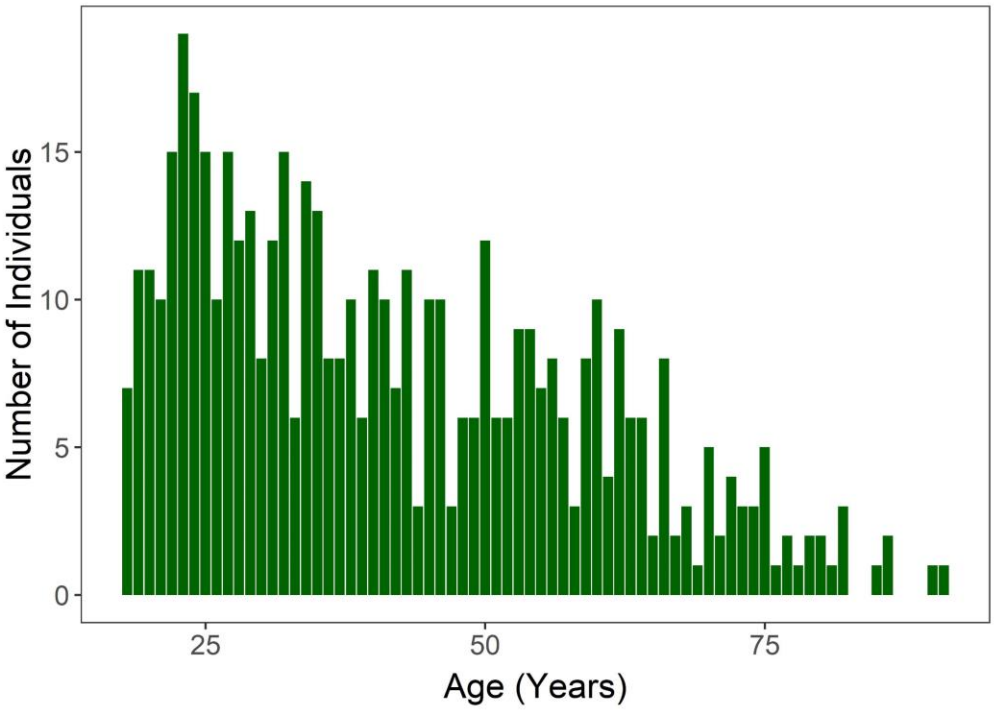

Figure 3.3. Distributions of ages represented in the HCIF sample.

The sample collected from the NMDID consisted of 381 individuals (274 males, 96 females, and 11 individuals of unknown sex). Ages ranged from 18 to 96 years old, with a median age of 45 years (Figure 3.4). The most common MOD was accident (n = 311) whereas only 12 individuals had a MOD of homicide, and 11 individuals had a MOD of suicide. There were 47 cases with a MOD of undetermined. The available metadata was dependent on its presence in the NMDID, which resulted in a greater

amount of missing data because of the stricter data collection environment. Even though it was a disadvantage to not work directly with the autopsy reports or associated documentation, the advantage of the NMDID was being able to document the fracture data from high resolution full body CT scans. The CT data was rendered using the software program Amira (Amira™, Thermo Fisher Software).

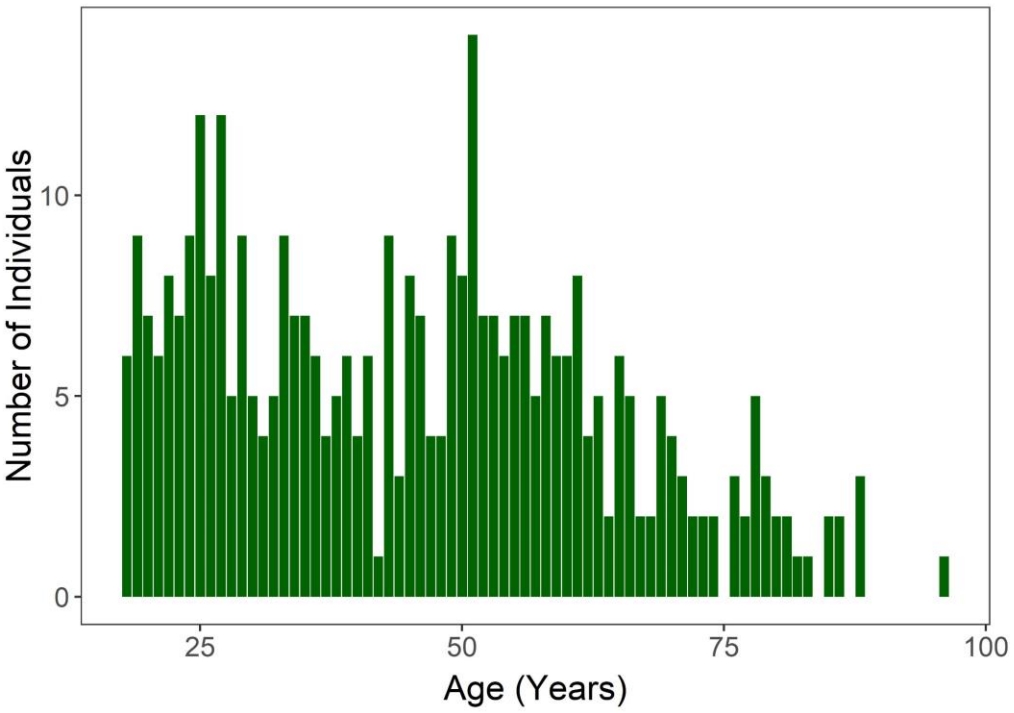

Figure 3.4. Distributions of ages represented in the NMDID sample.

Table 3.1. Number of individuals per medical examiner's office separated by known sex					
	WCRMEO	**NY OCME**	**HCIF**	**NMDID**	**Total**
Males	185	190	365	274	1014
Females	82	78	130	96	386
Unknown	0	3	1	11	15
Total	267	271	496	381	1,415

Table 3.2. Number of individuals per MEs office separated by known manner of death				
	WCRMEO	**NY OCME**	**HCIF**	**NMDID**
Homicide	7	10	7	12
Suicide	7	113	27	11
Accident	252	146	462	311

Variables Collected

Data Collection: Rib Fracture Data

If a fracture was present, then fracture variables, such as location, type, and completeness was collected per fracture. Anatomical rib location was defined based on standards for collection of rib fracture data by Love et al. (2013) and Ritchie et al. (2006). There were four discrete locations: anterior, anterolateral, posterolateral, and posterior.

The posterior region extends from the head of the rib to just lateral to the articular facet of the rib. This section is unique in its shape, size, and higher amount of cortical bone and therefore is a small, but biomechanically important. The posterolateral section begins at the lateral aspect of the articular facet to the most laterally projecting part of rib body, where the curve of the rib turns medially. The anterolateral section begins where the posterolateral section ends at the most laterally projecting point on the rib body and continues to either the anterior section of the rib or the rib end. The method used to determine the anterior portion of the rib was adapted from the Ritchie *et al.* (2006) method, in which the anterior portion is designated by observation of an imaginary line at approximately 36 degrees from the end of the posterior section through the mid-sagittal plane to intersect the anterior portion of the rib (Figure 3.5). The anterior section is defined as from the intersection of where the imaginary line crosses the rib to the midline. With this method, the size of the anterior section varies for each rib, but the designation includes structural geometry and anatomical similarity, rather than arbitrary designations. As argued by Ritchie *et al*. (2006), the anterior section of the rib varies anatomically, and as such, special ribs (one, eleven, and twelve) possess no anterior portion. In recreating this method, the practitioner should consult the original source of Ritchie *et al.* (2006) and use their best judgement to utilize this general measurement and their interaction with the bone to determine the appropriate anterior section. Rib fracture location was also mapped on a rib homunculus (Figure 3.6). The area of the rib that is fractured or compromised was indicated so that serial fractures, and injuries to the entire rib cage could be easily documented and later visualized.

Each fracture was classified as a specific fracture type. The fracture types utilized for this study were: incomplete, simple, oblique, buckle, displaced, and multi-fragmentary (Figure 3.7 – 3.12). The designations of simple, oblique, and multi-fragmentary were adapted from Harden and Agnew (2018). An incomplete fracture occurred when the fracture did not transect the entire rib and some bony tissue remained connected/uncompromised (Figure 3.7). A simple fracture was characterized as a fracture that transects the entire rib, but the two resulting segments were not displaced, and the fracture morphology was largely straight (Figure 3.8). Oblique fractures occur at an angle, and the rib is transected obliquely along the body of the rib (Figure 3.9). Buckle fractures were defined by Love and Symes (2004) and is an incomplete fracture that occurs on the pleural surface of the rib. The buckle fracture morphology consisted of any fracture that looked crushed or crumpled onto itself from the pleural surface (Love and Symes 2004) (Figure 3.10). Displaced fractures were classified as any complete fracture where the two segments of bone were separated, and the resulting segments were no longer in alignment (Figure 3.11). A multi-fragmentary fracture classification was given in one of two instances: 1) the fracture was comminuted and resulted in three or more

small bone fragments within a single anatomical segment, or 2) multiple related fractures occurred within a single anatomical rib segment (*e.g.*, butterfly fracture) (Figure 3.12).

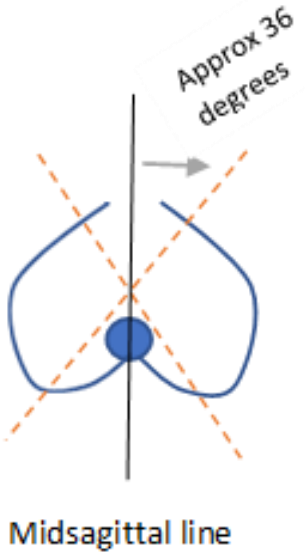

Figure 3.5. Graphic representation of the approximation of the angles used to determine anterior portion of the ribs.

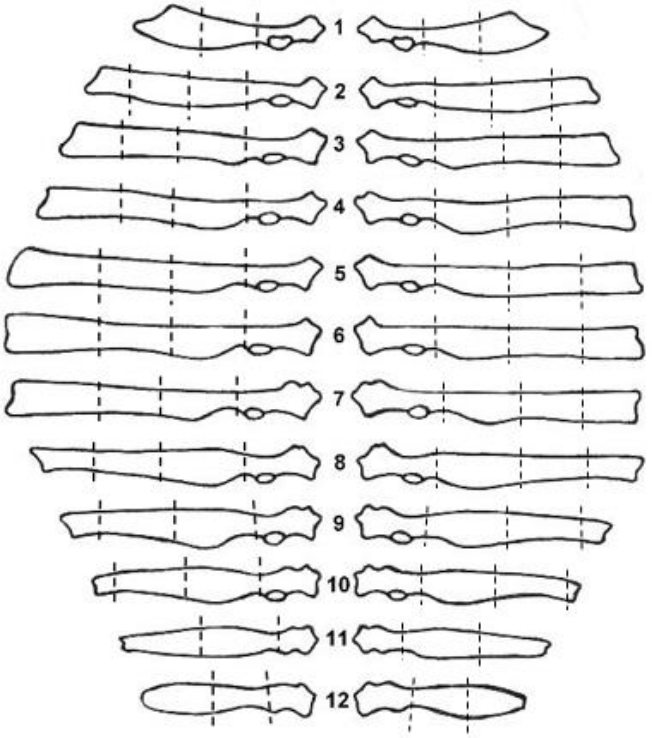

Figure 3.6. Homunculus with general anatomical location designations indicated by the dotted lines.

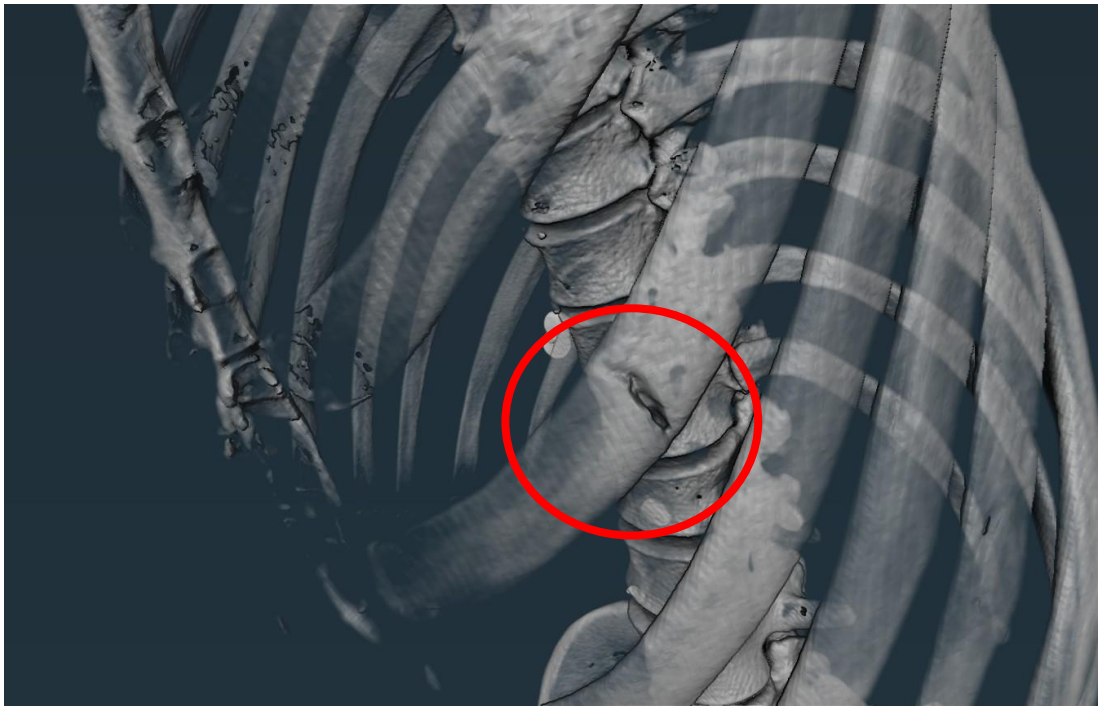

Figure 3.7. Example of an incomplete fracture (red circle) using Amira™ software. The fracture does not transect the entire rib, and there is some uncompromided bony tissue on the superior end of the fracture.

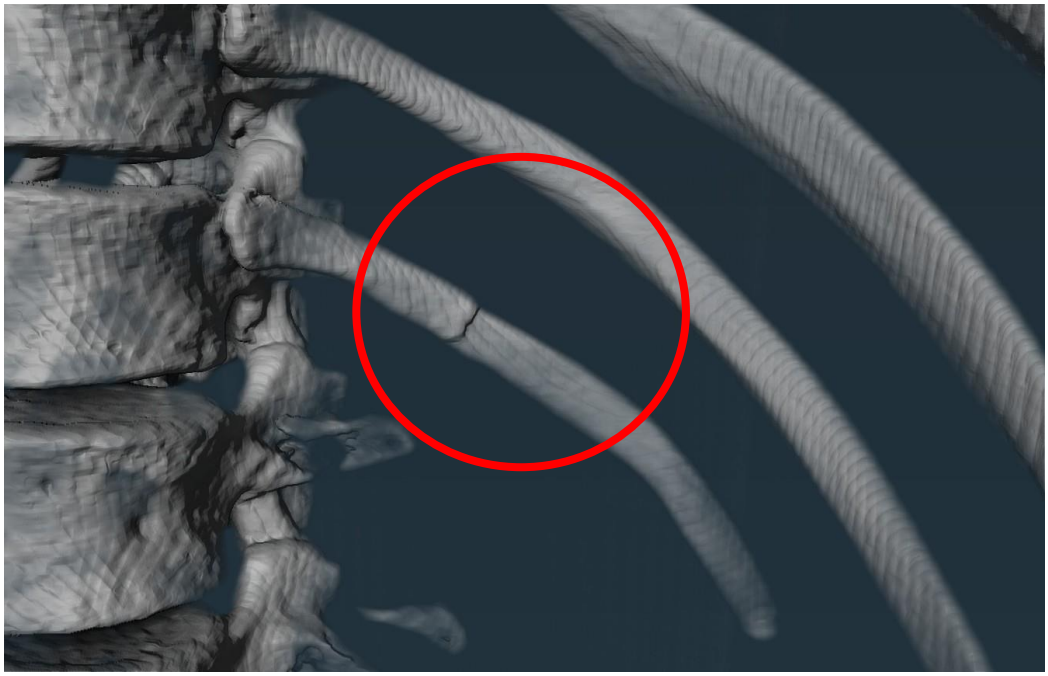

Figure 3.8. Example of a simple fracture using Amira™ software (red circle). Simple fractures are complete, but remain in alignment with the rest of the bone.

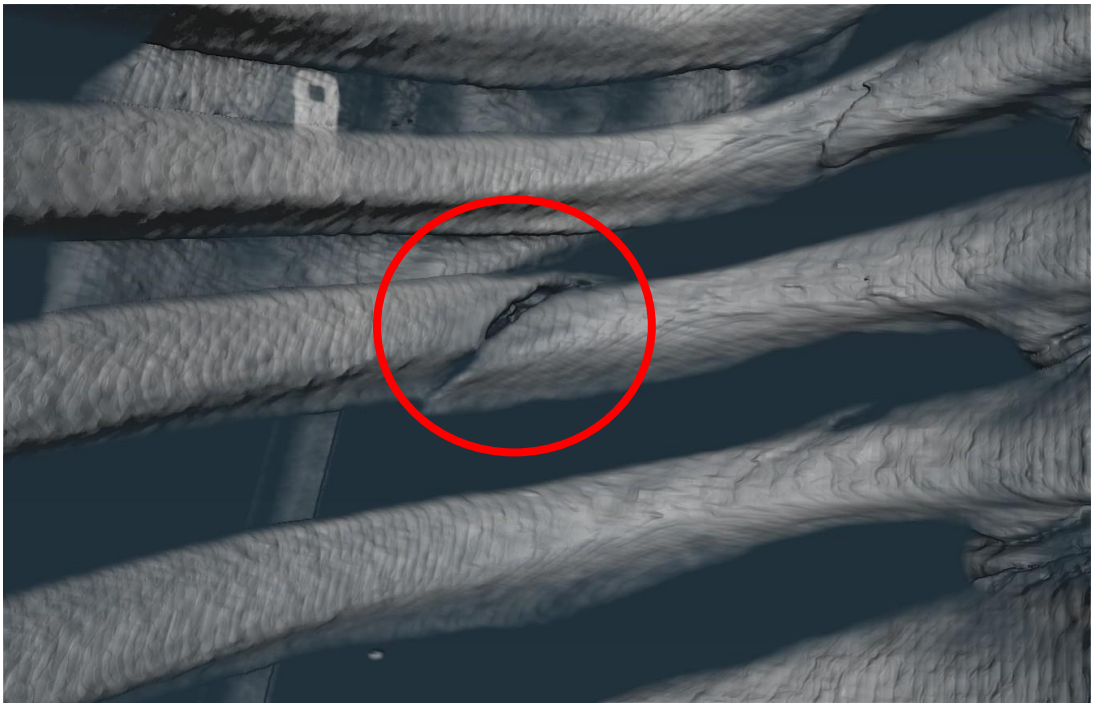

Figure 3.9. Example of an oblique fracture using Amira™ software (red circle). Oblique fractures occur at an angle from superior to inferior borders

Figure 3.10. Example of a buckle fracture using Amira™ software (red circle). As defined by Love and Symes 2004, a buckle fracture is an incomplete fracture on the pleural surface that occurs due to a failure of the cortical bone under compressional stress, and the bone has buckled in on itself.

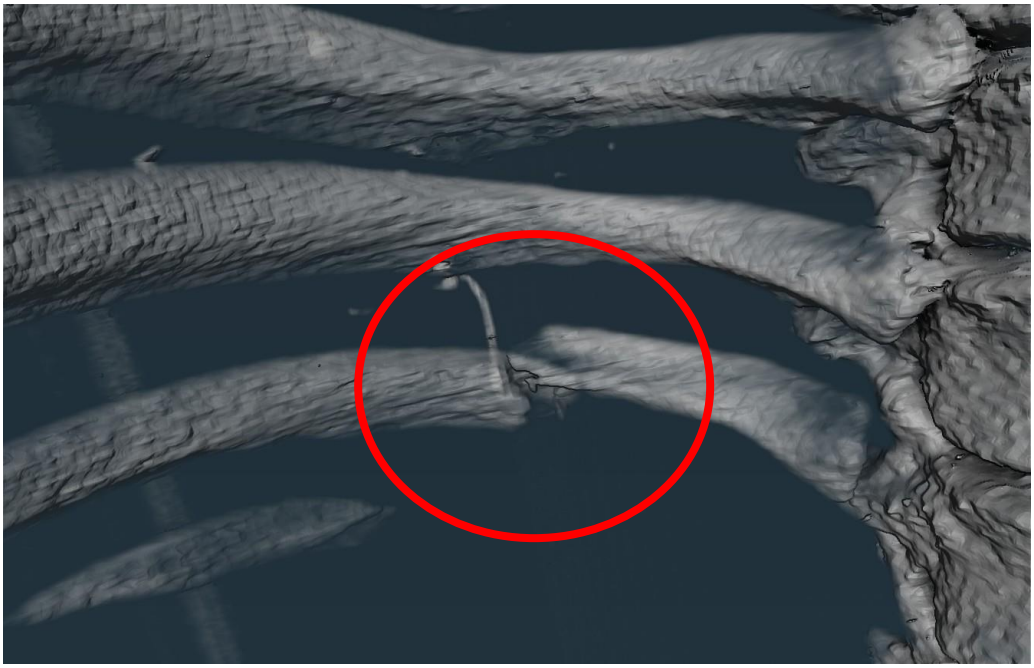

Figure 3.11. Example of a displaced fracture using Amira™ software (red circle). Displaced fractures indicate any fracture where the two resulting segments are no longer in

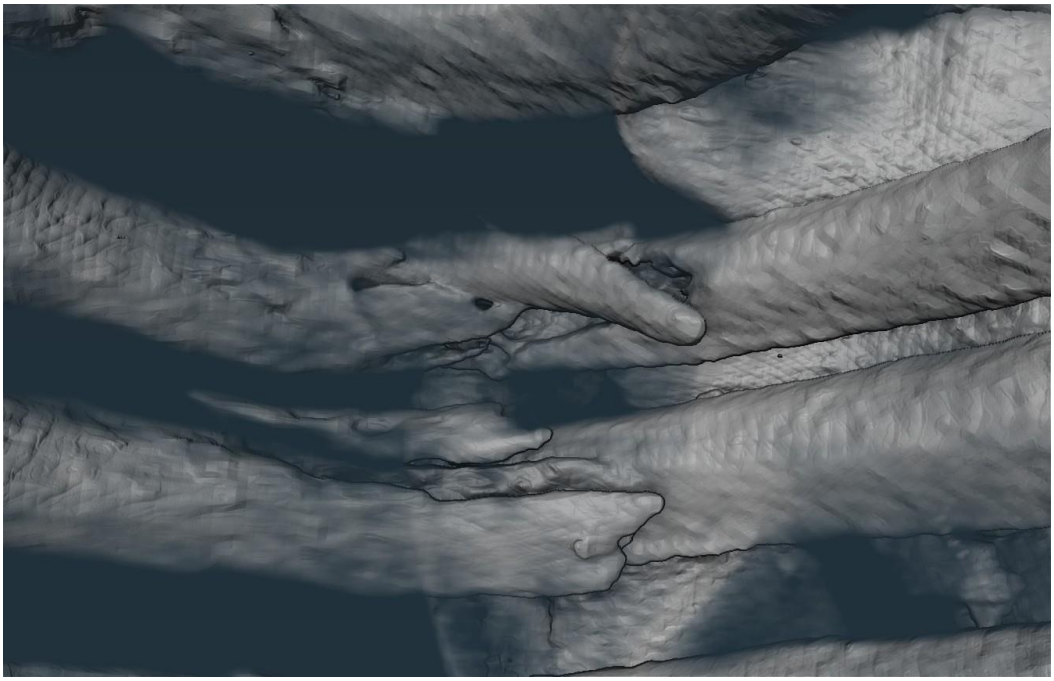

Figure 3.12. Example of multi-fragmentary fractures using Amira™ software (red circle). The ribs are comminuted and result in multiple small seperated sections of bone.

Data collection: Autopsy Report

Most data collected for this study relied heavily on autopsy reports from each location and depending on the institution, additional documentation, such as the death investigators' reports or the police reports, provided additional data. The supplemental reports generally contributed information to the death event, such as the height of the fall or if the individual was wearing a seat belt. However, there are no nationally accepted guidelines or standard operating procedures for death-scene investigation (National Medicolegal Review Panel 1999). Therefore, depending on the death event, the individual, and the operating procedures associated with each collaborating institution,

the supplemental demographic, health, and death event variables available per person widely varied. While specific details are present in all autopsy reports, the level of information regarding the sustained injuries also varied across institutions.

To retain data integrity, all language in the autopsy reports and metadata were preserved during data collection of individual-level information and demographics. For example, the institutions varied in how they recorded ancestry, or race, and the verbiage used in the autopsy reports was how it was recorded in the current research design. In contrast to the retention of individual-level variables, COD categories were created after data collection to more easily evaluate death events. Details provided for CODs were often unique to the pathologist, death investigator, or police report recordings and subsequently most individuals had a unique wording for COD details associated with the death event. The original COD terminology was retained and a new incident type variable was created to collapse related death events; the categories were “Fall”, “MVA”, “PVA”, “Train” and “Other”. The general “Other” category consisted of incidences that did not fit any definition perfectly such as hot air balloon crash, motorcycle rollover, etc. These five were specified because they presented with the highest frequency in the data. If rib fractures were documented in autopsy reports, autopsy images and x-rays were opened and examined to observe any visible fractures (see *Data Collection: Fracture Data Collection by Image Type)*. Often the pathologist would record side, location, and general information about the fractures. This information was noted and then verified with the accompanying images. Location classification differed between what the pathologists

used and the methods used for the current study, therefore fracture locations documentation relied on the images. For example, pathologists would often use designations such as, “the fourth rib is fractured at the midline of the clavicle”; in the current study, this would be classified as anterolateral. Fracture type was recorded whenever visible in the images, but on occasion when advanced imaging was not available and the fractures were not dissected out, fracture type was left blank.

One exception to the use of autopsy reports was the NMDID sample; in this case, the available metadata was what was previously chosen to be included in their database. Additionally, an autopsy report was not available from which to extract the fracture information. Therefore, CT slices were volume rendered into a three-dimensional model, which was examined for rib fractures. Once the fractures were identified, the fracture variables were recorded.

Data Collection: Fracture Data Collection by Image Type

Photographs

Photographic images were heavily relied upon to verify fracture data. Forensic photography procedures indicate that during autopsy all injuries should be thoroughly photo-documented (Marsh 2014; Connolly et al. 2016). Photos were usually taken of the external surfaces of ribs once visible during autopsy and a second set of photos were usually taken on the pleural surface of the rib cage once the thoracic cavity was cleared.

Further steps were taken in some MEOs to dissect out rib fractures, which would then provide an additional round of photo- documentation.

X-rays

Two MEOs, WCRMEO and HCIF, had radiographic images (x-rays) available for some decedents. Research has suggested rib fractures are difficult to observe in x-ray images (Crandall, Nathens, and Rivara 2004); therefore, x-rays were only used in conjunction with photographs in autopsy reports. However, x-ways provided *in situ* images of anterior and anterolateral fractures which helped to identify them prior to autopsy. In both collaborating institutions, the post-mortem x-ray images were generated prior to autopsy. As a result, the individuals were not always in proper anatomical position, and there may have been other obstructions in the visualization, such as clothing, medical devices, or debris.

CT Scans

The NMDID database was a unique data source in that the data collection was from full body CT images, rather than autopsy reports, photos, or any combination of the documentation. The scanning parameters were kVp 120, mAs 300, Scan length 600-800 mm, Scan FOV 350-699 mm, Pitch 0.817, Collimation 16 x 0.75, Rotation Time 1.0 s, Matrix 512 x 512. More information about the CT scanning process is available on the NMDID website (https://nmdid.unm.edu/). Amira™ software was used to volume render the CT images into a three-dimensional format. The threshold was set to 200 and was

modified to filter out the soft tissue to only leave the thoracic skeleton visible. These three-dimensional skeletal models were then able to be manipulated and rotated to identify any rib fractures present on an individual.

Data Collection: RibRecord Graphical User Interface

A graphical-user interface (GUI), named RibRecord, was developed by ComplexityNexus LLC for ease of secure data collection and efficiency in mapping fracture location. RibRecord consists of two windows that open simultaneously. The first window is for general data entry and the second window is a rib homunculus used to map fracture location (Figures 3.13 and 3.14). In the main data entry pane, all variables were collected through text entry, drop down menu, or radio buttons. Some variables such as “Health Notes”, “COD Details”, and “Case Notes” were free entry text boxes where useful information for each case could be recorded. The smaller text entry boxes for ID, Age, Weight, Height, COD were limited text entry that would only allow specific entries such as only letters or only numbers to prevent mistaken recordings. The drop-down options contain discrete options that were largely associated with demographic and health information. Once a record was input, a unique ID number was associated with each individual to ensure there was no identifiable information for future researchers.

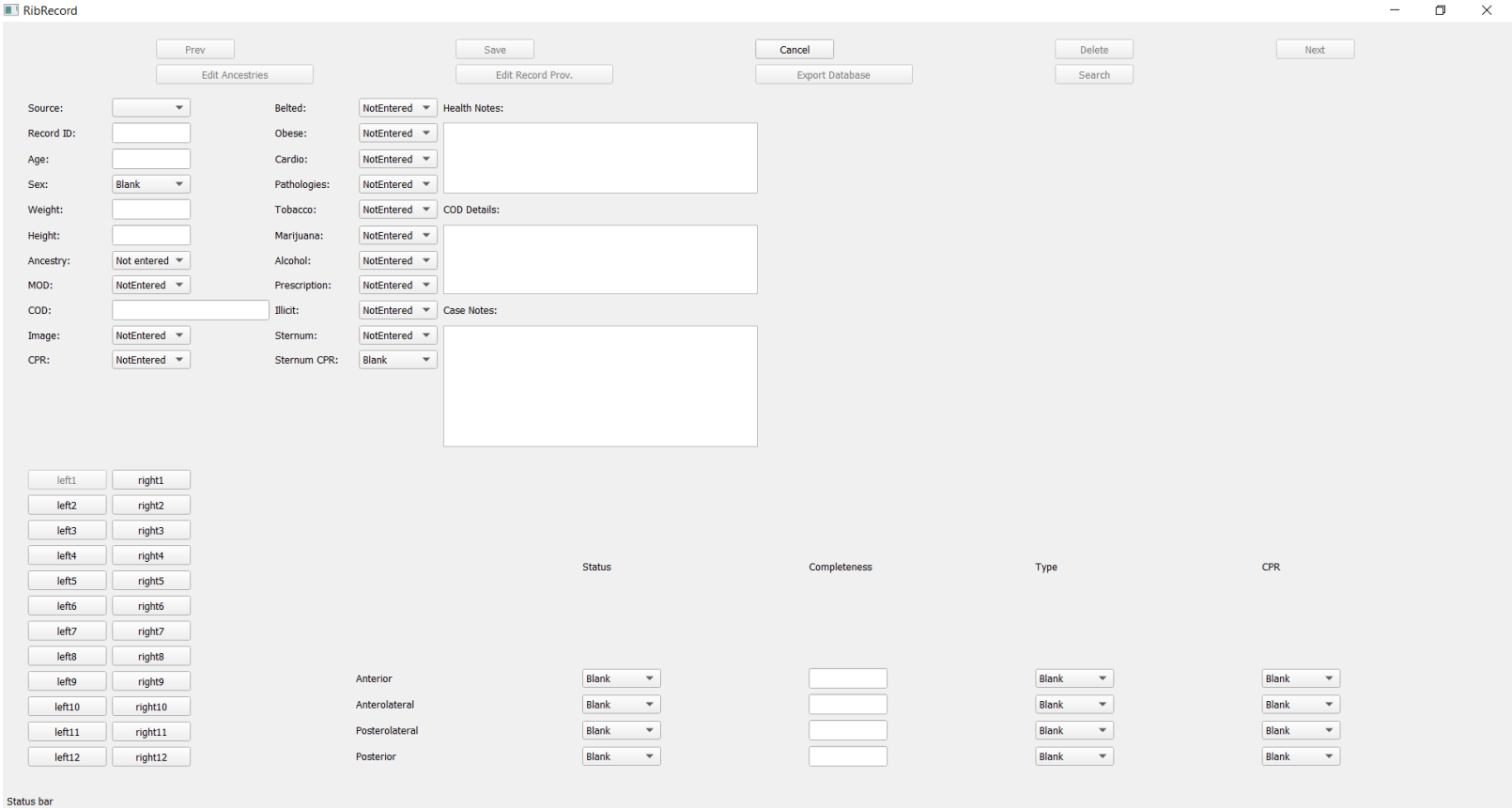

Figure 13.13. A screen capture of the RibRecord GUI. This image depicts the main page where demographic information and fracture variables were entered.

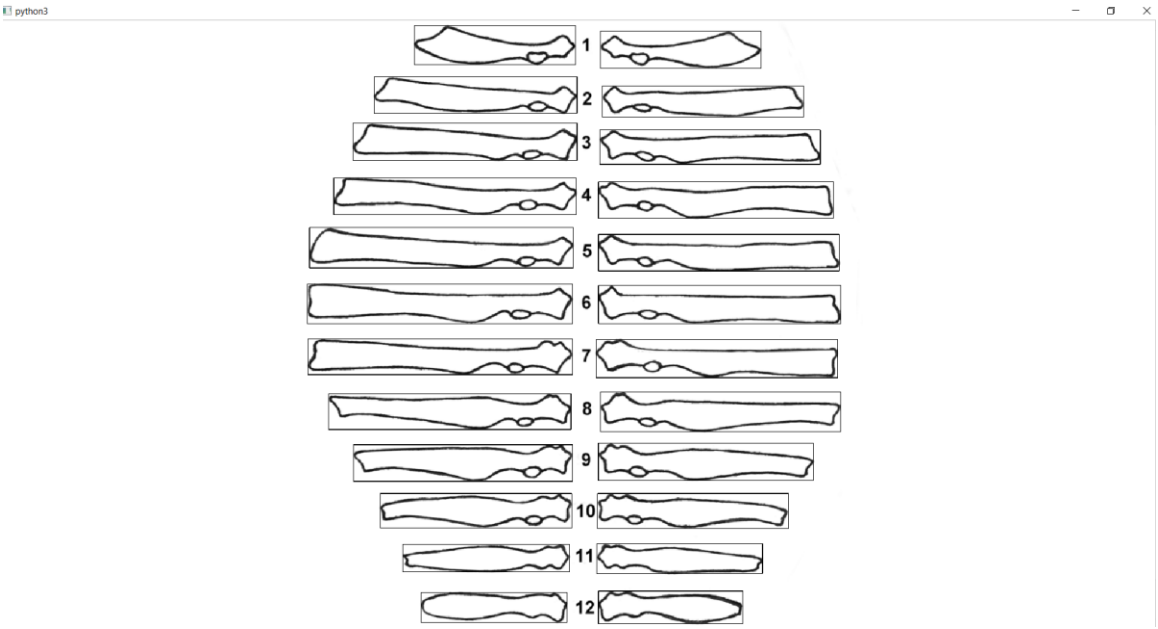

Figure 2~~3~~.14. A screen capture of the RibRecord GUI. This image depicts the secondary window of the rib homunculus where red squares were drawn to depict the exact location of fractures.

Fracture locations were mapped on the homunculus on the second window in RibRecord. The window contained a digital representation of a rib homunculus so that the exact location of the fracture could be marked. The cursor is used to create a red box on the image to demarcate the location of fracture. It is possible to create as many boxes on as many ribs as needed and the boxes can vary in size, to be as large or small as needed. Each box was given coordinates dictated by position on the image and were saved as separate variables so that they could be used in visualizations.

Chapter 4. Methods

Statistical Analyses

The resulting comma delineated excel files output from the RibRecord were analyzed using R 4.1.0 software and associated packages (R Core Team 2021a). General data cleaning, tidying, and recoding was conducted in R. The data were kept in both long and wide formats for analyses because the nested and unnested data structures addressed different research questions. Outliers were assessed visually by plotting the data in univariate and bivariate space with boxplots and scatterplots, which are commonly used in exploratory data analysis for outlier detection (Dovoedo 2011). Any individual or observation that was considered an outlier was investigated, then subsequently removed if deemed necessary, specifically if the data entry was determined to have occurred through an input error. Additional variables were created to capture different scales of the data. The continuous variable of age was used to create two new categorical variables. The one categorical age variable was created by filtering the individuals broad age groupings of young, middle, old, and advanced to better capture broad life history stages. The young group had individuals aged 30 years and younger, the middle group had individuals between 31 years and 45 years old, the old group had individuals between 46 years and 60 years, and the advanced group had individuals 61 years and older. A second age category was created that separated individuals into decade specific groups, which

still collapses the data into groups but may reveal more nuances because the scale is narrower.

Height and weight of each individual were explored individually but were also used to create a BMI category. The BMI was calculated using the traditional formula by Adolphe Quetelet, adjusted for the imperial system of measurement (Eknoyan 2007). Weight and height variables were transformed accordingly and then weight was divided by height, resulting in a numeric BMI score. The adult BMI score was used to determine ranges for BMI type and separate individuals based on their corresponding score (CDC 2020). Research has shown that BMI does not reflect health or weight reliably, but it is a good indication of general body size (CDC Body Mass Index: Considerations for Practitioners). Additionally, it is regularly used in other mortality and morbidity studies (*e.g.*, Brahmbhatt et al. 2017; Hoffmann et al. 2012; Bruni-Fitzgerald 2018), and therefore can be easily compared to other findings. BMI is of particular interest as it has also been evaluated in terms of its relationship with rib fractures (*e.g.*, Premaor, Comim, and Compston 2014).

Inter- and Intra-Rater Agreement Scores

Inter- and intra-rater agreement scores were calculated via Fleiss's Kappa test and percent agreement scores. Inter and intra-rater percent agreement scores are often used with categorical data to quantify the magnitude and direction of concordance rather than just the accuracy of the tool used to complete the scoring (McHugh 2012). Percent

agreement is calculated by summing the number of times the observers agreed divided by the overall number of observations and is therefore easy to interpret. A benefit of using this statistic is that it is directly interpretable (McHugh 2012). One limitation in using percent agreement is that the percentage is what the observers agreed on and does not include chance agreement into the score. Percent agreement is also biased towards variables with fewer levels and a chance exists that the agreement score may be overestimated (Scott 1955). Therefore, when using percent agreement, it is necessary to present a kappa score in concordance with the percent agreement (Park and Kim 2015).

To mitigate some of the pitfalls of percent agreement scores, Fleiss' Kappa was used. Fleiss's Kappa is a generalization for Scott's pi, which is a measure of reliability between two observers that compares the amount that they agreed (Scott 1955). Fleiss' Kappa negates the possible overestimation with percent agreement scores because this measurement is corrected for chance. However, in this research study, the specific benefit of Fleiss' Kappa is its ability to be used to test agreement among more than two raters and more than two categorical variables (Gisev, Bell, and Chen 2013; Zapf et al. 2016). A limitation of a Fleiss' Kappa is difficulty in interpretation, and possible influence by homogeneity of the data (Kraemer and Bloch 1988; Morris et al. 2008). While percent agreement scores may overestimate agreement, it is possible that kappa statistics underestimate agreement because of assumptions of rater independence (McHugh 2012). By including both statistics, there is allowance for sufficient interpretation of reliability; a high kappa score in conjunction with a high percent agreement indicate the variables

were reliably recorded. The *kappam.fleiss* function from the package 'irr' was used in R (Gamer, Lemon, and Fellows 2019).

Intra-rater and inter-rater agreement scores were completed on a sample of the NMDID data for ease of access, as it is a freely available database and does not require special permission. This was preferrable especially during the COVID19 pandemic as these images could also be viewed on a personal computer and did not require entry into a medical examiner's facility. Thirty total fractures were isolated from volume rendered CT images. The observers would evaluate the fractures and record location of fracture and fracture type. Because the number of fractures was primarily dictated by autopsy reports it was felt that these two variables were the most appropriate to check for reliability.

The data were collected on this sample twice by the author for intra-rater agreement, and by two outside observers. Neither outside observer had experience in trauma analysis or medical imaging and were provided written descriptions and exemplars for the fracture type as well as the homunculus used in Figure 3.6 to demonstrate the anatomical locations. Each outside observer was compared to the author via percent agreement and Fleiss' kappa. The intra-rater agreement was also performed in the same way, on the same sample of fracture images.

Frequency Distributions

Frequency distributions were created to help draw conclusions from the large datasets in a simplistic way. Frequency distributions are based on counts of the number of times a value occurs in a data set and a relative frequency is the percentage of an observation that falls within a certain class over the sum of all the data (Field, Miles, and Field 2012; Gibson 2013). This approach provides information on what values, and combined values, were the most common and uncommon in the dataset, which ultimately provide guidance for evaluation of fracture type and location when considering demographic variables. The benefits for utilizing frequency distributions lie in the ability to present large amounts of data in logical and compact form. Furthermore, they aid in interpretations as frequency distributions are inherently reflective of their parent population from where they are drawn, and therefore on some level the distributions can be attributed to overall patterns (Carver 1931).

Chi-squared & Kruskal-Wallis

The frequency distributions display the structure of the dataset, but statistical tests are needed to evaluate if there are statistically significant relationships in the distributions. Specifically, chi-squared and Kruskal-Wallis tests were performed on the categorical and continuous variables, respectively.

The chi-squared tests of independence evaluate the categorical variables in a crosstabulation, which displays the intersection of two categorical variables. A chi-squared test of independence tests if two variables are independent of one another by comparing predicted outcomes of an event happening by chance to the actual observation of the event occurring in the database (Magnello 2005). A variable is considered significant if the observed outcome differs from the predicted outcome with a $p < 0.05$; the null hypothesis is that there is no statistical relationship. Chi-squared does not have any assumptions that need to be met, but it is sensitive when some counts are less than five and when sample sizes are large (~500). Importantly, this means that the chi-squared tests are not influenced by imbalanced classes, and therefore within this dataset will not be affected by the uneven distribution of data (*e.g.*, high MVAs, more males within the sample, etc.) (Magnello 2005). Analyses were performed on the categorical variables and if sufficient data was available. The *chisq.test* function in the stats package was used (R Core Team 2021b). Some limitations with chi-squared required further testing. For example, small differences in large datasets appear statistically significant. Furthermore, chi-squared would not be appropriate on continuous data. Therefore, other statistical analyses were performed to ensure significance and provide interpretation of variables.

A Kruskal-Wallis test was used to test for significant relationships between the continuous and categorical variables. All variables were assumed to be independent, or not influence one another for the analyses. A Kruskal-Wallis is used to compare the medians of two or more groups, and is the non-parametric sister statistic to the Analysis

of Variance (ANOVA) (Field, Miles, and Field 2012; Kruskal and Wallis 1952). Kruskal-Wallis was chosen because it is more robust to violations of the assumptions than ANOVA (McDonald 2014). The Kruskal-Wallis test has a special kind of distribution known as the chi-squared distribution and is an extension of the rank-sum test (Field, Miles, and Field 2012). The *kruskal.test* function of the 'stats' package in R was used (R Core Team 2021b).

If there are no differences in the medians among any of groups (*i.e.*, categorical variables), the p-value will be larger than 0.05, and it can be determined that there is no statistically significant relationship between the variables. However, if there is at least one statistically meaningful difference, the p-value associated with the Kruskal-Wallis tests will be less than 0.05 and considered a significant finding. If the Kruskal-Wallis tests determines a result to be significant then a Dunn's Test was performed. A Dunn's Test is a focused comparison of the median ranks and indicates what variables specifically are statistically significant between the compared groups. The *dunn.test* from the dunn.test package was employed (Dinno 2017). The function computes a Dunn's test (1964) and reports the results among multiple pairwise comparisons after a Kruskal-Wallis test among *k* groups (Kruskal and Wallis 1952). The *dunn.test* in R provides further interpretation of the median differences of the continuous variables per levels of the categorical variable. The p-values are adjusted using the Holm method (1979) for multiple comparisons. The Holm method of adjustment counteracts the effects of

multiple comparisons and ensures that each subsequent test is not rejected. An adjusted p-value less than or equal to 0.05 was considered significant.

Conditional Probability Statements

Rather than solely providing a statement regarding significance of relationships, conditional probabilities were also calculated to provide a quantification of the probabilistic differences in the results. Conditional probabilities reflect the likelihood that a particular event will occur, therefore facilitating interpretation for the practitioner. A conditional probability is calculated based on weighted probabilities, compared to normal probabilities. Specifically, it is the probability that a certain event will occur (A) *given* some other event has already occurred (B) (Waterman 2017). A conditional probability is calculated as the probability of A given B or P(A|B). If the variables are independent of one another and the one event occurring has no influence on the other occurring, the probability of one can be removed so the notation is simply the P(A). However, if the variables are dependent on one another then the conditional probability is calculated as the probability of A and B occurring or P(B)P(A|B). Conditional probabilities were calculated for all relevant categorical variables, given the probability of another categorical variable. For example, the conditional probabilities of an individual's BMI were calculated given that a particular fracture type had occurred. The proportional results of the conditional probabilities were multiplied by 100 to provide percentages.

Multiple Correspondence Analysis

The variables were also used in multiple correspondence analysis (MCA) using the *MCA* function in the FactomineR package (Husson et al. 2008). This analysis is used to observe underlying structures in a dataset and analyze underlying relationships among several categorical dependent variables at one time. An MCA is conducted by creating a multi-way contingency table which is then transformed into an indicator matrix, and simple classification analysis is applied (Abdi and Valentin 2007). The variables are projected onto a Euclidean plane, visualized as a biplot, and the variance-covariance of each variable is displayed through its location on the plot. The longer vector length a variable is, or how far away it is from the axis, indicates that variable has higher discrimination abilities within the data. The cosine, or the angle created between two points, indicates the correlation between two corresponding variables. The smaller the angle, the stronger the relationship (Abdi and Valentin 2007). Within the biplot MCA analyzes the pattern of relationships among categorical variables and can be considered a generalization of principal component analysis (Abdi and Valentin 2007). Additionally, the MCA offers corroboration of statistical relationships identified in the previous statistical analyses, which is especially important considering the sensitivity of chi-squared to large sample sizes. Specifically, it can be used for analysis of qualitative data using a multidimensional scale analysis (Hoffman and De Leeuw 1992). This can further illustrate if multiple variables have a relationship within the dataset and provide further information on what relationships may have an influence on fracture. Categorical variables that were found to be of interest through the previous tests were used in conjunction with one another to further illustrate the relationships within the dataset, and

relationship between the incident variables, fracture variables, and demographic variables.

Random Forest Analysis

A random forest analysis (RFA) is a machine learning technique, specifically an ensemble method, that can be used for classification. An RFA uses a series of decision trees, which use recursive binary splitting to separate the predictor space based on the mode, or the most often observed categorical variable, to classify the data into one of the desired variables. Decision trees are used as an easily interpretable method of classification, and are particularly useful as they are robust to outliers and errors within the data, have few assumptions, and can handle heterogenous data (*i.e.*, ordered, categorical, or mixed data types) (Louppe 2015). As an ensemble method, RFA utilizes many decision trees to provide a more accurate classification.

In an RFA each tree selects a random group of variables at each node, and then makes the best split based on the training set data features. The variable that is determined to be the best at discrimination, or separation of the observations is used at each node. Variables that are highly influential, will be higher up in the decision tree, and importance will decrease with each “branch” and separate the variables into classifications. Each tree in the forest “casts a vote” based on the training data and classification error and the variable is classified using the majority vote (Hastie, Tibshirani, and Friedman 2008). A strength of this analysis is that it removes any

correlation, and each tree classifies the data independently to arrive at the best answer. Because the multiple trees implemented in a RFA can cause the data to be noisy, bagging is employed, which is a technique that reduces variance and results in unbiased models (Biau 2012).

Obviously, an important aspect to RFA is the random selection of variables. To create the test and training dataset, variables are selected at random from the sample and replaced. As such, it is possible to grab the same observation multiple times and other observations not at all. The Out of Bag error (OOB) is the average error using predictions form the trees that do not contain their respective bootstrap sample. This provides a generalized accurate estimate of forest (Louppe 2015). The OOB error is also used to determine the variables that were able to contribute most to the analysis. As the variables better at discriminating are higher within the trees, the OOB is calculated and recoded at each node, and normalized by the standard error. As the utility of the variables decrease, so do the associated OOB scores, which are then used to determine variable importance (R Core Team 2021a).

To conduct the RFA on this data, all demographic variables and incident variables were used to classify the data into fracture characteristic variables. For example, variables like age, weight, height, ancestry, etc. were used to attempt to classify fracture location, or fracture type. As RFA is susceptible to imbalanced classes (Louppe 2015), the dataset was first down sampled such that there were equal numbers of the outcome variable to ensure there was no bias. Additionally, each of the RF models were trained with a subset

of the data (75%) and a separate test set (25%) was used to validate the model's performance. A similar classification accuracy between the training and the test set indicates the model is not overfit and it is generalizable to an independent sample.

Chapter 5. Results

Reliability Scores: Intra-Rater and Inter-rater agreement

Two inexperienced observers collected fracture data to calculate inter-rater reliability and the author collected fracture data twice to calculate intra-rater reliability from a set of volume rendered CT images of thirty-one rib fractures from four individuals. Approximately 48 hours passed between the intra-rater's first and second observations. Intra-rater percent agreement for fracture location was 90.3% (n = 28/30). Fleiss' Kappa was also calculated and the agreement score classified as very good (K = 0.834) (Landis and Koch 1977). The reliability scores for fracture type were slightly lower than those for fracture location; the intra-rater percent agreement was 80.6% (n = 25/31) and the associated Fleiss' Kappa score was 0.743, which is considered to be good reliability (Landis and Koch 1977).

An inter-rater percent agreement was calculated between the author and two additional observers (Observer A and Observer B) in a pairwise approach. When comparing the fracture location scores between Observer A and the researcher, the percentage agreement was 90.3% (n = 27/31) and the Fleiss' Kappa was considered very good (K= 0.835, p-value < 0.05) (Landis and Koch 1977). Comparisons between Observer B and the researcher revealed a lower percentage agreement (77%, 24/31) and Fleiss' Kappa score (K = 0.645, p < 0.05) for fracture location. Fleiss' kappa was also calculated among all three raters with an overall kappa score of 0.72 (p = 0), which is

considered good agreement. The overall good outcome of these scores, especially considering the lack of experience in trauma analysis or working with medical imaging, implies that the fracture location can be reliably determined.

Type of fracture was then analyzed between the observers in a similar pairwise approach. Observer A and the researcher achieved a percent agreement score of 70.9% (n= 22/31) and a Fleiss' Kappa score that classifies as 'good' ($K = 0.607$, $p < 0.05$). The highest discordance between observers occurred with incomplete ($K = 0.516$) and simple fractures ($K = 0.517$). Percent agreement between the researcher and Observer B was 61.29% (n = 19/31) and the Fleiss' Kappa was moderate ($K = 0.482$, $p < 0.05$). The discordance in the comparisons was greatest for simple ($K = 0.139$) and incomplete ($K = 0.262$) fractures. Fleiss' Kappa was also conducted among the three observers and achieved an overall kappa of 0.499, which is considered moderate agreement. Similar to the individual pairwise comparisons, the levels with the greatest discordance occurred among simple ($K = 0.27$) and oblique ($K = 0.311$) fractures; the third greatest discordance was with incomplete fractures ($K = 0.34$).

The high kappa values and high percent agreement for fracture location for both the inter-rater and intra-rater demonstrate that these variables can be reliably observed. Type of fracture had lower percent agreement and kappa values in both intra- and inter-rater percent tests compared to fracture location. However, the intra-rater values were substantially higher than the inter-rater scores. There is no precedent that has been established regarding the acceptable reliability threshold for features evaluated in trauma

analysis. Furthermore, only 6 of the 31 comparisons of fracture type were incorrect for the intra-rater comparisons. Considering there were six levels of fracture type to choose among, it was decided that fracture type was reliable, but may be more dependent on experience and visibility of fractures.

Descriptive/Summary Statistics of the Sample

The total sample includes 1,415 individuals (Table 5.1). Males (n =1013; 72%) comprised a much larger portion of the sample than females (n = 386; 27%) and there were several individuals (n = 15) of unknown sex. All individuals died between 2015 and 2020 and were between the age of 18 and 96 years at the time of death (Figure 5.1). Ages ranged from 18 to 96 years for males with a mean age of 44.83 years, and ages ranged from 18 to 92 years for females with a mean age of 46.32 years. When further considering sex with age (age/sex variable), there were more younger females and more older males (Figure 5.2).

Table 5.1. Number of males and females per medical examiner office, and number of fractures per group

	WCRMEO	**NY OCME**	**HCIF**	**NMDID**	***Total***
Individuals (sexes pooled)	267	271	496	381	1,415
Males	185	190	365	274	1013
Females	82	78	130	96	386
Fractures	4329	5957	8610	5957	24,853

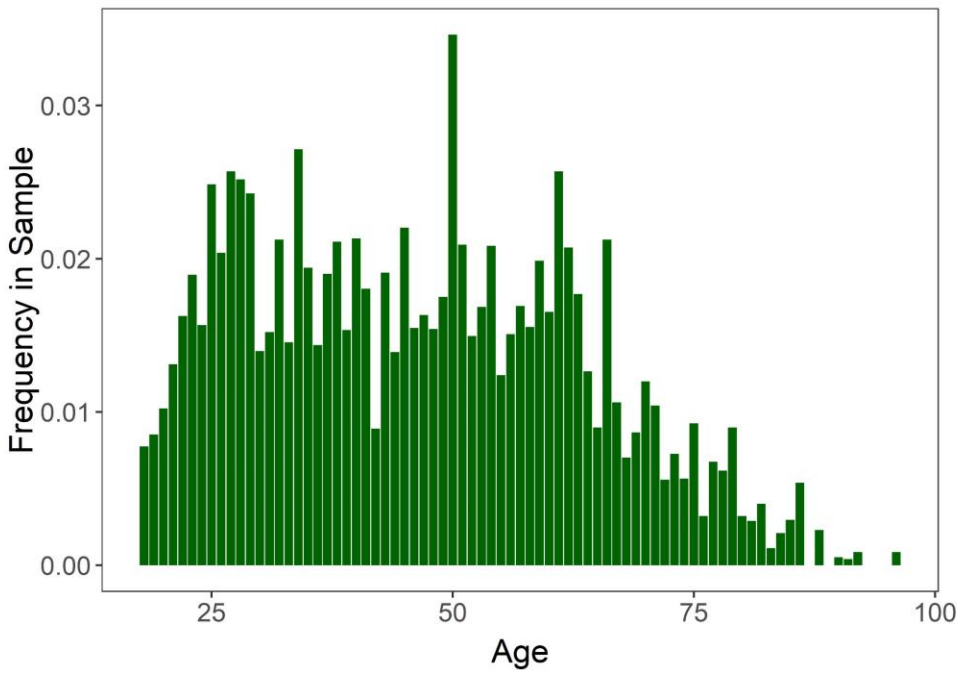

Figure 5.1. Age distribution of the sample.

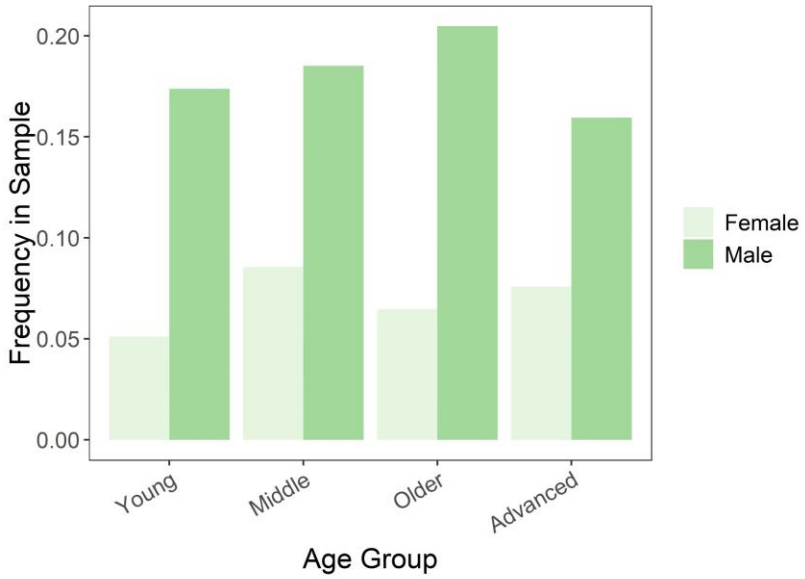

Figure 5.3~~2~~. The frequencies of age groups separated by males and females within the

Males were on average taller and heavier than females in the sample (Figure 5.3). BMI was calculated to better capture the general phenotype. Depending on BMI score, individuals were grouped into one of four categories based on the imperially adjusted Quetelet BMI scale (Eknoyan 2007): underweight, normal, overweight, and obese. The category with the most individuals was obese (37.4%), followed closely by overweight (32.8%), and then normal (25.4%); the underweight category had the fewest individuals (4.2%). There was a larger number of females in the healthy and overweight categories and a larger number of males in the obese and overweight categories (Figure 5.5).

The most common MOD was accidental deaths (n = 1171, 87%), with suicide comprising 10% (n = 158) of the total sample, and homicide comprising only 1% (n = 36) of the total sample. Cause of death was most frequently associated with MVAs (50%, n = 699), PVAs (29%, n = 335), falls from height (10%, n=193) and pedestrian versus train (1.8%, n = 26) . The remaining 188 cases had a variety of unique CODs (10%). Males and females presented with comparable percentages in the MOD and COD categories. For example, 85.9% of females and 87.9% males had a MOD of accident, and 54% of females and 48.7% of males had a COD of MVA.

Because data collection at numerous institutions does not adhere to the same policies and procedures, the dataset included high amounts of missing data. However, most of the missing data was associated with the supplemental health, death event, and biological data that was not pertinent to the primary objectives of the research. Some

examples of this data include if CPR was used on site, or if the individual had a history of tobacco, drug, or alcohol use.

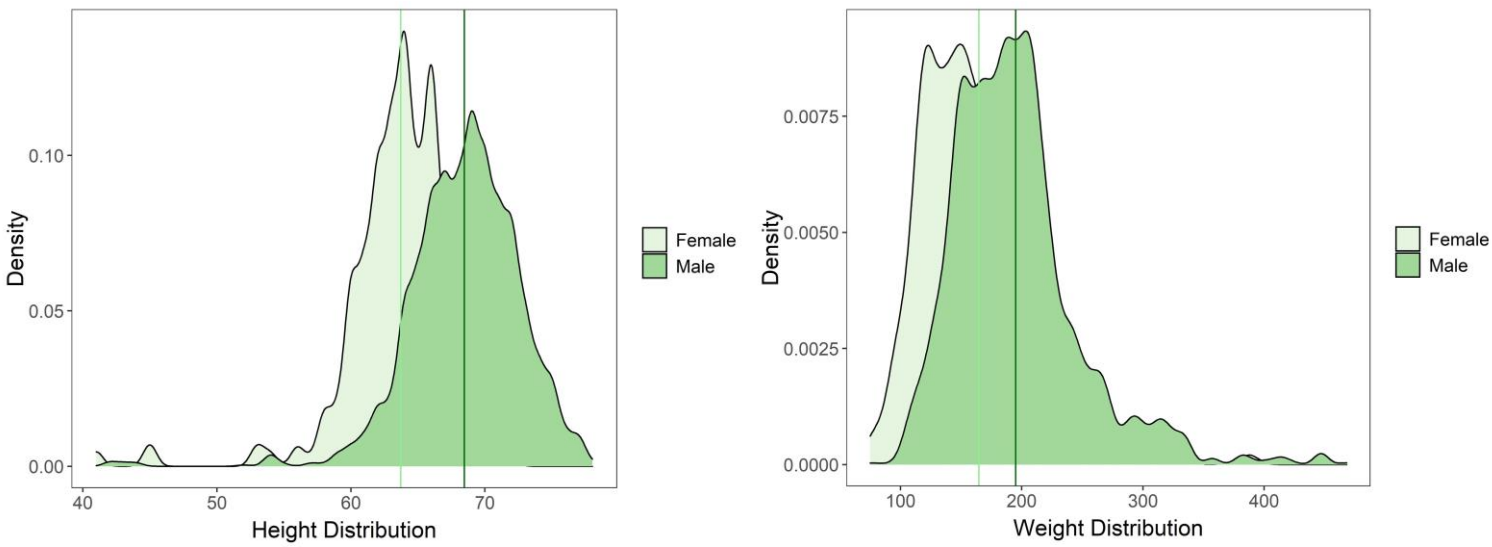

Figure 5.3 - Height (left) and weight (right) distribution in the sample. The vertical line illustrates the mean of the sample.

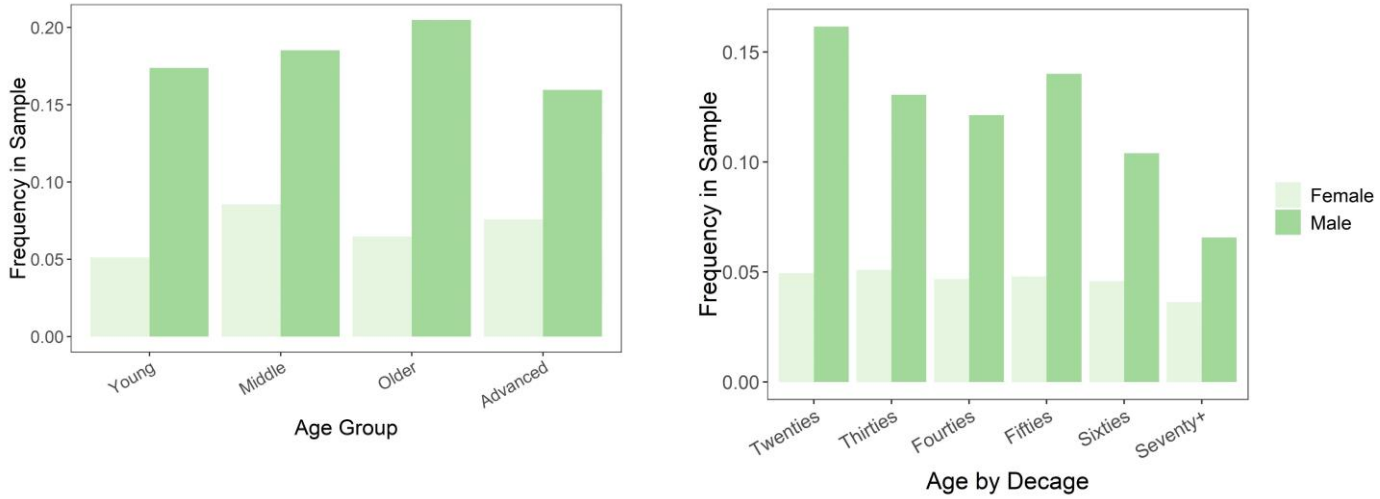

Figure 5.4. Distribution of ages by age group (left) and by decade separated and sex (right).

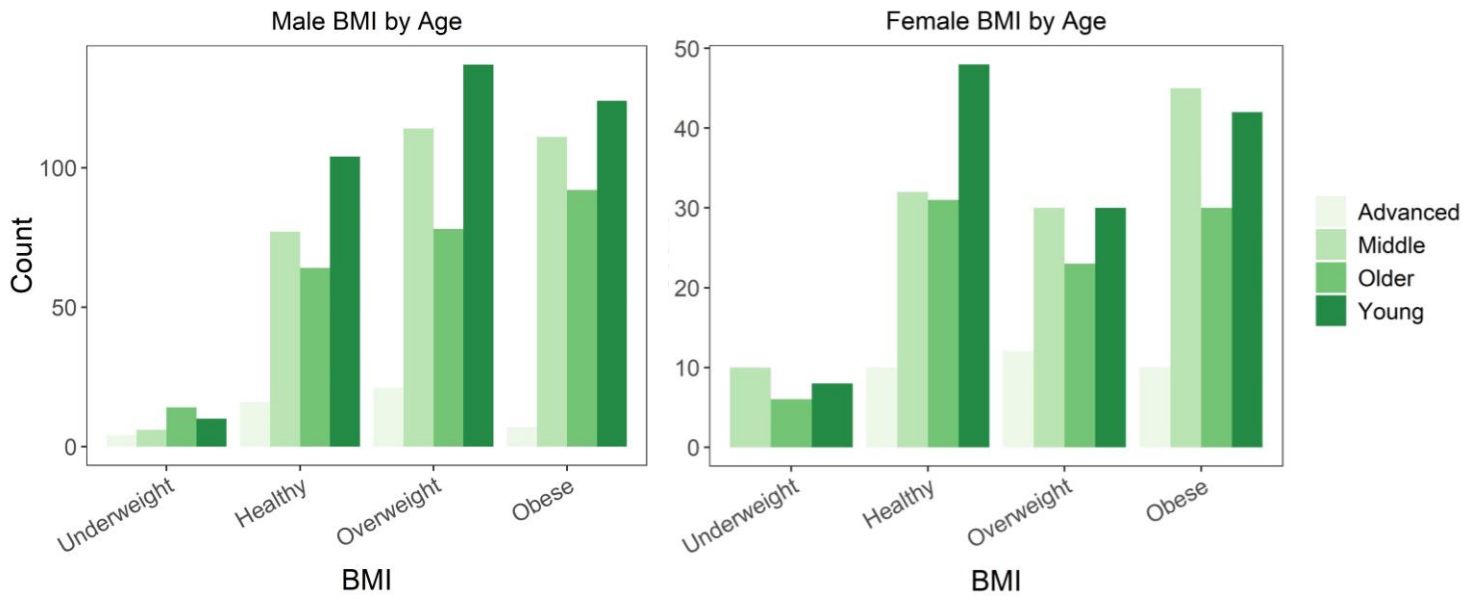

Figure 5.5. Distribution of BMI by age group for males (left) and females (left).

Fracture Variable Data

A total number of 24,853 fractures were collected from the 1415 individuals. Of the fractures that were recorded as present, 23,760 had an associated fracture type. The distribution of fractures was normal (Figure 5.6) and ranged from 1 fracture to 58 fractures; the median number of fractures was 23 and the mean was 24. When considering the number of fractures per individual, the distribution is right skewed, though it does have a slight plateau, which results in both a mean and a median of 16 fractures per person (Figure 5.7). Figure 5.8 depicts a scatterplot of number of fractures

by age. Loess lines emphasize the slight increase in the number of fractures per person from young to middle age, but then the number of fractures per person stabilizes even though age is increasing. There is also no obvious – or statistical – difference between males and females for the number of fractures and chronological age.

Frequencies were calculated to observe the distribution of categorical fracture variables individually and then in combination with other demographic and fracture level variables. While the same individual presented with numerous fractures, all analyses considered the fractures as independent events. Fractures occurred almost equally on left (50.8%) and right (49.1%) sides of the rib cage. The most fractured ribs were the third through sixth ribs (11.5% to 11.9%) and the eleventh (3.3%) and twelfth (2%) ribs incurred the least number of fractures (Table 5.2, Figure 5.9). Anatomical location of fractures occurred mostly along the body of the rib; the most frequently fractured locations were posterolateral (43%) and anterolateral (38%) (Figure 5.10). The least frequently fractured locations were anterior fractures (6.5%) and posterior fractures (11%). The most common fracture type was displaced (59%), followed by simple fractures (23%), and then multi-fragmentary (7.3%) (Table 5.3, Figure 5.11). Buckle, incomplete, and oblique had the smallest frequencies in the dataset (Table 5.3).

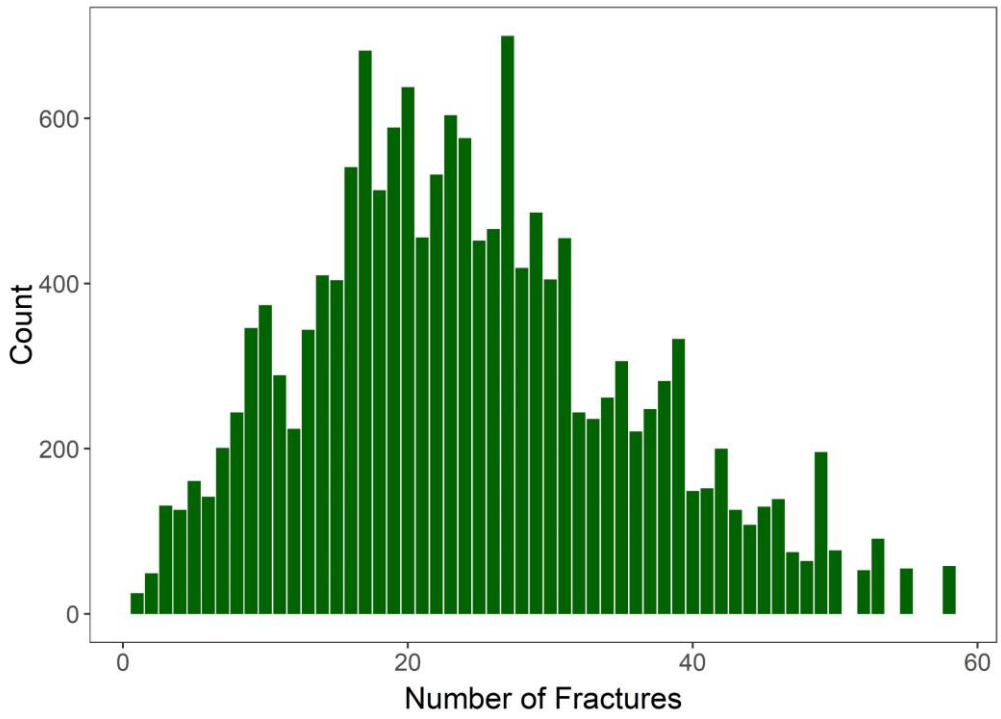

Figure 5.6. Distribution of counts of number of fractures within the dataset

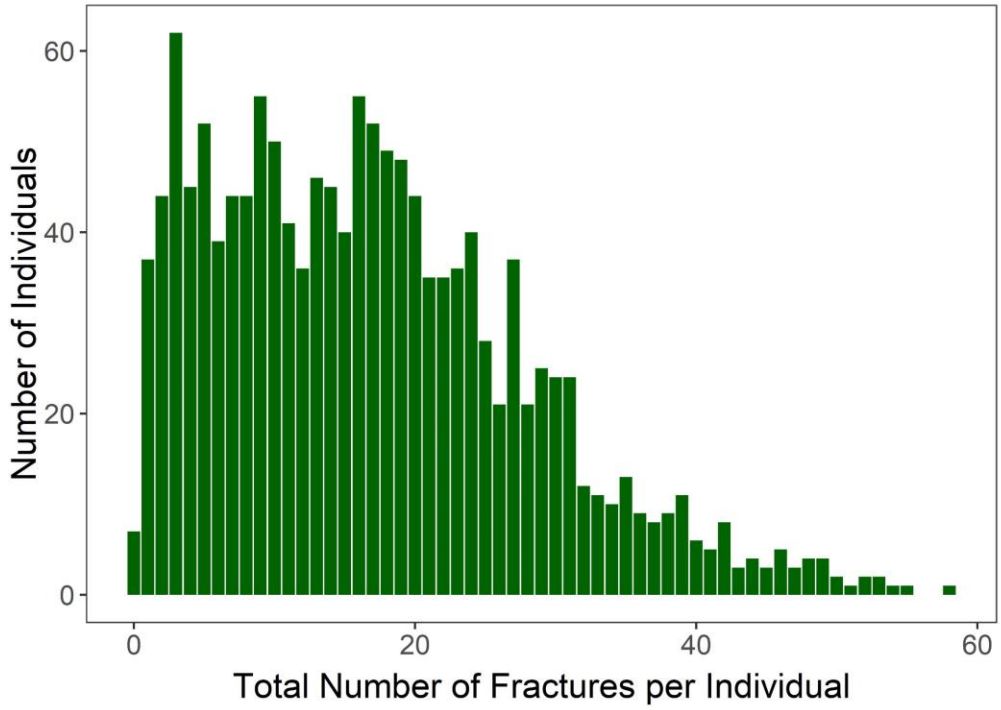

Figures 5.7. Numbers of Fractures per individual

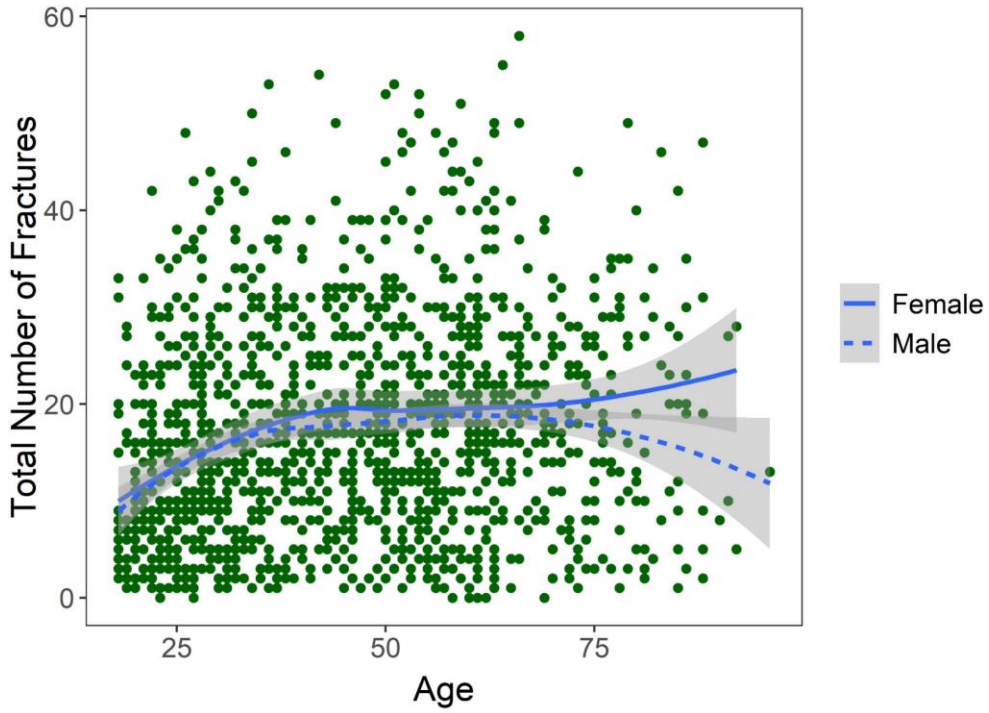

Figure 5.8. Number of fractures by age. Loess lines indicate the average number of fractures plateaus in the forties and continues to be consistent until approximately 70 years of age. Negligible differences exist between males and females with until older ages (~70 years).

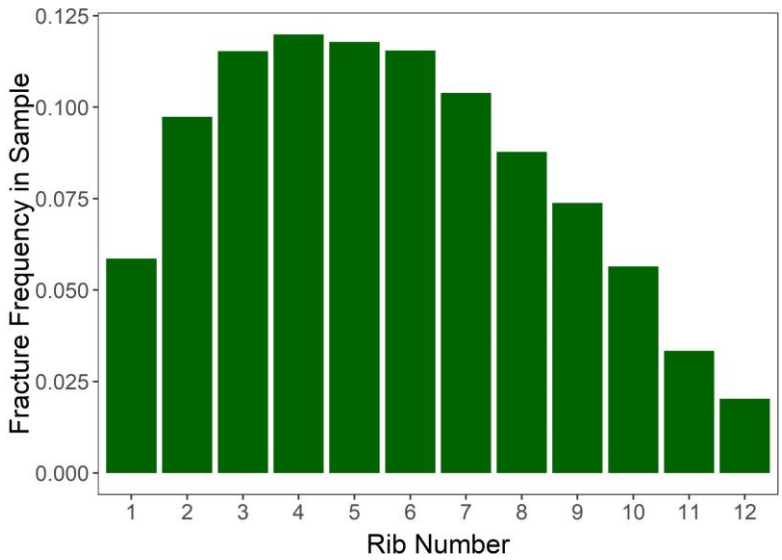

Figure 5.9. Frequency of fracture per rib number

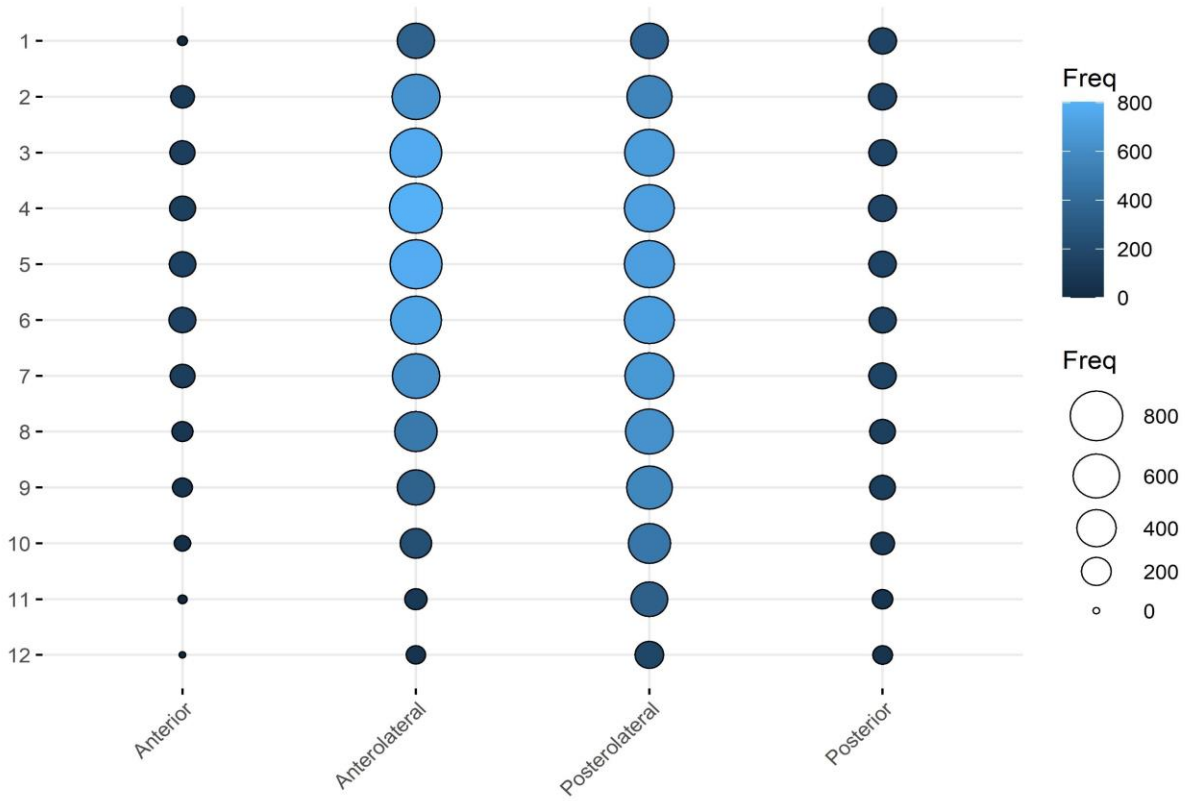

Figure 5.10. Balloon plot depicting frequency of fractures per anatomical location (x-axis) and rib number (y-axis).

Table 5.3. Frequency of Fracture Type within the Dataset	
Fracture Type	**Frequency**
Buckle	3.8%
Displaced	59.0%
Incomplete	2.7%
Multi-fragmentary	7.2%
Oblique	3.0%
Simple	23.9%

Table 5.2. Frequency of Fracture for each rib	
Rib Number	**Frequency**
Rib 1	5.8%
Rib 2	9.7%
Rib 3	11.5%
Rib 4	11.9%
Rib 5	11.7%
Rib 6	11.5%
Rib 7	10.3%
Rib 8	8.7%
Rib 9	7.3%
Rib 10	5.6%
Rib 11	3.3%
Rib 12	2.0%

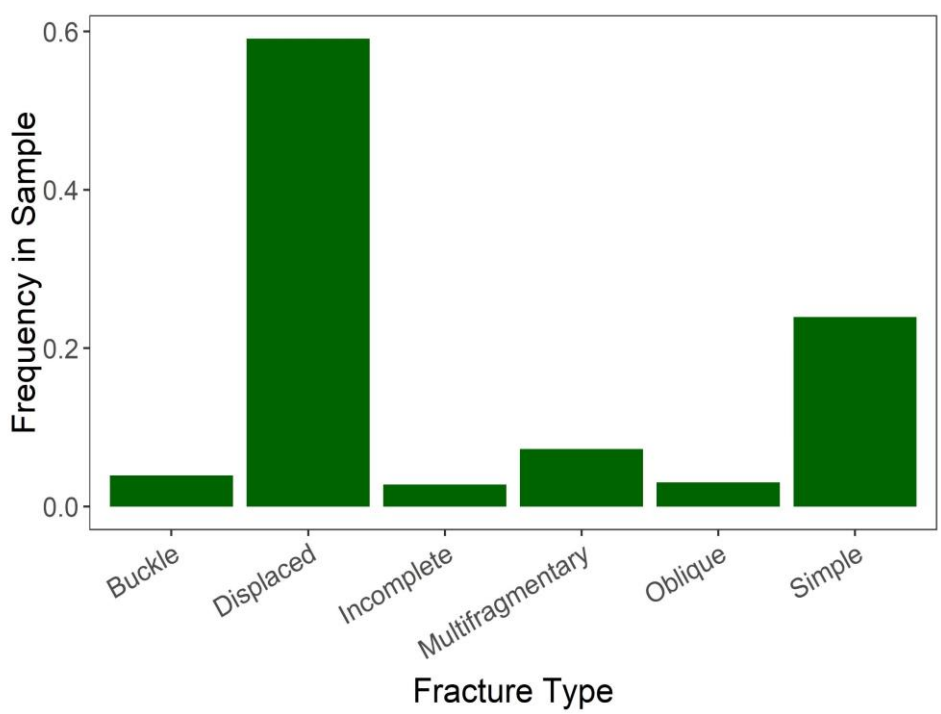

Figure 5.11. Frequency of fracture type within the sample

While raw frequencies are important for understanding the distribution of the data, the reality is that none of the individual-level or fracture-level variables are independent of one another. Combining variables and creating contingency tables elucidates relationships that may commonly occur among the individual-level variables and the fracture-level variables. When the frequencies related to simple fractures in the dataset were examined, simple fractures occurred at the highest frequency in accidental deaths (94.7%), on the fourth rib (11.5%), in the middle age group (27.5%), and when age and sex were both considered, middle-aged males (19.6%).

Buckle fractures occurred most frequently, and almost equally, in the young (< 35 years, 26.9%) and advanced (> 60 years, 27.1%) age groups. However, when age was explored by decade, buckle fractures occurred in individuals 29 years and younger more frequently (24.5%) than any other decade (Figure 5.12). In conjunction with age, young (21.7%) and older (22.5%) males had much higher frequency of buckle fractures than any female age group (5.2%,8.2%, respectively). Buckle fractures occurred most often in the anterolateral (62.2%) and anterior (27.4%) locations, and most frequently on rib six (14.7%), five (13.9%), three (13.3%), and seven (13.1%). Buckle fractures were absent on ribs one, eleven, and twelve (Figure 5.13).

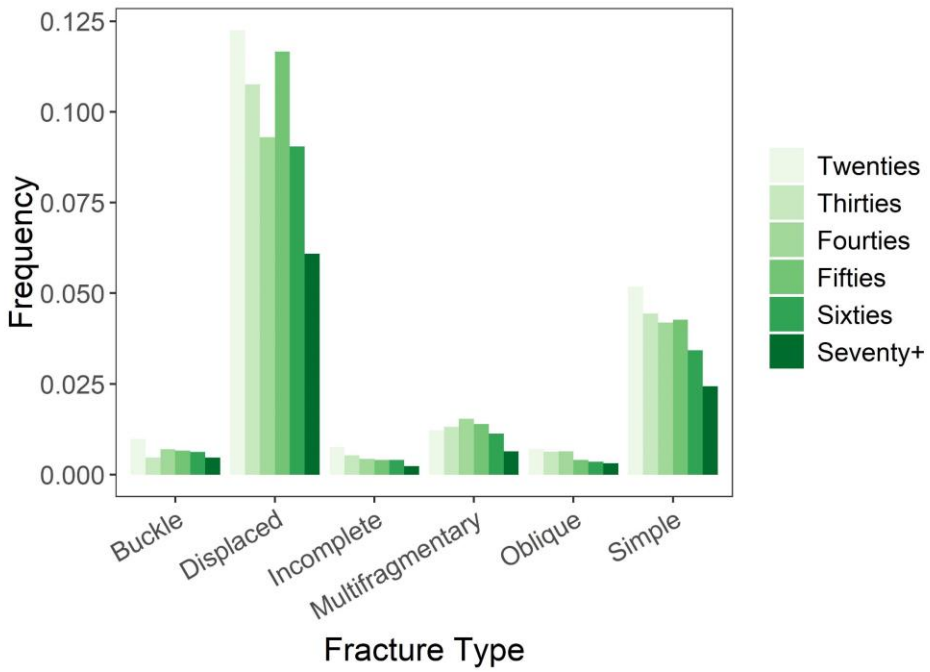

Figure 5.12. Frequency of fracture type separated by age group

Multi-fragmentary fractures occurred most often in the posterolateral region (48.8%), on ribs four (11.7%) and seven (11.5%), in obese individuals (35.7%), and in individuals in the older age category (seventy-five years and older, 30.7%). When considering sex and age, older males had the highest frequency of multi-fragmentary fractures (26.1%).

Oblique fractures occurred most often in obese individuals (42.5%) and in the middle (31.4%) and young (25.1%) age groups. When considering sex and age, middle-

aged males had the highest frequency of oblique fractures (22.7%). However, considering age by decade revealed oblique fractures occurred most often in individuals 29 years and younger (22.6%). Oblique fractures occurred in high frequencies posterolaterally (52.7%) and on rib three (12.4%), six (12.2%), and seven (12%).

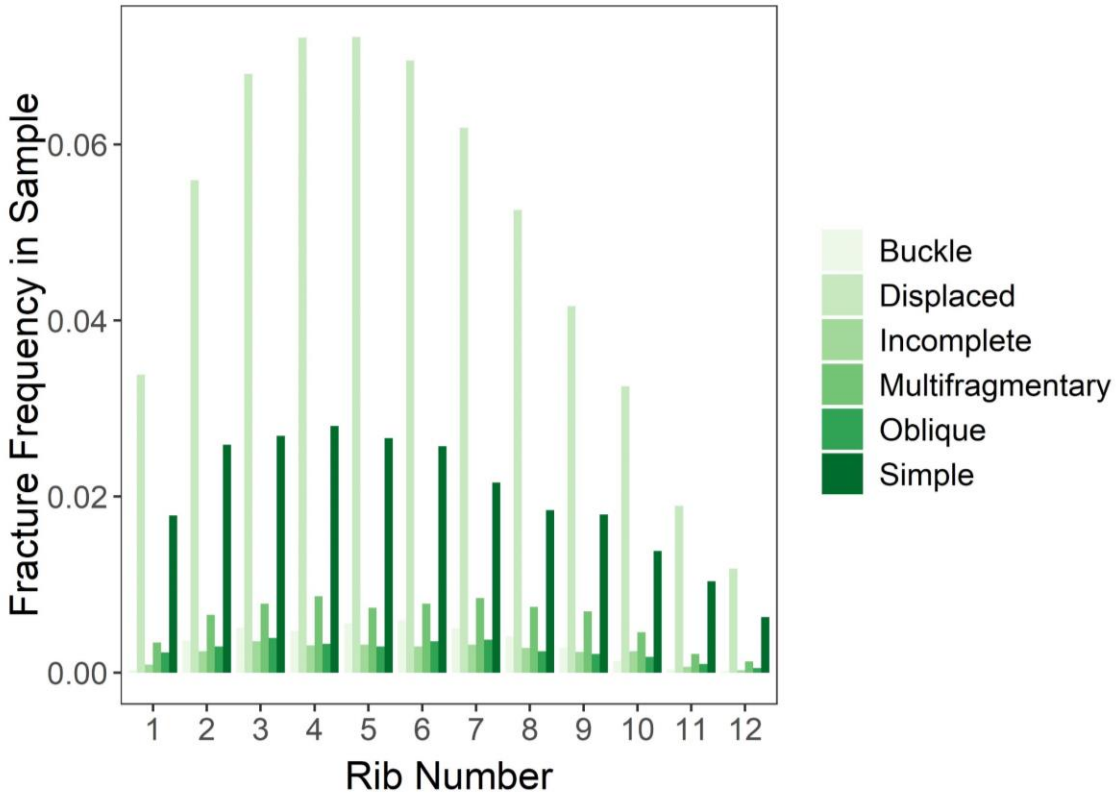

Figure 5.13. Frequency of type of fracture per rib number.

Displaced fractures did not appear to be biased towards any age groups, as it was present at almost equal levels in the broad categories (young: 21.6%, middle: 27.5%,

older: 26.9%, advanced: 23.8%). However, when age and sex were both considered, older males had the highest frequency of displaced fractures (20.3%). Displaced fractures most frequently occurred in the two lateral regions, with posterolateral incurring a slightly higher percentage (45.1%) compared to anterolateral (38.9%).

When considering fracture variables and body size (BMI), all fracture types occurred more frequently in the higher BMI categories than the smaller BMI groups (Figure 5.14). The underweight BMI group had a notably higher percentage of displaced fractures compared to all other fracture types and the healthy BMI group had a notably higher proportion of incomplete fractures than any other group. Generally, those in the obese group fractured at higher frequencies in all locations than all other BMI groups (Figure 5.15). However, frequencies between overweight and obese groups were similar in the anterior location. Those in the underweight group had much lower frequency of fractures in the anterior and posterior locations.

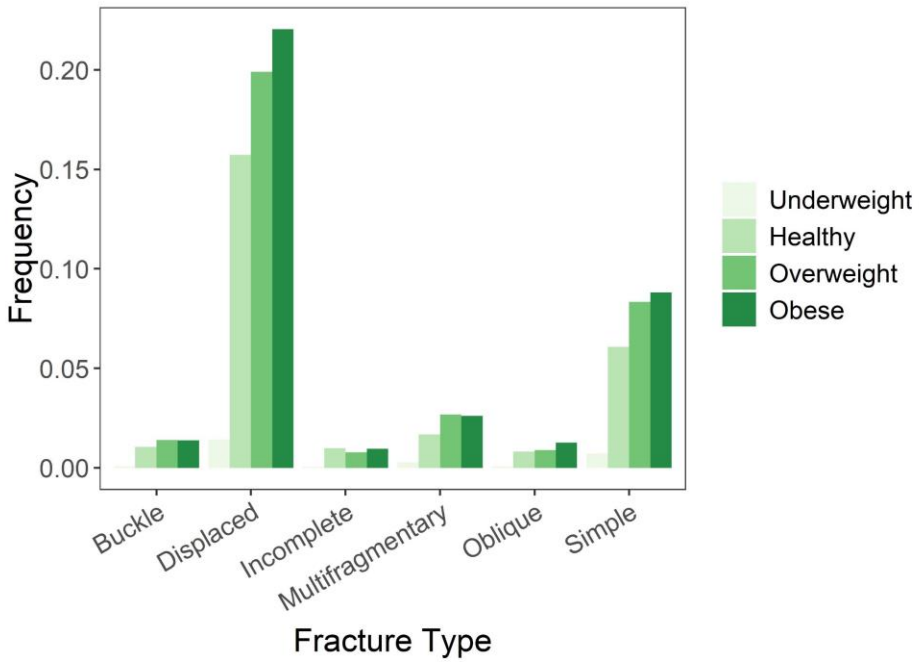

Figure 5.14. Frequency of fracture type separated by BMI

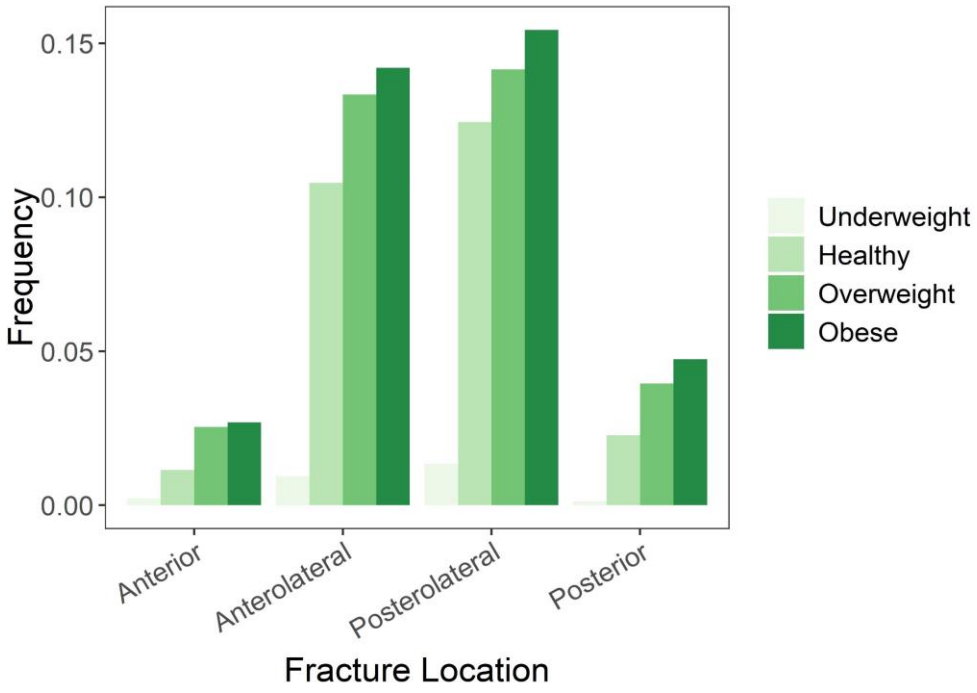

Figure 5.15. Frequency of fracture location by BMI

Chi-squared Tests

While frequencies inform what variables, and combination of variables occurred the most or least frequently in the dataset, it does not indicate if the relationships are statistically significant. Chi-squared tests were performed to test for significant relationships among fracture variables, demographic variables, and incident variables.

Anatomical location of fracture was explored by broad age category, sex, BMI, MOD, COD, rib number, and fracture type. In general results for chi-squared tests of age group, sex, BMI, rib number, MOD and COD were all found significant. However, when looking at significance per location, only rib number, fracture type, and broad age category had a statistically significant relationships with all anatomical locations based on the chi-squared tests. Specifically, fractures on the anterior portion of rib cage had significant relationships ($p < 0.05$) with age category, sex, COD, rib number, and BMI. Anterolateral fractures were also found to have significant relationships ($p < 0.05$) with age group, COD, rib number, and type of fracture. Posterolateral fractures shared the same significant relationships as the anterolateral fractures, with the addition of having a significant relationship with BMI. Sex, BMI, and rib number were found to have significant relationships with posterior fractures (Table 5.6). Overall, anatomical location had many statistically significant relationships that spanned all demographic and fracture level variables, except sex. Both sex and MOD were found to be significant with the general fracture location variable, but not in relation to any specific locations.

Table 5.6. P-values associated with chi-squared tests of individual fracture locations; mod is omitted as no significant relationships were observed						
Fracture Location	**Age Group**	**Sex**	**BMI**	**Rib Number**	**Fracture Type**	**COD**
Anterior	$p = 0.013$	$p < 0.001$	$p < 0.001$	$p < 0.001$	$p < 0.001$	$p < 0.001$
Anterolateral	$p < 0.001$	__	___	$p < 0.001$	$p < 0.001$	$p < 0.001$
Posterolateral	$p < 0.001$	___	$p < 0.001$	$p < 0.001$	$p < 0.001$	$p < 0.001$
Posterior	$p = 0.005$	___	$p <0.001$	$p <0.001$	$p <0.001$	___

Fracture types were considered with broad age category, sex, BMI, MOD, COD, rib number, and location. Age group, BMI, location of fracture, rib number and COD showed significant relationships with fracture type. Specifically, fracture location had a statistically significant relationship ($p < 0.05$) with all fracture types and COD had a statistically significant relationship for all fracture types except incomplete fractures. Age group had significance ($p < 0.05$) with all fracture types except simple fractures. Rib number was significant for all fracture types except oblique and displaced fractures. BMI had a significant ($p < 0.05$) relationship with multi-fragmentary and incomplete fractures (Table 5.7). When looking at individual ribs, location was significant for all ribs except the seventh rib, and fracture type was significant for second rib and seventh rib. Sex and BMI had the fewest number of significant relationships with fracture type.

Table 5.7. P-values associated with chi-squared tests of individual fracture type.						
Fracture Type	**Age Group**	**Sex**	**BMI**	**Rib Number**	**Fracture Location**	**COD**
Incomplete	p = 0.007	___	p < 0.001	p =0.05	p < 0.001	___
Buckle	p < 0.001	___	___	p < 0.001	p < 0.001	p < 0.001
Simple	___	___	___	p < 0.001	p < 0.001	p < 0.001
Oblique	p = 0.02	___	___	___	p < 0.001	___
Displaced	p = 0.004	___	___	___	p < 0.001	p < 0.001
Multi-fragmentary	p = 0.008	p = 0.03	p < 0.001	p = 0.03	p < 0.001	p < 0.001

To better capture demographic information, a new variable that combined age and sex was created (age*sex). A chi-squared test was conducted between the categorical variable and all fracture data. The age/sex variable was found to be significant for all anatomical locations and all fracture types (except buckle fractures) and had no significant relationship with rib number (Tables 5.7).

Table 5.8. P-values from the chi-squared tests for fracture location and combination of Age & Sex.	
Fracture Location	**Age*Sex**
Anterior	p < 0.05
Anterolateral	p < 0.05
Posterolateral	p < 0.05
Posterior	p < 0.05

Table 5.9. P-values from the chi-squared tests for fracture type and combination of the Age & Sex.	
Fracture Type	**Age*Sex**
Buckle	$p = 0.15$
Displaced	$p < 0.05$
Incomplete	$p = 0.01$
Multi-fragmentary	$p < 0.05$
Oblique	$p < 0.05$
Simple	$p < 0.05$

Kruskal-Wallis Test

Age, stature, weight, and number of fractures per individual are continuous variables, and therefore Kruskal-Wallis tests were employed to identify statistically significant relationships between these variables and the categorical fracture variables. Age, weight, height, and number of fractures presented with significant ($p < 0.05$) relationships with location of fracture and type of fracture (Table 5.10). Weight and number of fractures were found to be significant ($p < 0.05$) with rib number, whereas both age and height had no significant relationship with rib number. While a Kruskal-Wallis test informs if at least one comparison has a significant relationship, it does not provide post-hoc pairwise comparisons to reveal what pairwise comparison dominates

(*i.e.*, is significant) (Dinno 2017). Therefore, Dunn's tests were performed to further explore the relationships.

Table 5.10. Results of Kruskal-Wallis Test; asterisk and bold font indicate a statistically significant relationship.

	Location	**Type**	**Number**
Age	chi-squared: 82.731 df: 3 **p – value: <0.05 ***	chi-squared: 31.224 df: 5 **p – value: < 0.05 ***	chi-squared: 9.1528 df: 11 p – value: 0.6078
Height	chi-squared: 71.209 df: 3 **p – value: < 0.05 ***	chi-squared: 15.172 df: 5 **p – value: < 0.05 ***	chi-squared: 15.351 df: 11 p – value: 0.167
Weight	chi-squared: 94.369 df: 3 **p – value: < 0.05 ***	chi-squared: 11.632 df: 5 **p – value: < 0.05 ***	chi-squared: 20.84 df: 11 **p – value: < 0.05 ***
Number of Fractures	chi-squared: 114.9 df: 3 **p – value: < 0.05 ***	chi-squared: 938.52 df: 5 **p – value: < 0.05 ***	chi-squared: 145.89 df:11 **p – value: < 0.05 ***

The results of the Dunn's test indicated the mean differences among the continuous variables of age, weight, and height and the categorical levels of the fracture variables. The output of a *dunn.test* in R provides all possible pairwise comparisons among groups and provides the z-statistic, p-value, and degrees of freedom for each comparison (Dinno 2017). Results are reported below, but the full Dunn's test results for all comparisons are provided in the appendix (Appendix 1.3). Mean differences in age were found to be significantly different between anterior-anterolateral groups, anterolateral-posterior groups, anterolateral-posterolateral groups, and posterior-posterolateral groups (Table 5.11). Mean differences in age were also identified as

significantly different between fracture types. Significant differences in age were identified between buckle-incomplete fractures, displaced-incomplete fractures, multi-fragmentary-incomplete fractures, multi-fragmentary-oblique fractures, displaced-simple fractures, incomplete-simple fractures, and multi-fragmentary-simple fracture groups (Table 5.14). Finally, mean differences in age were significantly different between first-fourth, first-fifth, first-sixth and first-seventh rib group means (Appendix 1.3).

Mean differences in weight were found to be significant for all anatomical fracture locations. Specifically, differences in weight were found to be significantly different between buckle-incomplete fractures, oblique-incomplete fractures, displaced-oblique fractures, multi-fragmentary-oblique fractures, and oblique-simple fracture groups (Table 5.15). Mean differences in weight were found to be significantly different between tenth-second, tenth-third, tenth-fourth, tenth-fifth, tenth-sixth, tenth-seventh, eleventh-second, eleventh-third, eleventh-fourth, eleventh-fifth, eleventh-sixth, and fourth-ninth ribs (Appendix 1.3).

Mean differences in height were found to be significantly different between anterior-anterolateral, anterior-posterolateral, anterior-posterior, posterior-posterolateral. Mean differences in height were found to be significantly different among fracture types. In particular, between buckle-displaced fractures, buckle-simple fractures, displaced-multi-fragmentary fractures, and multi-fragmentary -- simple fractures (Table 5.16). Finally, mean differences in height were found to be significantly different across the rib numbers. The pairwise comparisons that were significant include: tenth-third, tenth-

fourth, tenth-fifth, tenth-sixth, eleventh-third, and eleventh-fourth ribs. All other differences were not found to be significant (Appendix 1.3).

Table 5.11. Dunn Test output for Age and Location; asterisk indicates significant relationship

	Anterior	Anterolateral	Posterior
Anterolateral	-2.79 0.003*		
Posterior	0.177 0.430	3.714 0.000*	
Posterolateral	1.979 0.024*	9.070 0.000*	2.202 0.014*

Table 5.12. Dunn Test output for Weight and Location; asterisk indicates significant relationship

	Anterior	Anterolateral	Posterior
Anterolateral	7.000 0.000*		
Posterior	3.091 0.001*	-4.200 0.000*	
Posterolateral	8.474 0.000*	2.688 0.004*	6.015 0.000*

Table 5.13. Dunn Test output for Height and Location; asterisk indicates significant relationship

	Anterior	Anterolateral	Posterior
Anterolateral	7.728 0.000*		
Posterior	5.593 0.000*	-1.485 0.0688	

Posterolateral	8.278 0.000*	0.929 0.176	2.113 0.017*

Table 5.14. Dunn Test output for Number of Fractures and Location; asterisk indicates significant relationship

	Anterior	**Anterolateral**	**Posterior**
Anterolateral	-0.384 0.351		
Posterior	-7.491 0.000*	-10.350 0.000*	
Posterolateral	-2.773 0.003*	-4.515 0.000*	7.504 0.000*

Table 5.15. Dunn Test output for Age and Type; asterisk indicates significant relationship

	Buckle	**Displaced**	**Incomplete**	**Multi-fragmentary**	**Oblique**
Displaced	-0.700 0.242				
Incomplete	2.560 0.005*	3.866 0.000*			
Multi-fragmentary	-0.941 0.173	-0.057 0.284	-3.688 0.000*		
Oblique	1.538 0.062	2.633 0.004*	-1.014 0.155	2.596 0.005*	
Simple	0.885 0.188	3.505 0.000*	-2.408 0.008*	2.542 0.006*	-1.139 0.127

Table 5.15. Dunn Test output for Weight and Type; asterisk indicates significant relationship					
	Buckle	**Displaced**	**Incomplete**	**Multi-fragmentary**	**Oblique**
Displaced	1.478 0.070				
Incomplete	2.376 0.008*	1.781 0.038			
Multi-fragmentary	1.646 0.050	0.662 0.254	-1.185 0.118		
Oblique	-0.533 0.297	-2.018 0.022*	-2.746 0.003*	-2.119 0.017*	
Simple	1.852 0.032	0.987 0.162	-1.349 0.089	-0.048 0.481	2.343 0.010*

Table 5.16. Dunn Test output for Height and Type; asterisk indicates significant relationship					
	Buckle	**Displaced**	**Incomplete**	**Multi-fragmentary**	**Oblique**
Displaced	2.814 0.002*				
Incomplete	1.451 0.073	-0.537 0.296			
Multi-fragmentary	1.085 0.139	-2.021 0.022*	-0.653 0.257		
Oblique	0.446 0.328	-1.937 0.026	-0.967 0.167	-0.501 0.308	
Simple	2.786 0.003*	0.207 0.418	0.599 0.275	1.994 0.023*	1.953 0.025

Table 5.17. Dunn Test output for Number of Fractures and Type; asterisk indicates significant relationship					
	Buckle	**Displaced**	**Incomplete**	**Multi-fragmentary**	**Oblique**
Displaced	2.814 0.002*				
Incomplete	1.451 0.073	-0.537 0.296			
Multi-fragmentary	1.085 0.139	-2.0214 0.022*	-0.653 0.257		
Oblique	0.446 0.328	-1.937 0.026	-0.967 0.167	-0.501 0.308	
Simple	2.786 0.003*	0.207 0.418	0.599 0.275	1.994 0.023*	1.953 0.025

Conditional Probabilities

Contingency tables were used to calculate conditional probabilities for those variables that were observed to influence fractures in the previous analyses to better understand the relationships. Tables were created for as many variables as possible, and due to the size of the dataset not all were included. The tables indicated to be most useful are reported here. Conditional probabilities were calculated between COD related incidents and fracture location. Individuals with a COD related to a fall from height, pedestrian vs. train, and the general category of “other” COD types had the highest conditional probability of posterolateral fractures (fall: 54.9%, train: 67.1%, other: 42.5%). Individuals with a COD related to MVA or PVA had relatively even probability

of anterolateral and posterolateral fractures (MVA anterolateral: 40.5%; posterolateral 40.4%; PVA anterolateral: 40.8%, posterolateral: 44.0%).

Conditional probabilities were then calculated for fracture location with the continuous demographic variables of age, weight, and height, all of which displayed significance in the Kruskal-Wallis tests. The probability of an anterior fracture occurring in a healthy/normal sized adult is 16.9%, whereas the probability of an anterior fracture occurring in an obese individual is 40.5%. Similarly, the probability that a healthy person incurs a posterior fracture is 19.5%; the probability increases to 42.6% for an obese individual to incur a posterior fracture.

Age group was found to be significant in all four locations of fracture within the chi-squared tests; therefore, probabilities were calculated for age by decade and location of fracture. If presented with an anterior, posterior, or posterolateral fracture, the probability that the individual was younger than 29 years was highest (23.6% anterior, 22.4% posterior, 22.9% posterolateral). The next highest conditional probability associated with a posterior or anterior fracture was for those in their thirties (anterior 18.6%, posterior 20.5%). The probability of an anterior fracture in all other decades was under 16%, and for posterior and posterolateral fractures in all other decades were less than 19%. Given an anterolateral fracture, the probability of the individual being in their fifties was highest (20.8%).

When considering fracture type, there is a high probability of an oblique fracture in obese individuals (42.5%) compared to a 25.3% probability of an oblique fracture in an

individual with normal BMI. The results of the chi-squared tests demonstrated significant relationships between incomplete fractures and multi-fragmentary fractures and BMI. In the healthy BMI group, the highest probability of incomplete fractures was in the healthy group (34.9%), followed by obese (33.9%). The BMI groups with the highest probability of multi-fragmentary were the obese (35.7%) and overweight (35.3%) groups. When further examining incomplete fractures with age, the youngest (39.4%) and middle age (31.4%) groups had the highest probability of incomplete fractures; in comparison the advanced group only had a 6% probability of exhibiting an incomplete fracture. Buckle fractures occurred most often in the anterolateral (62.3%) and anterior (27.5%) locations, compared to posterolateral (8.1%), and posterior (2.1%) locations. Furthermore, buckle fractures occurred most often in the two youngest groups: young (33.5%) and middle (33.2%) groups, compared to the older (27.2%) and advanced groups (6.2%). Multi-fragmentary fractures have the highest probability in older individual (41.3%).

Multiple Correspondence analysis

Multiple correspondence analyses (MCA) were conducted to depict underlying relationships among the data and visualize them via a biplot. A biplot is a two-dimensional representation of the variance within the data. Additionally, MCAs were conducted to further investigate the validity of previously identified important relationships. The more acute the angle between the variables (*i.e.*, how close they are in proximity) in the plots, the more influential the variables are to one another.

Age group and fracture type were used in the first analysis (Figure 5.16). The vertical line at zero separates the broad age groups; the middle age group is on the left, and the older, and advanced ages are on the right, while the young age group straddles the line. On the top half of the biplot are incomplete, buckle, simple, and oblique fracture types. Simple, incomplete, buckle, and oblique fractures are on the same plane as the young age group and their proximity emphasizes a relationship. Older and advanced broad age groups represent everyone 60 years and older. Close to the 60+ years individuals are displaced and multi-fragmentary fracture types. The middle age group is closer to displaced fractures. Incomplete and buckle fractures appear the furthest away from the axis, and therefore indicate that they are the best at discriminating between the data.

A relationship was observed within the chi-squared tests between COD and location and type of fracture. Figure 5.17 illustrates the relationships between location of fracture and COD. Posterolateral fractures occur in closest proximity to falls from height, and pedestrian-train incidences. The acute angle created by the proximity of these variables indicates an underlying relationship within the data. MVA and PVA CODs are found about equidistant from both posterolateral and anterolateral fractures, while anterior and posterior fractures are closest to MVA. However, the COD class of “other” and posterolateral fracture occur at a higher than 90-degree angle from one another, which indicates there is not a relationship between those two variables as chi-squared had indicated.

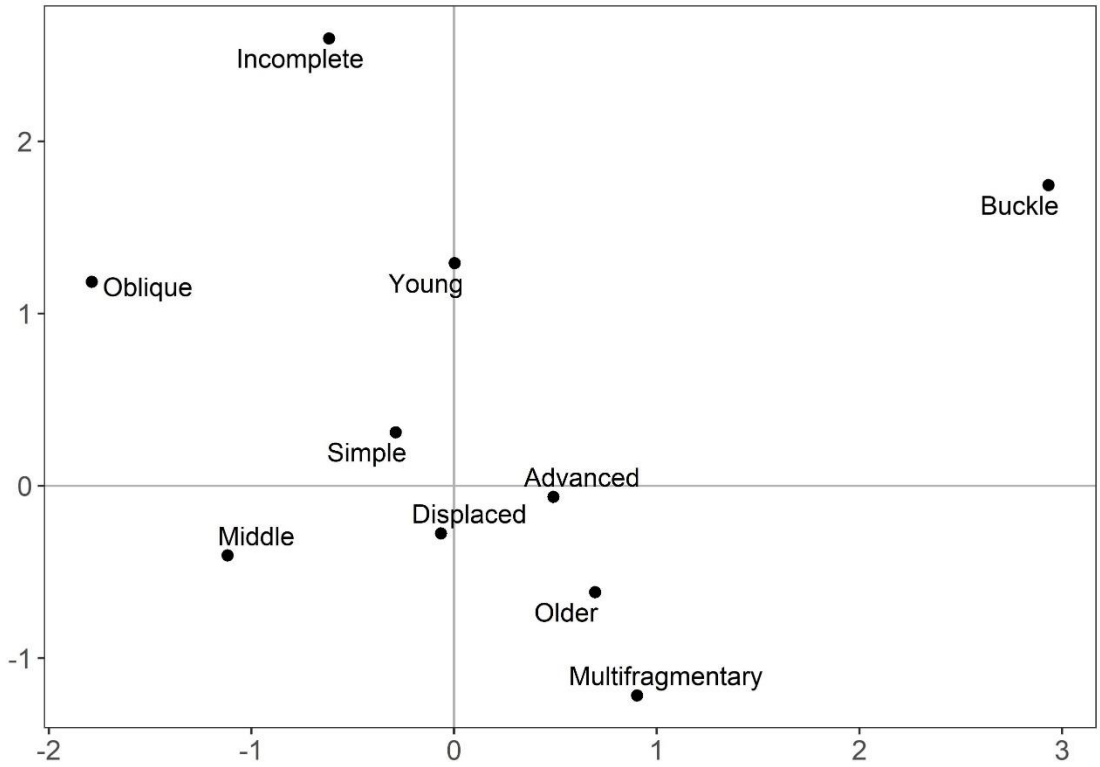

Figure 5.16. MCA biplot depicting the relationship between age group and fracture type, where the x and y axis represent the two principal components which describe the most variance in the data.

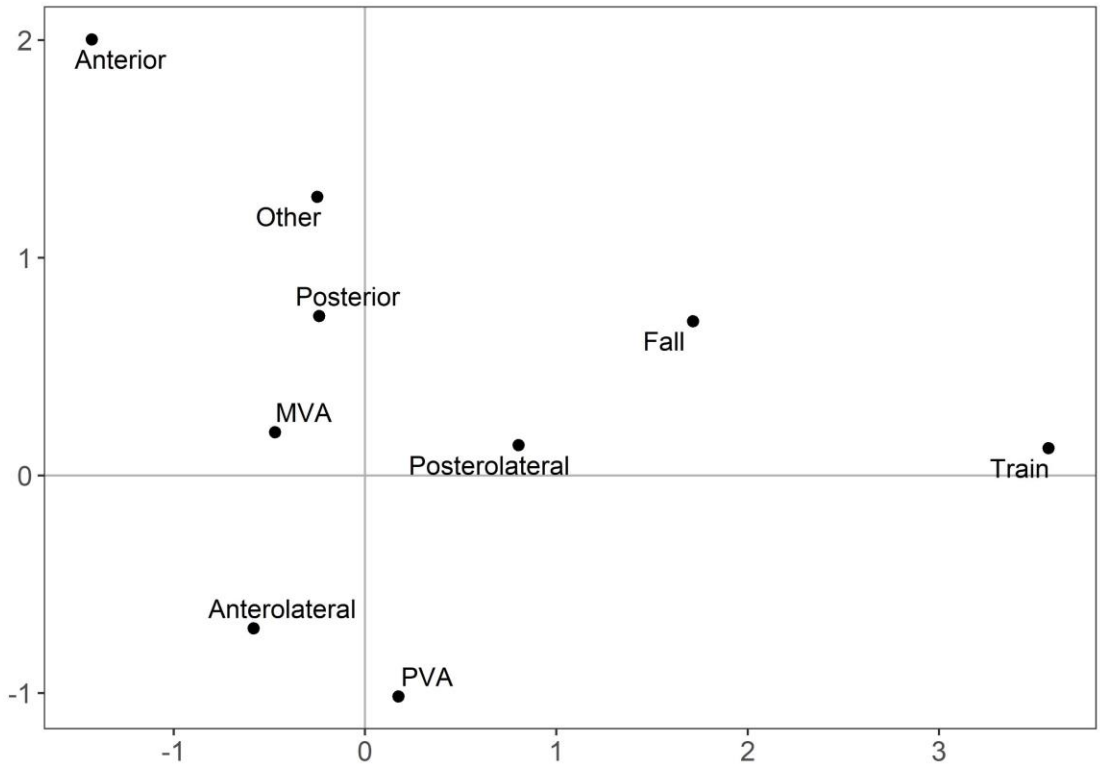

Figure 5.17. MCA plot depicting the relationship between COD and fracture location variables.

The MCA between COD and fracture type displays a MVA related COD being relatively close to all fracture types. Displaced fracture types are relatively similar distances to MVA, falls from height, and other COD types. The lack of distinguishable clustering within the biplot suggests the high number of MVA and PVA COD types, as well as the high number of displaced fractures may be influencing the results from the chi-squared (Figure 5.18).

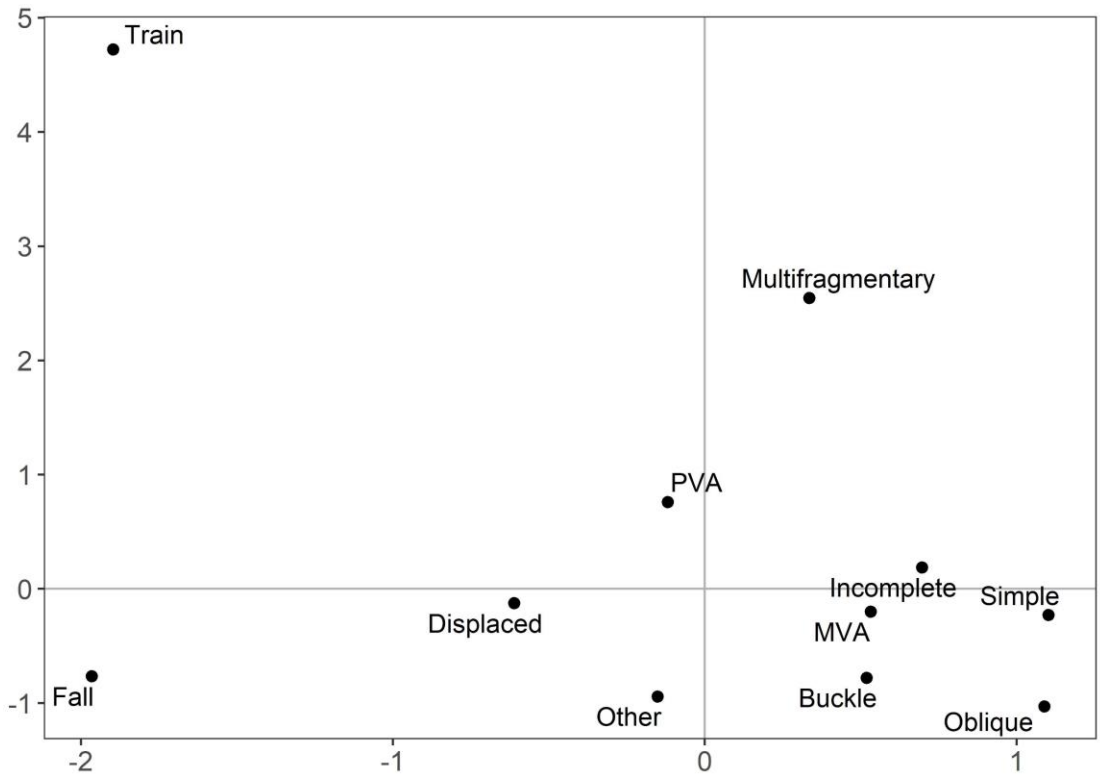

Figure 5.18. MCA biplot depicting the relationship between COD type and fracture type.

Fracture type and fracture location variables were used in an MCA analysis to observe if the underlying structure of the relationship supported previous analyses that indicated statistically significant relationships (Figure 5.19). The posterior location is closest in proximity to oblique and simple fractures, and the anterior location is closes to buckle fractures. Both displaced and multi-fragmentary fracture types are similar distances from posterolateral and anterolateral fractures. Incomplete fractures are closest to anterolateral fractures as well.

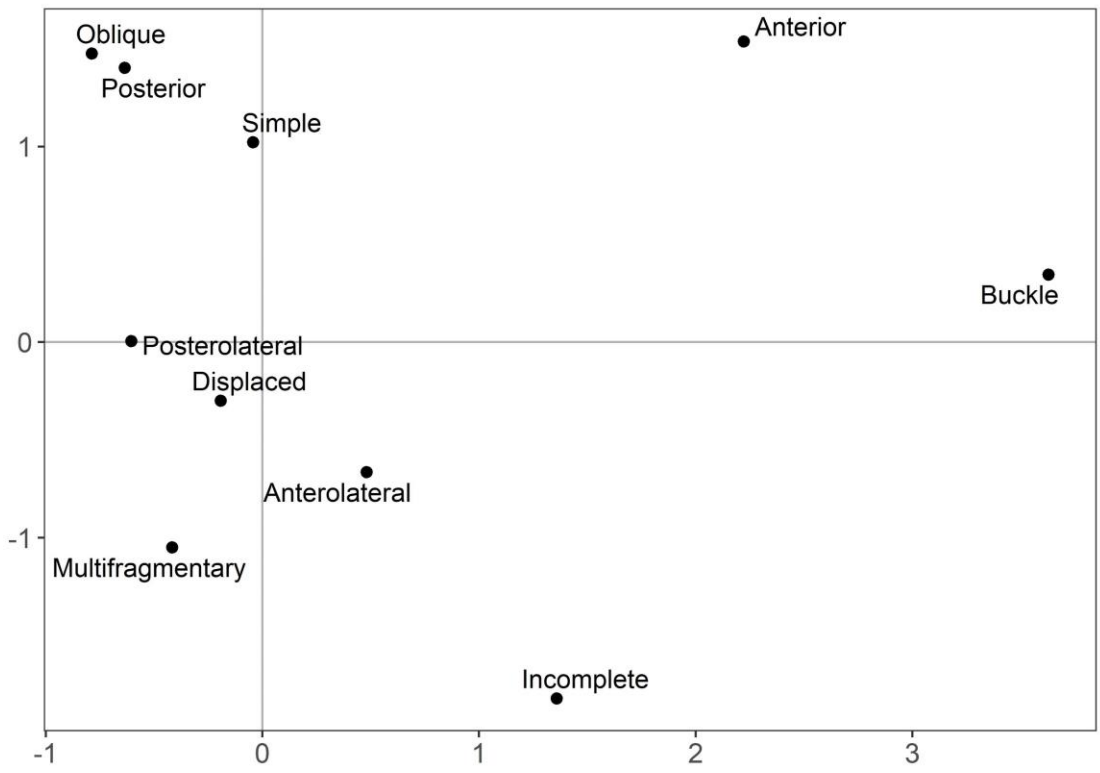

Figure 5.19. MCA biplot depicting the relationship between fracture type and fracture location.

MCA was then used to analyze the relationships among broad age categories and anatomical locations (Figure 5.20). Middle and young age groups are separated from older and advanced ages on the vertical axis. Older and advanced age groups are closer to the anterolateral fractures, where young individuals are closer to anterior and posterior fractures, and the middle-aged group is closest to posterolateral fractures. As there are clear separations between the quadrants it can be assumed that age is related to location of fracture in the data. The same analysis was performed on Age/Sex category and

anatomical location to observe any differences that might occur between the sexes. Some trends remained similar, such as both young male and female groups were closest to anterior fracture locations. Males in the middle age group remained closest to posterolateral, however middle-aged females were now grouped with advanced age females and older males, which were closest to the anterolateral fracture category (Figure 5.21).

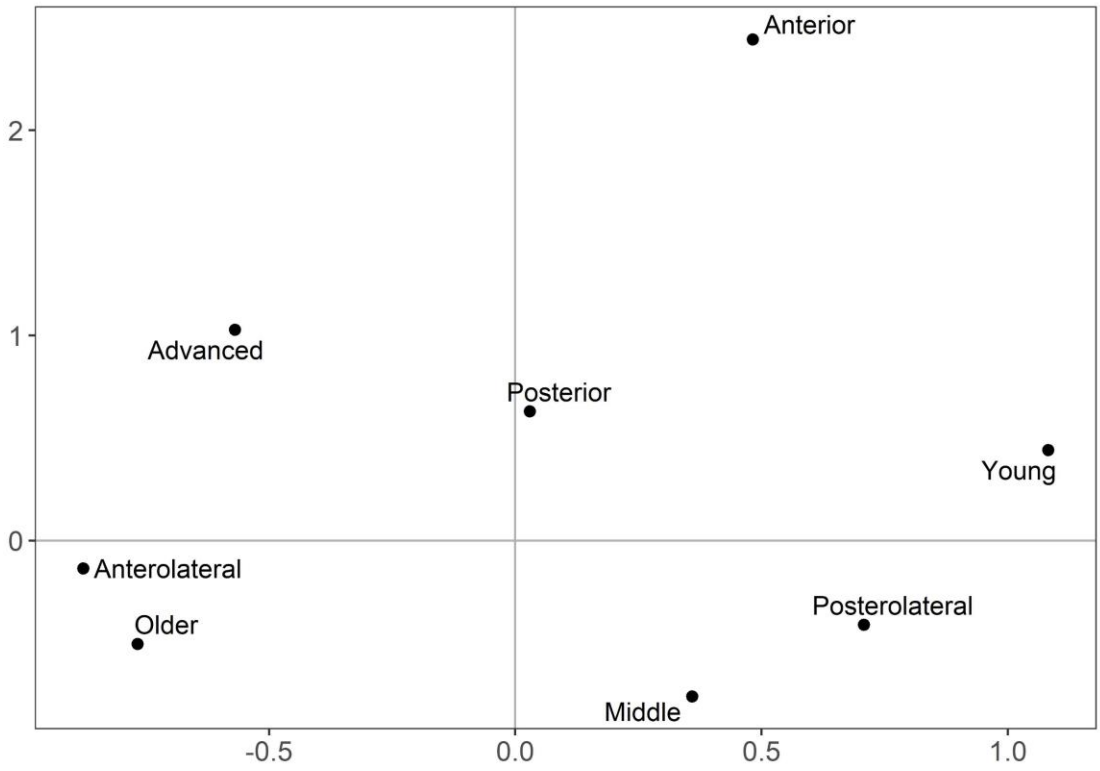

Figure 5.20. MCA biplot depicting the relationship between age group and fracture location.

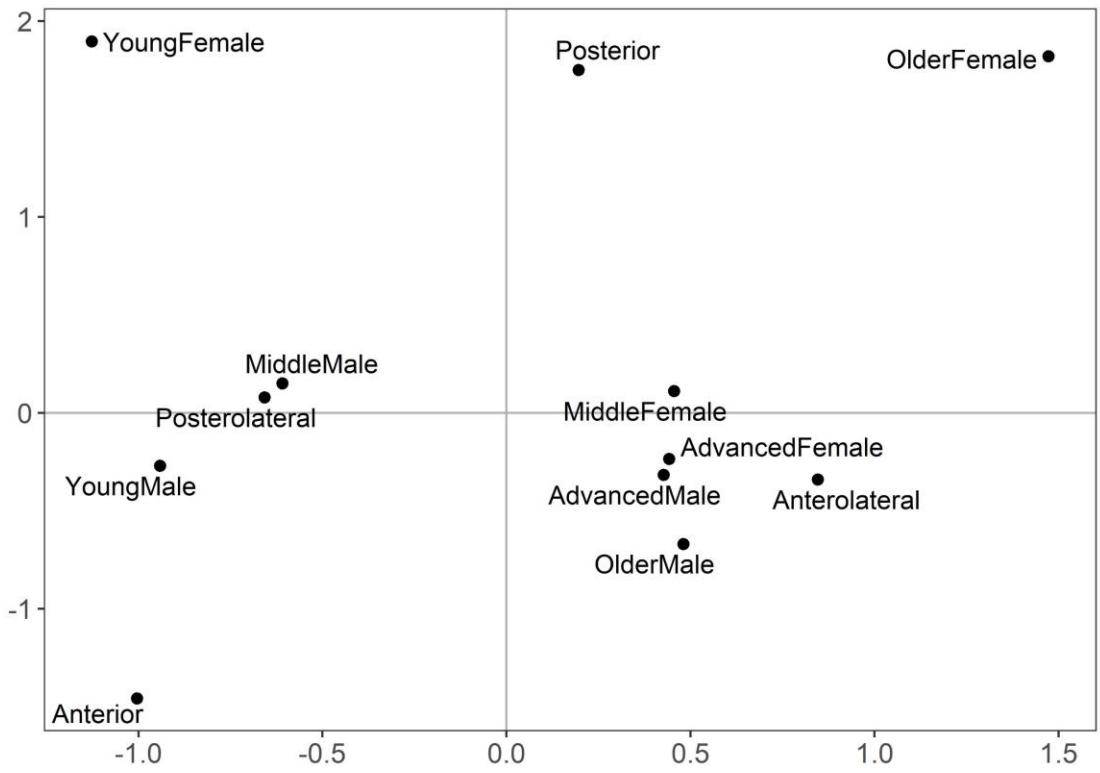

Figure 5.21. MCA biplot depicting the relationship between the combined age and sex variable, and fracture location.

BMI was then analyzed with fracture type (Figure 5.22). When projected on the coordinate plane, individuals classified as obese were very close to the 0,0 point, and close in proximity to displaced and simple fractures. Individuals classified as healthy were in the same quadrant as incomplete, and buckle fractures. Simple fractures also appeared in proximity to individuals classified as overweight.

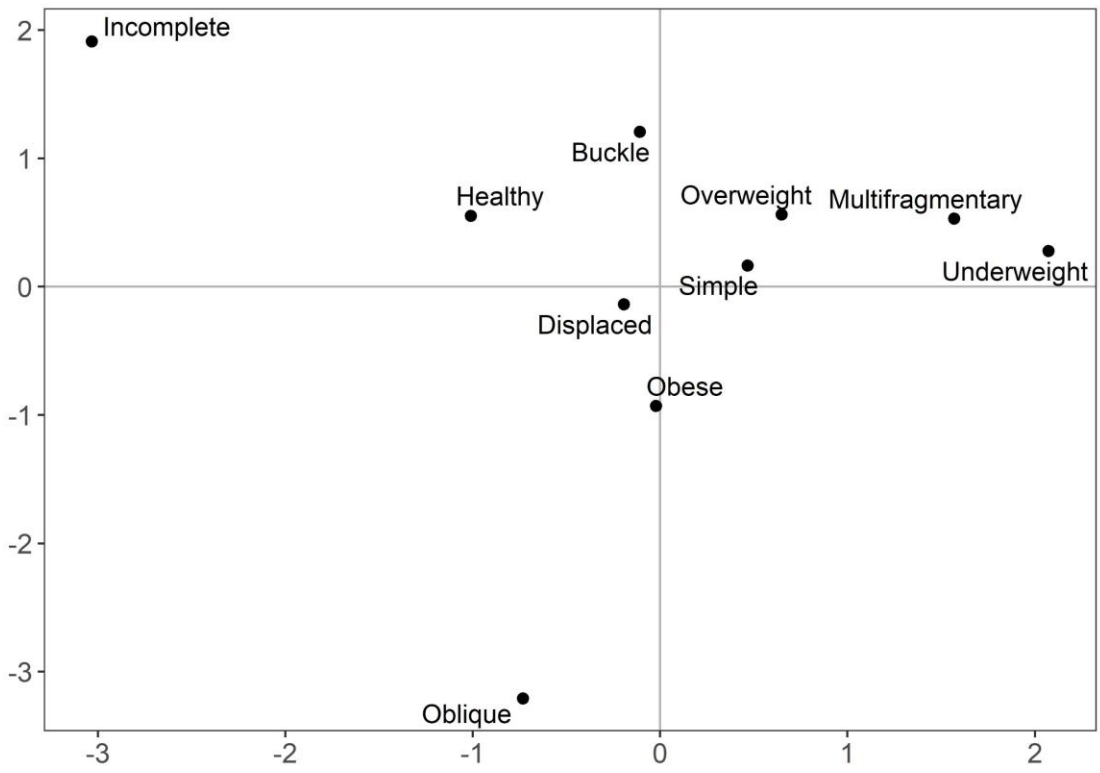

Figure 5.22. MCA plot depicting the relationship between fracture type and BMI variables.

Fracture location and BMI were then used in an MCA (Figure 5.23). The BMI categories were separated on the horizontal axis with overweight and obese on the right, and underweight and healthy on the left. Furthermore, they were then separated by the y-axis, with each category in its own quadrant. Posterior fractures appear in closest proximity to a BMI of obese, and anterior fractures appear in the same quadrant as overweight individuals. Based on the positions, the lateral anatomical locations are strongly linked with healthy individuals and then with underweight individuals.

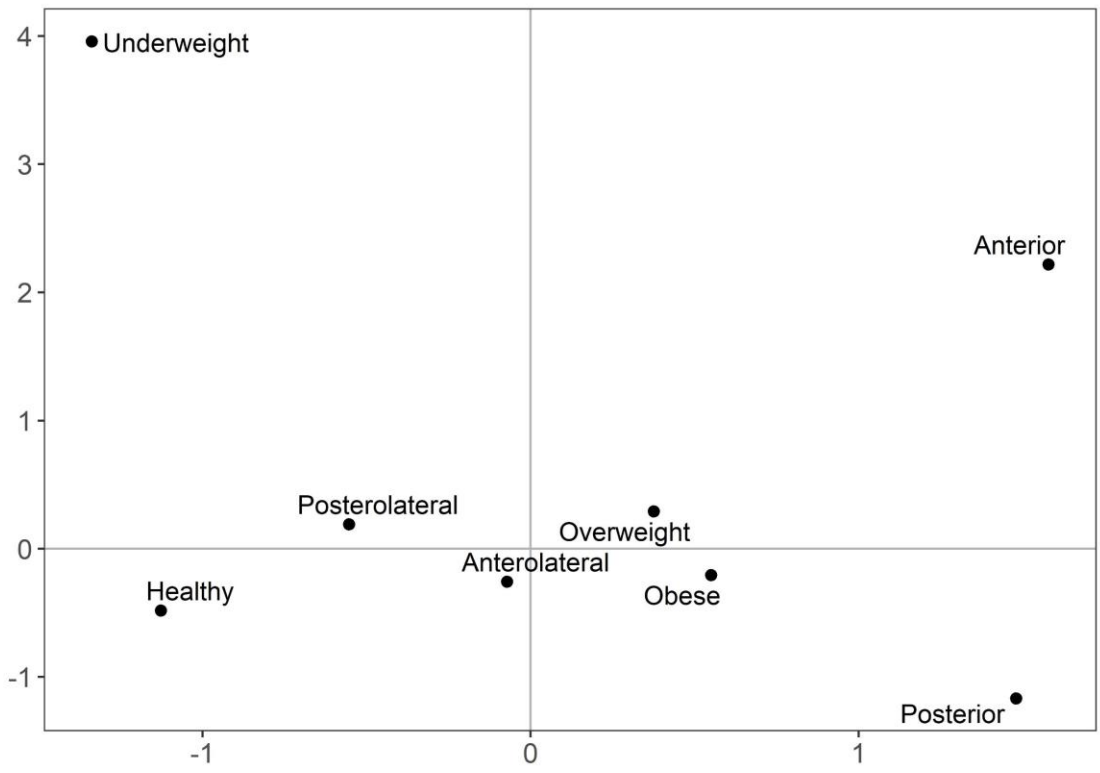

Figure 5.23. MCA plot depicting the relationship between BMI and fracture location variables.

Classification with Random Forest Analysis

Random Forest Analysis (RFA) was used to better understand the predictive power of MOD, COD, and the demographic variables in the prediction of location of fracture and type of fracture. Because of the high prevalence of fractures in the anterolateral and posterolateral locations (*i.e.*, they have a combined frequency of 81% of the fractures), the classes were clearly imbalanced, which could influence the results.

Classification algorithms attempt to minimize error rate, which in an imbalanced class can cause false negative and false positive classifications. To combat this, the sample was down-sampled. Down-sampling randomly subsets the sample so that the frequencies of the majority classes are comparable to those in the minority classes, rather than focus on minimizing error. Importantly, down-sampling can be done in RFA without data loss (Kuhn and Johnson 2013). The first RF model used location of fracture as the outcome variable (four levels) and age, sex, BMI, ancestry, COD, MOD, side, and fracture type as the predictor variables. The analysis was run using 500 decision trees and resulted in an accuracy of 56.89%. The model identified age (100%), side (23.15%), and sex (10.98%) to be the variables that contributed most to classification (Table 5-18).

A second RF model using location of fracture as the outcome variable was developed. This time, BMI was removed and replaced with weight (continuous) and height (continuous), while all other variables were kept the same. This model resulted in a classification accuracy of 56.48%. When exploring variable importance, the variable that was indicated to have the most importance within the model was weight (100%), age (91.17%), and height (64.1%) (Table 5-18). The confusion matrix illustrated a high misclassification between anterolateral and posterolateral locations. Therefore, anterolateral and posterolateral were collapsed into a single category of lateral. Anatomically anterolateral and posterolateral are sections of the body of the rib that have similar cross-sectional characteristics, therefore it was possible to collapse these variables without compromising the data. The predictor variables were age, sex, COD, MOD,

weight, height, side, ancestry, and fracture type. The classification accuracy increased to 67.49% and weight, age, and height were identified as the most important in classifying fracture location.

Fracture type classification through RFA was performed on similarly down-sampled data using 500 decision trees and age, sex, ancestry, COD, MOD, weight, height, side, and location of fracture to classify type. As there were so few observations of these data types, the classification sample excluded missing, and incomplete fracture types. The accuracy of this classification model was 50.0%. Weight, age, and height were again the variables identified by the model as most important in classification (Table 5-19).

Table 5-18. Random Forest Analysis for classification of fracture location.

	Predictor Variables	**Classification Accuracy**	**Variables of importance**
Location ***4 levels***	Age, Sex, BMI, Ancestry, COD, MOD, Side, and Fracture Type	56.89%	Age (100), side-right (23.15), sex – male (10)
Location ***4 levels***	Age, Sex, Ancestry, COD, MOD, Weight, Height, Side, and Fracture Type	56.48%	Weight (100), Age (91.2), Height (64.02)
Location ***3 levels***	Age, Sex, Ancestry, COD, MOD, Weight, Height, Side, and fracture type	67.49%	Weight (100), Age (90.5), Height (63.20)

Table 5-19. Random Forest Analysis for classification of fracture type.		
	Predictor Variables	**Classification Accuracy**
Type ***5 levels***	50.0%	Weight (100). Age (97.9), Height (72.4)

Chapter 6. Discussion

A large, geographically diverse, retrospective sample of rib fracture data of this magnitude has never been accumulated in forensic anthropological research prior to this project. This sample was comprised of 1,415 individuals from six states across the United States resulting in 24,853 documented rib fractures. This study is the first to expose large scale rib fracture patterns, to provide foundational statistical analyses to facilitate interpretations of rib fractures, and to associate and corroborate trends between experimental and retrospective research designs. By exposing the expected fracture patterns, it also provides an opportunity to reveal unexpected or unique fracture patterns. Knowing the interrelationships of the variables, both the normal and less common, can be considered by practitioners and may help in interpretation of fracture patterns. The probabilistic statements can be used to further help practitioners substantiate interpretations, move beyond description and observation, and clearly demonstrate the strong relationship between biomechanical principles and likelihoods of fracture characteristics. A discussion about the pertinent findings, advice and limitations for interpreting rib fractures, and options for application and future avenues of research are addressed below.

Common Injury Patterns: What is normal?

While every fracture level variable was present in the data, there were obvious trends that revealed normal patterns. *Ribs three through seven were the most frequently fractured, anterolateral and posterolateral were the most prevalent locations of injury, and there were more displaced and simple fractures than any other type of fracture.* The mean number of fractures exhibited per person was 16. The loess line in Figure 5.8 displayed a positive slope between 20 and ~35 years of age, but then plateaued and was not impacted by increased age.

The high number of rib fractures per individual in the current study may be reflective of the deceased population from which the data were collected. Research on rib fractures in medical literature has indicated that rib fractures are associated with mortality in approximately 10% to 12% of patients (Jentzsch et al. 2020; Sharma et al. 2008). These studies also indicated a linear relationship between higher number of rib fractures and mortality; usually there is a high likelihood of mortality with over ~5 rib fractures (Sharma et al. 2008). Other potential idiosyncrasies of this sample have to do with fracture location. While this sample incurred fractures most frequently on ribs three through seven, medical literature indicates the most common rib fractures are located on ribs seven through ten. Again, this difference between the current study and clinical literature could suggest a difference in living versus deceased samples, which also further substantiates the relationship between mortality and rib fractures (Vavalle et al. 2013; Poole and Myers 1981). Clinical literature also suggests mortality associated with rib

fractures increases with certain covariates, such as age and obesity (Abdulrahman et al. 2013; Elkbuli et al. 2021). While the age distribution in the sample is relatively normal and not left-skewed to incorporate a larger number of older individuals, the higher number of overweight and obese individuals may contribute more to higher mortality rates associated with blunt force thoracic trauma.

Interestingly, the number of fractures per individual did not increase as age increased and the number of fractures by age did not differ by sex. However, females in the advanced age group had similar patterns to males in the older age group, which indicates that earlier onset osteoporosis in women might be influencing likelihood of fracture (Alswat, 2017). There were an extraordinary number of fractures per individual though, which is again likely linked to mortality and collecting data from a deceased sample.

Fracture Characteristics

Rib Number

Overall, normal fracture patterns for this dataset were determined to be on most of the true ribs (three through seven) and the least number of fractures were located on ribs one, eleven, and twelve. While the most common rib fractures in living individuals were on ribs seven through ten, there still existed a high frequency of fractures on ribs three through seven were reflected in other real-world based studies, specifically, they occur

regardless of differing mechanisms of fracture, such as from physical activity (McDonnell, Hume, and Nolte 2011) or impactions and CPR related fractures (Kang et al. 2021; Yang, Lynch, and O'Donnell 2011). As "true" ribs have direct articulations with the sternum, the points of constraint caused by these articulations might influence their ability to deflect stress when under loading conditions. Furthermore, on average cortical bone is thinner on ribs three through seven, which could contribute to a lack of stiffness (Lynch 2015). Experimental research has shown that ribs closer together in the rib cage often fracture similarly, as the geometry of closer ribs are more similar to one another, while those further away from each other within the rib cage fracture in dissimilar ways (Kemper et al. 2005). Ribs three through seven share many similarities in shape and articulation, and subsequently it can be concluded that they would fail similarly.

Ribs one, eleven, and twelve were fractured least often in this dataset. These three ribs are the most abnormal in size, cross section, and shape in comparison to the rest of the ribs and are the most superiorly and inferiorly located ribs. Furthermore, their anterior articulations differ comparatively to the rest of the rib cage. Ribs eleven and twelve have no anterior articulation, and the anterior articulation of the first rib is a synchondrosis, not a cartilaginous joint. The anatomy of the first rib is wider anteriorly to posteriorly with thicker cortical bone, and tight articulations both anteriorly and posteriorly. This may indicate that it is less susceptible to strain under anterior loading, as can occur during an MVA. Ribs eleven and twelve have no anterior articulations and therefore do not

experience stress in the same manner as the rest of the rib cage. Furthermore, the direction of loading may be different applied to the lower ribs in comparison to non-floating ribs. With these three ribs being the most superior and most inferior in the rib cage, it may indicate they do not incur direct loading during impaction, and other variables may be involved in fracture of these ribs. *Interestingly, weight was the only continuous variable found to have a significant relationship with rib number. Individuals who were classified as obese had more fractures to ribs eleven and twelve; specifically, probability of fracture to rib eleven is 67.1% in obese and overweight individuals in comparison to 25.9% in healthy BMI individuals, and the probability of fracture to rib 12 is 71.3% in obese and overweight individuals compared to 24% in healthy BMI individuals.* In a study by Ejima et al. (2017), obese individuals had a higher frequency of fractures in lower ribs. Therefore, the relationship between a larger body size and increased stress on the lower ribs is plausible.

Fracture Location

Anterolateral and posterolateral locations incurred the most fractures for all groups throughout the entire sample. The high frequency of fractures to these locations is not surprising as these two locations make up a large section of the rib and constitute the entire rib body. Furthermore, cross-sectional geometry remains largely consistent along the body of the rib whereas it is drastically different than the anterior and posterior locations. Because the rib cage is an enclosed unit there are no articulations to provide buttressing along the rib bodies when loading is applied, subsequently stress may be

deflecting laterally from the points of constraint anteriorly and posteriorly. Notably, lateral locations on the rib are also found to incur a high amount of fractures in other real-world and bioarcheological contexts and experimental research (Agnew et al. 2018; Agnew 2015; Crandall, Nathens, and Rivara 2004; Matos 2009). Therefore, the rib body can be interpreted as being more susceptible to fracture than the anterior and posterior locations.

The ‘lateral’ section of the ribs makes up most of the length of the rib and it is possible that if the number of anatomical locations on the body was increased, then the results could glean even more nuanced information. As is, the location categories most likely do not capture the anatomical differences that mitigate stress and strain to these locations. However, the current definitions were created from osteologically identifiable locations and are used regularly in rib trauma research (*e.g*., Ritchie et al. 2006; Love et al. 2013; Agnew et al. 2018). As there is always a balance in research design, additional locations could have also caused lower kappa values as there are few markers on the rib body to indicate a new section.

Because of the high number of fractures in the lateral sections, the greatest interpretative impacts are linked to posterior and anterior fractures. Anatomically anterior and posterior locations vary from the body of the rib and from each other in substantial ways. The posterior rib has thicker cortical bone and tight (supportive) articulations with the vertebral column. The anterior ribs are often wider and possess more trabecular bone with flexible anterior articulations to the costal cartilage. Because these anatomical areas

exhibited less fractures than the lateral locations, it became essential to better understand which variables may contribute to fracture.

Anterior fractures were found to be significant with age within the dataset. This may indicate that the change in material properties of bone with age may be more apparent in the anterior portion of ribs than other anatomical locations. *A strong negative relationship between trabecular bone structure and age, and increased trabecular atrophy with age, leads to a logical assumption that the portion of the rib with the greatest ratio of trabecular bone to cortical bone may be more impacted by age than other rib locations with a lower ratio of trabecular bone to cortical bone (Weinstein and Hutson 1987; Majumdar et al. 1997).*

Posterior fractures were found to be more common in instances related to large body size; individuals with posterior fractures had 42.6% probability of having a BMI category of obese. For example, the rib cage morphology of an obese individual changes to accommodate additional fat tissue, which causes ribs to lie more parallel to the transverse plane and consequently incur a higher number of fractures (Ejima et al. 2017) (Figure 6.1). Furthermore, Agnew *et al.* (2018) showed a decrease in peak yield strength in the ribs of obese individuals compared to underweight and normal BMI individuals. *The material and structural differences that occur in the bones of obese individuals, and the higher amount of stress associated with a higher BMI, may be increasing the likelihood of fracture in the posterior location.*

Fracture Type

All fracture types were present in the dataset, but the most common fracture type was overwhelmingly displaced fractures. Displaced fractures have been shown to have a relationship with high speed impactions, especially in relation to MVAs (Scheirs et al. 2018). The high prevalence of MVAs in the dataset could be influencing the high frequency of displaced fractures in the dataset. Yet, there were high frequencies of displaced fractures associated with falls from height, PVAs, and other COD types. This indicates that displaced fractures are common across the most frequent CODs. Displaced fractures also had a significant relationship to broad age group in the chi-squared analyses and the MCA depicted displaced fractures closest to older individuals and relatively distant to all other age groups. Unfortunately, no age group had a substantially higher conditional probability for a displaced fracture because it was common for all age groups.

Displaced fracture was chosen to be used as a fracture type because of the frequent use of it in the clinical literature, including in the medical examiner's office, to describe a fracture. Some literature discusses the connection between severity of injuries and the number of displaced fractures (Chien et al. 2017). Additionally, displaced fractures are linked to injury severity on the AIS scale, which is used in trauma research and vehicular accidents (Gennarelli and Wodzin 2006). Considering its use in clinical literature and its link to severity of injury, it was retained as a unique fracture type.

However, this may have resulted in a few limitations and therefore a catalyst for modifying future research. First, displaced is not usable for all forensic anthropology practitioners since there are analyses conducted on skeletal remains; displacement is not recordable once there is loss of soft tissue. Second, simple and oblique fractures can be categorized as being displaced or non-displaced. Therefore, 'displaced' should be a discrete feature of the fracture but not the sole fracture characteristic. Future research may benefit from displaced being a binary characteristic that is supplemental to fracture types of simple, oblique, multi-fragmentary, wedge, *etc*. In the current study, the chi-squared tests only showed a significant relationship with COD and simple (non-displaced) fractures; the conditional probability of an individual incurring a simple fracture from an MVA was 59.8%. A different classification scheme for 'displaced' should be considered in future research as it may lead to greater understanding of simple and oblique fractures and other covariates.

The fracture types that were less common in the dataset (*e.g.*, oblique, buckle, and multi-fragmentary fractures), revealed how age influences fracture type. All "abnormal" fracture types had significant relationships with specific age groups. The young age group had the highest conditional probabilities of incurring a buckle fracture (26%), incomplete fracture (29%), or oblique fracture (25%). Studies have shown that ribs of younger individuals have the ability to resist more force before fracture (Kang et al. 2021; Jingwen, Rupp, and Reed 2012). Furthermore, Larsson et al. (2021) observed that there is a general 10% decrease in the amount of strain an individual's ribs can undergo

without failure with each increasing decade. *Therefore, it is reasonable that the higher elasticity of ribs in the youngest age group is associated with incomplete and buckle fractures and the less resilience in older individuals is what leads to the conditional probability of those exhibiting multi-fragmentary fractures (54.5% in those over 55 years old).* Notably, the advanced age group was not associated with the highest probability of any fracture type; however, the MCA plot (Figure 5.16) clearly suggest that multi-fragmentary fractures are more associated with older and advanced age groups than any other age group. Agnew *et al.* (2018) noted the reduced ability to withstand strain in older individuals. *Therefore, it stands to reason those fractures in older individuals are not necessarily more severe, as some may assume multi-fragmentary fractures would indicate; in fact, older individuals may just present with skeletal elements with a lower yield point, and comparably the bone undergoes less strain before failure.*

Buckle fractures have been stated in the literature as occurring more often on the anterior portion of the rib (Yang, Lynch, and O'Donnell 2011; Love and Symes 2004). The current study corroborates the claims and provides probabilistic statements to demonstrate its likelihood of occurrence. *A buckle fracture has a 27.6% probability of occurring anteriorly and a 62.8% probability of occurring anterolaterally, and a 7.9% probability of occurring posterolaterally and a 1.7% probability of occurring posteriorly***.** While this statement clearly demonstrates the differential relationships with fracture types and location, one cannot discuss anterior fractures, without discussing CPR and CPR-related fractures. Research suggests that approximately one-third of individuals who

receive CPR incur rib fractures (Kralj et al. 2015) and the fractures initiating because of CPR are 7.8 times more likely to be incomplete or buckle fractures than those incurred via MVA (Scheirs et al. 2018; Yang, Lynch, and O'Donnell 2011). Of those individuals on whom CPR was performed, only a small number had recorded CPR related fractures. Very rarely was fracture data provided if fractures were related to CPR or the COD related incident. In the instances that CPR fractures occurred they were usually recorded separately to the rest of the perimortem trauma in the autopsy report. Because CPR related fractures are not considered related to the COD, it is possible the pathologists did not record them, and therefore it is unlikely that many of the fractures recorded in this dataset are reflective of CPR. Therefore, CPR related fractures most likely do not constitute a large portion of the fractures in the dataset and the buckle and incomplete fractures that are present are likely because of trauma and not CPR. However, if future research could obtain CPR information for their entire sample, the trends would be verified.

Variable Influence on Fracture

Demographic variables relating to age and body size had significant relationships with all fracture variables. The continuous variables of age, weight, and height, and their categorical counterparts also had the highest conditional probabilities on the presence, type, and location of fracture. This was substantiated in the RFA analysis, which revealed

that age, weight, and height offered the greatest contributions to the classification of fracture location. *Together these results indicate that fracture presence, location, and type are more related to the material properties and anatomy of the ribs than the incident that caused the fractures. Therefore, knowing the biological profile and BMI of an individual can aid in determination of normal or abnormal fracture patterns. The strong relationship between location and fracture type and the phenotype, could also suggest the trauma data may be informative in estimating components of the biological profile*. More broadly, these results implore anthropologists to incorporate biomechanical principles in trauma analysis. The incorporation of biomechanical principles has been suggested in most publications on blunt trauma (*e.g*., Symes et al. 2012; Daegling et al. 2008; Galloway, Wedel, and Zephro 2013; Love and Symes 2004); however, the authors are overwhelmingly referring to analysis of tension and compression. Even then, word choice is misleading and anthropologists should refer to tensile and compressive stresses experienced by the bone (Yamada and Evans 1970). *In contrast, biomechanical principles are referring to the structural geometry and material properties of the bone, which can predominantly be informed by the age and health of the individual.*

To date, trauma analysis in forensic anthropology largely focuses on the description of fractures, and what can be interpreted from the observable patterns (*i.e.*, speed, implement, etc.). This research indicates that interpreting the implement or scenario of blunt force trauma to the ribs, as is often attempted in forensic anthropology with long bones or cranial trauma, might not be feasible with ribs. The anatomy,

structural geometry, and material properties of ribs are specifically suited to protect the thoracic viscera and therefore *should* function differently than other skeletal elements with different functions (*i.e*., skeletal movement). *The material properties, and structural geometry of bone ultimately dictate its response to applied loads, and ultimate failure, which in practice are what anthropologists are dependent on for trauma interpretation. This research indicates that trauma research should not solely be focused on the speed at impact or fracture characteristics, but instead take a more holistic view of the individual, their health, size, and the function of that bone to study trauma in the future.*

Bone biomechanics are dependent on material and structural properties, which is inherently linked to the individual. Historically, anthropologists would have linked severity of injury to type of fracture and number of fractures (*e.g.*, Galloway, Zephro, and Wedel 2013). However, this research has highlighted that a large portion of the algorithm that has been ignored is the individual features of that bone itself. Material properties have been found to be consistent within an individual, across all ribs (Li et al. 2010). Therefore, we can now interpret that an increased number of rib fractures indicates changes in structural geometry and material properties of bone related to with age or body size (Mccreadie and Goldstein 2000; Agnew 2015; Shi et al. 2014). The variables that were combined to best represent health and phenotype of an individual (*i.e.*, age, sex, and BMI), were shown to have significant relationships with the presence, type, and anatomical location of fractures. For example, as an individual ages their rib cage shape changes; therefore, the structural geometry of the bone changes (Shi et al. 2014). In

Figure 6.1 the change in general shape and furthermore, the material properties (visible through image quality/transparency) with age can also be noted between the middle-aged individual and the advanced age individual. Specifically, within this research, age had a significant relationship with most types and locations of fracture.

An original intent of this research was to identify common fracture patterns based on the death incident, as is done in epidemiological research. Previous research has demonstrated that MOD is strongly correlated with injury patterns and specifically what skeletal elements are impacted (Hulse, Stull, and Knight 2021). Essentially, thoracic injuries are most associated with accidental deaths and blunt force trauma (Prahlow and Byard 2012), which contributes to understanding the overwhelmingly large number of accidental deaths (87%) compared to all other MOD classifications in this dataset. Considering the MOD was not controlled for, this pattern illuminates the striking relationship between blunt trauma to the thorax and accidental deaths. While this relationship is not novel (e.g., Hulse, Stull, and Weaver 2018; Prahlow and Byard 2012), it does yield its own probabilistic statement: there is a probability of 82.7% that fatal blunt trauma to the chest is associated with a MOD of accident.

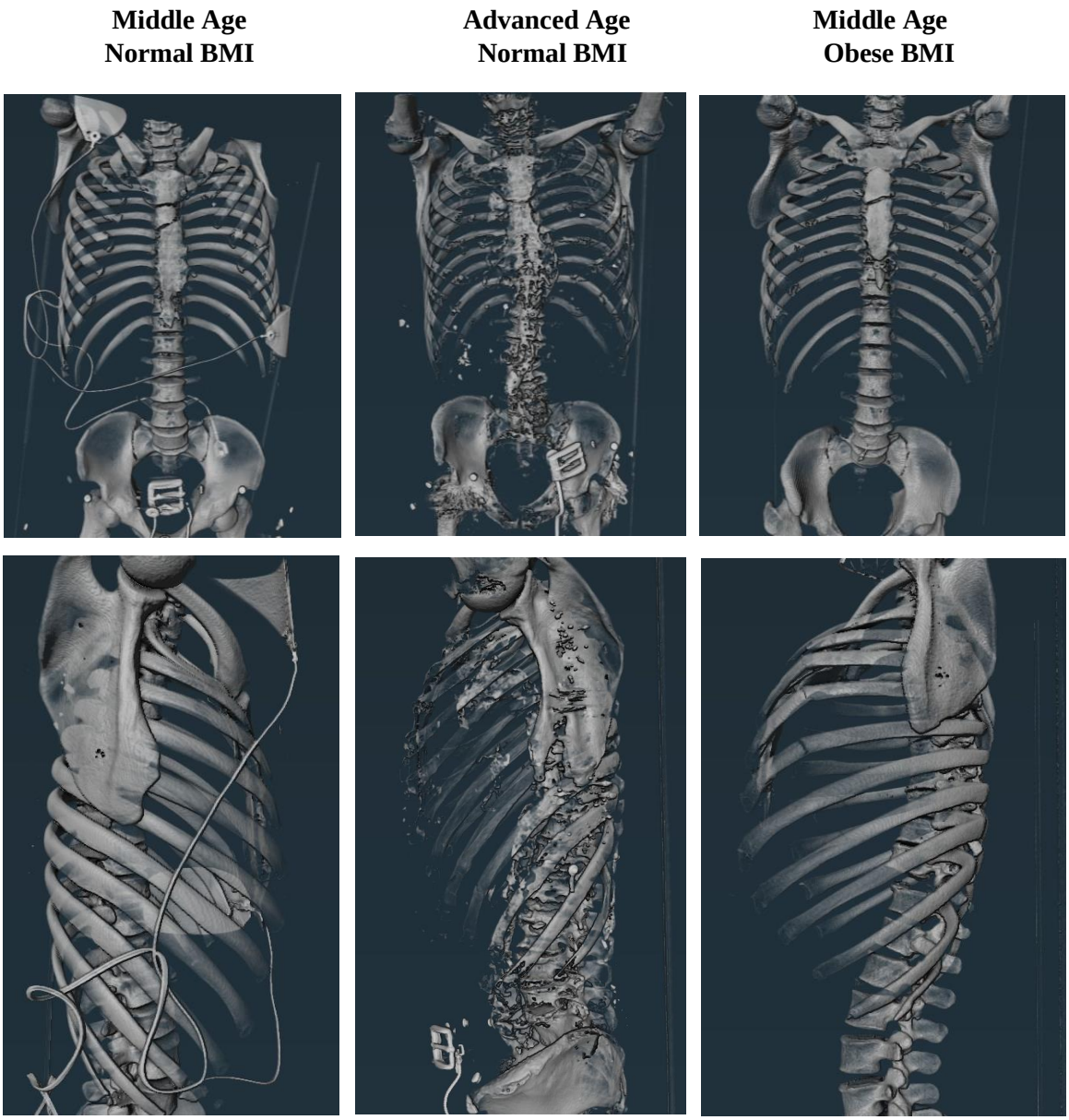

Figure 6.1. Examples of volume rendered CT images used for data collection. On the far left is an example of a middle-aged individual in the healthy BMI category. The middle images depict an individual in the advanced age group of normal BMI, and the far right images depict a middle age individual in the obese BMI category.

In contrast to MOD, COD was significant for both type and location of fractures, but further explorations did not reveal any notable patterns. These relationships, or lack thereof, were also apparent in the RFA results, which had higher variable importance scores for demographic variables than the death incident variables. These results are not terribly surprising in the lens of biomechanics. *The injury mechanism has significant relationships on anatomical location of the injury (broadly, not within the ribcage) (Hulse, Stull, and Weaver 2018), but the fracture characteristics are related to the material and structural properties of the bone, which are influenced by demographic variables.*

Tools for Substantiation

Recommender System and tRauma

In conjunction with this research, a graphical user interface (GUI) called "tRauma" was created using R (R Core Team 2021a). The GUI houses the dataset and allows users the ability to manipulate the data thereby letting anyone explore the data as they see appropriate. tRauma utilizes multiple content filtering techniques to filter rows and/or columns based on the user's needs and then will subsequently visualize the data through a heat map or bar chart (Figures 6.2-6.4). The heat map is organized into a general homunculus/anatomical form and provides counts and distributions of rib fractures per rib number and location. The bar charts visualize counts based on one or

two demographic variables of interest that are specified by the user. After the user inputs the variables of interest, the secondary function of tRauma is to use a recommender system algorithm to return the top five most similar rib trauma cases from the database (Figures 6.2-6.4). The GUI was made freely available for students, researchers, and practitioners through the shinyapps.io.

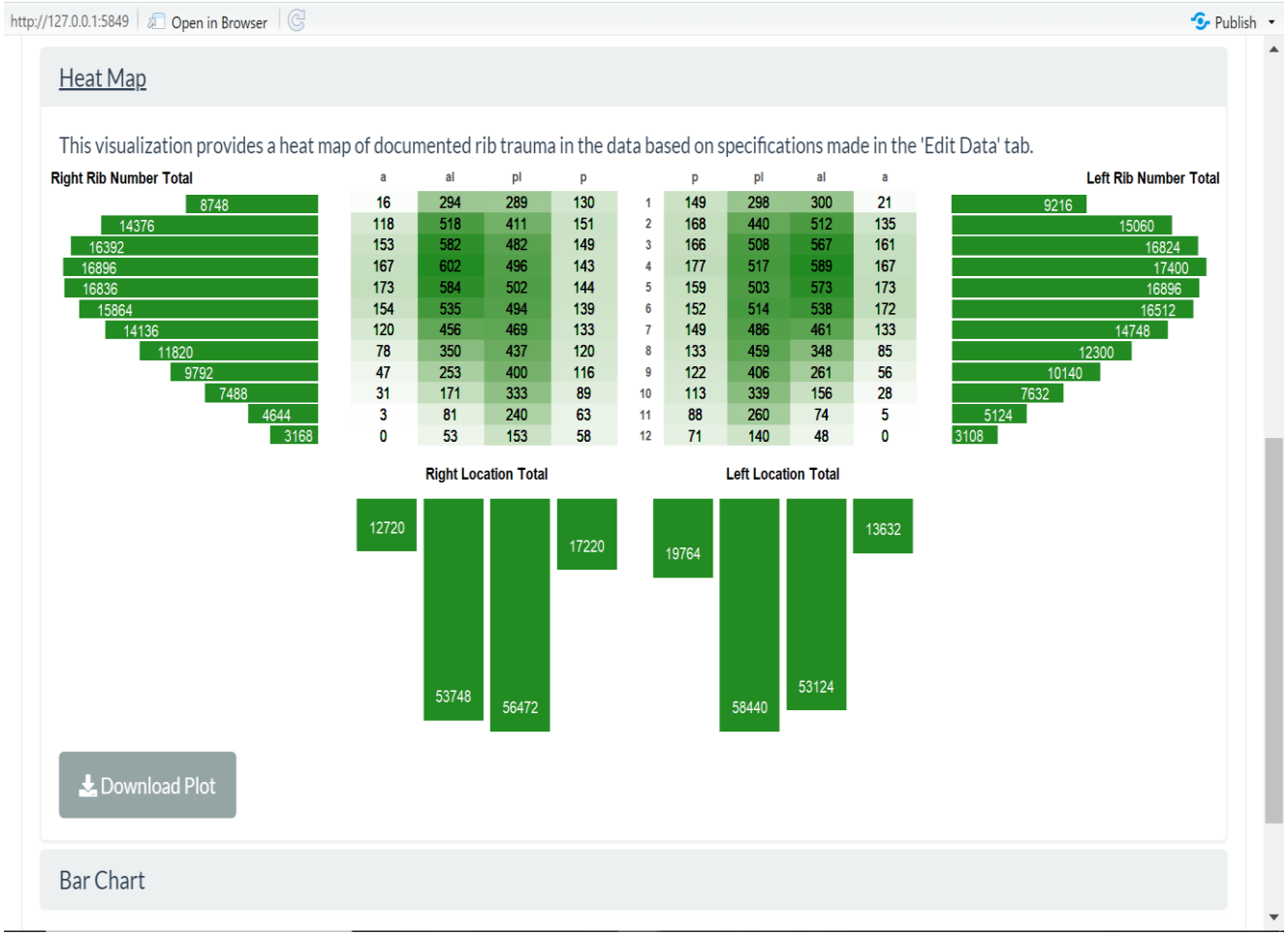

Figure 6.2. A screen capture from the tRauma GUI which illustrates an example of the heat map feature. The heat map illustrates the most frequently fractured locations, and the count of fractures per rib number, and anatomical location, based on the variables the practitioner has input.

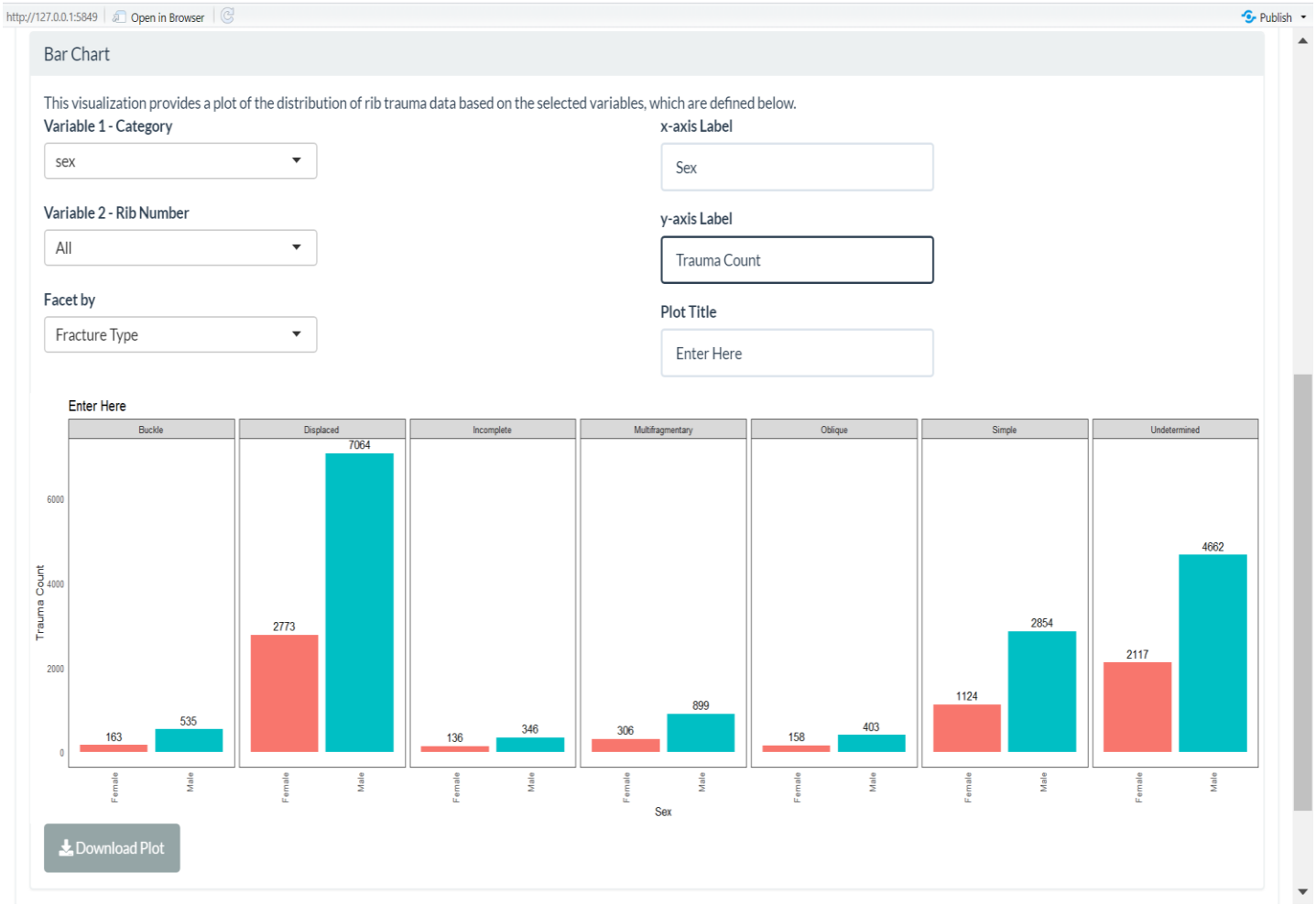

Figure 6.3. A screen capture indicating the bar chart feature within tRauma. The practitioner can specify demographic variables they wish to explore and bar charts of all relevant information.

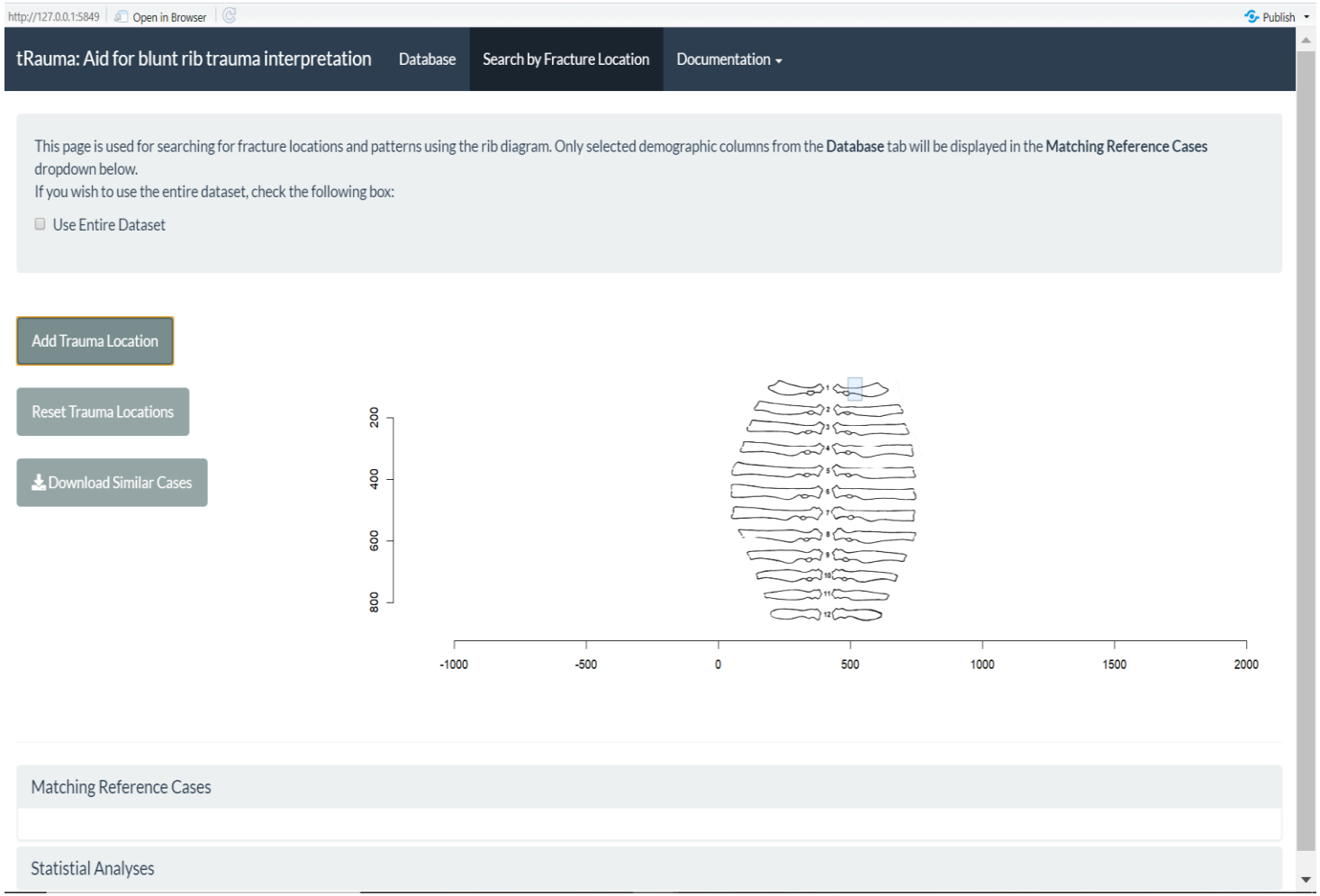

Figure 6.4. Screen capture of the rib homunculus where a practitioner can map exact fracture locations and the recommender system within the tRauma will return the most similar cases in regard to fracture location and demographic variables.

Substantiation of Anecdotal Claims and Experimental Research

A substantial outcome of this research is that it corroborates and substantiates many instances of anecdotal findings from case studies or concepts noted during experimental rib trauma research. For example many experimental studies have shown the anterolateral locations to be the most commonly fractured location in three point bending and impaction tests of individual ribs (Daegling et al. 2008; Agnew 2015; Agnew et al. 2018), which is also what was found in the current study. Additionally, the results of this study reflect the research conducted in other fields and has reached similar conclusions as to how an individual's health, age, sex, and other demographic variables are influencing bone fracture. Research on experimental impact trauma and fracture simulations with software such as the Global Human Body Model Consortium or similar human modeling have been focused on demographic variables as a main component of fracture presence and variability (Mccreadie and Goldstein 2000; Agnew 2015; Ejima et al. 2017; Gayzik et al. 2008; Kang et al. 2021; Jingwen, Rupp, and Reed 2012; Schafman et al. 2016; Vavalle et al. 2015; Agnew et al. 2018; Shi et al. 2014). The influence of varying demographics on fractures and injury has always been an object of study in epidemiological and medical research (Ottochian et al. 2009; Brahmbhatt et al. 2017; Hoffmann et al. 2012; Newell et al. 2007; Stillion and McDowell 2002; Beck et al. 2000; Chuang et al. 2016; Mccreadie and Goldstein 2000; Lynch 2015; Carter et al. 2014, *etc.*).

The high agreement of identified patterns between experimental trauma and this research also indicated that experimental research might be more analogous to real world trauma scenarios than previously thought. As such, this study brings to the forefront that trauma analysis in forensic anthropology should follow in the example of experimental and medical literature and research how demographic and health variables influence biomechanics of fracture, which could provide better insight to downstream interpretation of fracture characteristics and patterns. Minimally, the comparable findings suggest that experimental trauma and cross-sectional data could be combined to increase power and verify findings.

Limitations, Considerations, and Future Directions

As with all research, some limitations were inherent to the research design and the mediums used to collect the data. The research was designed to try to collect as much data relevant to the intrinsic and extrinsic variables as possible, such as health information, contributing factors to death indicated by the pathologist, if resuscitation was attempted or not, *etc*. While there are standard variables reported in every autopsy, there are also idiosyncrasies with each death event, which are recorded differently across medical examiners offices and forensic pathologists. Therefore, many variables were collected in the current study only if present in the autopsy report and associated

documents. Subsequently, there was much missing data for the superfluous variables that limited statistical analyses.

A large portion of this data relied on imaging modalities that have their own advantages and disadvantages. There is always a possibility that some fractures were not reported in the autopsy report and/or obscured from view in the photographs for verification. Because the pathologist's report was ranked highest in terms of fracture identification/verification, it was rarely the case that a fracture was recorded solely based on imaging. In contrast, the NMDID data collection was entirely based on the rendering of the CT images and a full evaluation of the ribcage because autopsy reports were unavailable. Therefore, it is possible that the resolution of the CT scan and the image smoothing effects could have obscured the image of incomplete or simple fractures. Nonetheless, CT images represent the entire rib cage *in situ* and can be manipulated and moved in three-dimensional space to easily observe fractures without being dependent on autopsy notes or photographs (Table 6.1).

Table 6.1. Summary of number fractures for each medical examiner's office. Regardless of imaging technique used per ME office, the median and mean number of fractures remains largely the same.

	Median Number of Fractures per ME Sample	Mean Number of Fractures per ME Sample
WCRMEO	23	24.79
NY OCME	22	24.31
HCIF	23	23.84
NMDID	23	23.95

Another limitation of data collection for this research lies in the subjectivity of the variables recorded. Little to no data exist for the agreed-upon acceptable cut off for reliability or agreement scores within trauma analysis. Nevertheless, fracture location had a high kappa value in both pairwise analyses and both percent agreement scores are well above chance. Based on the values, location of fracture can be reliably observed. Type of fracture had lower percent agreement scores in both pairwise tests, and the kappa value between the researcher and observer B was only “moderate” (Landis and Koch 1977). However, all percent agreements were better than probability of chance agreement. As the areas of disagreement were primarily on incomplete and simple fractures, it is possible that the outside observers had difficulty differentiating the definitions or that fracture type identification may be more experience dependent than fracture location. Future research should further investigate if the error is more associated with the lack of experience working with imaging modality or in the identification of fracture types more in general.

While the agreement scores in this research are considered acceptable, it was difficult to draw comparisons between the fracture patterns in this research and other rib fracture research, primarily because there is no standardized methodology or definition for anatomical location and rib fracture type. The lack of standardization on the fracture terminology is problematic and should be resolved to improve both practicing professionals and research designs. Minimally, fracture terminology and location data should be stated as part of best practices in forensic and biological anthropology.

At the time data collection began, there were only a few adult rib fracture classification methods and none in forensic anthropology (*e.g.*, Ritchie et al. 2006; Meinberg et al. 2018). Consequently, an amalgamation of multiple published methods was used, with some fracture characteristics adapted from MVA research, juvenile rib classifications, and preliminary research presented at conferences on upcoming rib fracture classification schemes (Ritchie et al. 2006; Love et al. 2013; Harden and Agnew 2018). A lack of standardized methods and terminology leads to discordances in results from different researchers. In the time since data collection began, methods for classifying fractures have been published, such as Harden, Kang, and Agnew (2019). Standardized and reliable methods on how to collect rib fracture information would allow for more thorough research in the future and directly comparable findings across numerous fields and projects.

Chapter 7. Conclusions

Best practices in forensic anthropology state that all trauma interpretations should be "based on scientifically valid methods and principles, beyond observation and documentation," (SWGANTH Trauma 2011). Yet, experimental research is expensive and requires a large, multidisciplinary team and very few donor-based or cadaveric collections conduct experimental bone trauma research. These considerable limitations have contributed to most trauma publications to be based on case studies (*e.g.*, Passalacqua and Rainwater 2015; Garvin and Langley 2020), which have conclusions that cannot be extrapolated to other situations with any degree of confidence or statistical support. This study is the first to accumulate a large-scale geographically diverse, retrospective rib trauma sample in biological and forensic anthropology. Furthermore, it is the first to statistically analyze the relationships among rib fracture characteristics collected from the entire rib cage, demographic variables, and death events yielding insight to fracture patterns and ultimately facilitating interpretation of rib trauma.

Normal fracture patterns consisted of displaced and simple fractures to ribs three through seven located anterolaterally and posterolaterally. It is likely that MOD did not have any relationship with fracture patterns because of the extraordinary number of accidental deaths compared to suicide and homicide. Considering the MOD was not controlled for, this pattern corroborated the striking relationship between blunt trauma to the thorax and accidental deaths. While this relationship is not novel (e.g., Karadayi et al.

2011; Scheirs et al. 2018; Poole and Myers 1981), it does yield its own probabilistic statement: there is a probability of 87% that blunt trauma to the chest is associated with a MOD of accident.

An important outcome from this research is the significance of demographic variables in influence of fracture. It is common for introductions and background information to trauma research to discuss biomechanical principles (*e.g.*, Passalacqua and Rainwater 2015; L'Abbé et al. 2019; Symes et al. 2014), and guidelines for trauma analysis in forensic anthropology even state that one should have a grasp of intrinsic and extrinsic variables that may influence fracture (SWGANTH Trauma 2011; Daegling et al. 2008). Yet, these are never specifically discussed regarding *how* it should be considered when looking at a rib fracture. Age, weight, and other health variables are known to influence the material properties of bone. In the current study age was consistently found to be significant in location and type of fracture. Younger individuals within the sample had a significant relationship with incomplete fractures, while older and advanced age groups were more often associated with multi-fragmentary and displaced fractures. As an individual ages rib stiffness increases, the angle of the rib becomes less severe, and trabecular bone decreases (Gayzik et al. 2008; Agnew 2015; Weinstein and Hutson 1987). The material properties associated with these age changes influence type of fracture; the young healthy bone can deflect stress more easily and thus leads to more incomplete fractures, the older more brittle bone cannot deflect stress and thus leads to multi-fragmentary fractures. L'Abbé *et al*. (2019) indicate that fracture type does not

always contribute to forensic anthropological interpretations, as they are medical descriptions, however with the information uncovered in this research, fracture type may provide information on bone health at time of fracture.

Body size, as indicated through BMI in this study, was also found to influence some fracture characteristics. Specifically, weight was the most important variable in classifying fracture location based on the RFA. Individuals with higher BMI (overweight and obese) had a higher conditional probability of incurring posterior fractures, as well as lower rib fractures. The structural changes to the thoracic cavity that occur at higher weights, such as lessening of the rib angle, can be determined to contribute to presence of fracture in these locations (Compston et al. 2014)

Rib fracture patterns are heavily dependent on the demographic variables of an individual and the associated material and structural changes that occur to the bone. Experimental trauma and motor vehicle research have determined similar outcomes to the current research, and heavier focus has been placed on exploring cross-sectional geometry and material properties influence on rib fractures (*e.g.*, Schafman et al. 2016; Kang et al. 2021). However, until this study, it was not known if the patterns exposed through experimental research were observable in real world contexts. As such, this research helps bridge the gap between experimental research and real-world scenarios. *Furthermore, the commonalities between experimental research and the current study's real-world findings suggest a greater ability to extrapolate isolated bone-by-bone approaches to ribcage interpretations thereby arguing that derived hypotheses from*

other situations may be reasonable. This salient finding suggests that experimental trauma research has a greater impact to practitioners than previously thought and that retrospective studies and experimental studies can work in tandem. Future research should strive to develop standardized methodologies to record fracture location and fracture type. Practitioner driven findings should inform experimental and retrospective studies such that a collective movement can be made towards statistically substantiated analyses. Additional efforts to increase data sharing and access will only advance all fields working towards the same research goals. As such, a freely available GUI was created using the data collected as part of this study to provide practitioners of all experience levels and all fields the ability to better understand the patterns and complexities of rib fractures.

References

Abdi, Hervé, and Dominique Valentin
2007 Multiple Correspondence Analysis. Multiple Correspondence Analysis: 1–13.

Abdulrahman, H., I. Afifi, A. El-Menyar, et al.
2013 Clinical Outcomes of Multiple Rib Fractures: Does Age Matter? European Journal of Trauma and Emergency Surgery 39(6): 605–611.

Agnew, Amanda M
2015 The Effect of Age on the Structural Properties of Human Ribs. Journal of the Mechanical Behavior of Biomedical Materials: 13.

Agnew, Amanda M., Michelle M. Murach, Victoria M. Dominguez, et al.
2018 Sources of Variability in Structural Bending Response of Pediatric and Adult Human Ribs in Dynamic Frontal Impacts. *In* Pp. 2018-22–0004. https://www.sae.org/content/2018-22-0004/, accessed October 19, 2021.

Agnew, Amanda M., Michelle Schafman, Kevin Moorhouse, Susan E. White, and Yun-Seok Kang
2015 The Effect of Age on the Structural Properties of Human Ribs. Journal of the Mechanical Behavior of Biomedical Materials 41: 302–314.

Alswat, Khaled A.
2017 Gender Disparities in Osteoporosis. Journal of Clinical Medicine Research 9(5): 382–387.

Beck, T.J, C.B Ruff, R.A Shaffer, et al.
2000 Stress Fracture in Military Recruits: Gender Differences in Muscle and Bone Susceptibility Factors. Bone 27(3): 437–444.

Berryman, Hugh E., Alicja K. Kutyla, and J. Russell Davis
2010 Detection of Gunshot Primer Residue on Bone in an Experimental Setting-An Unexpected Finding. Journal of Forensic Sciences 55(2): 488–491.

Biau, Gerard
2012 Analysis of a Random Forests Model. Journal of Machine Learning Research 13: 1063–1095.

Body Mass Index: Considerations for Practitioners
N.d.: 4.

Brahmbhatt, Tejal S., Michael Hernon, Charles Jeffrey Siegert, et al.
2017 Trauma and BMI Mortality. Current Obesity Reports 6(2): 211–216.

Bruni-Fitzgerald, Karen R.

2018 Review of Article: Obesity and Clotting: BMI Independently Contributes to Hypercoagulability after Injury. J Trauma Acute Care Surgery. 2015 January;78(1):30-38. Journal of Vascular Nursing 36(4): 216–217.

Carter, Patrick M., Carol A.C. Flannagan, Matthew P. Reed, Rebecca M. Cunningham, and Jonathan D. Rupp
2014 Comparing the Effects of Age, BMI and Gender on Severe Injury (AIS 3+) in Motor-Vehicle Crashes. Accident Analysis & Prevention 72: 146–160.

Carver, Harry C
1931 The Concept and Utility of Frequency Distributions: 5.

CDC
2020 Healthy Weight, Nutrition, and Physical Acivity. Cdc.Gov. https://www.cdc.gov/healthyweight/assessing/bmi/adult_bmi/english_bmi_calculator/bmi_calculator.html.

Chien, Chih-Ying, Yu-Hsien Chen, Shih-Tsung Han, et al.
2017 The Number of Displaced Rib Fractures Is More Predictive for Complications in Chest Trauma Patients. Scandinavian Journal of Trauma, Resuscitation and Emergency Medicine 25(1): 19.

Christensen, Angi M., Christian M. Crowder, Stephen D. Ousley, and Max M. Houck
2014 Error and Its Meaning in Forensic Science. Journal of Forensic Sciences 59(1): 123–126.

Chuang, Jung-Fang, Cheng-Shyuan Rau, Pao-Jen Kuo, et al.
2016 Traumatic Injuries among Adult Obese Patients in Southern Taiwan: A Cross-Sectional Study Based on a Trauma Registry System. BMC Public Health 16(1). http://www.biomedcentral.com/1471-2458/16/275, accessed April 1, 2020.

Compston, Juliet E, Julie Flahive, David W Hosmer, et al.
2014 Relationship of Weight, Height, and Body Mass Index With Fracture Risk at Different Sites in Postmenopausal Women: The Global Longitudinal Study of Osteoporosis in Women (GLOW): WEIGHT, HEIGHT, BMI, AND FRACTURE RISK. Journal of Bone and Mineral Research 29(2): 487–493.

Connolly, Andrew J., Walter E. Finkbeiner, Philip C. Ursell, Richard L. Davis, and Walter E. Finkbeiner
2016 Chapter 7. Autopsy Photography and Radiology. *In* Autopsy Pathology: A Manual and Atlas. Third edition. Pp. 80–89. Philadelphia, PA: Elsevier.

Crandall, Marie L., Avery B. Nathens, and Frederick P. Rivara
2004 Injury Patterns among Female Trauma Patients: Recognizing Intentional Injury: The Journal of Trauma: Injury, Infection, and Critical Care 57(1): 42–45.

Crowder, Christian M., Jason M. Wiersema, Bradley J. Adams, Dana E. Austin, and Jennifer C.

Love
2016 The Utility of Forensic Anthropology in the Medical Examiner's Office. Academic Forensic Pathology 6(3): 349–360.

Crowder, Christian, and Laura Rosella
2007 Assessment of Intra- and Intercostal Variation in Rib Histomorphometry: Its Impact on Evidentiary Examination. Journal of Forensic Sciences 52(2): 271–276.

Daegling, David J., Michael W. Warren, Jennifer L. Hotzman, and Casey J. Self
2008 Structural Analysis of Human Rib Fracture and Implications for Forensic Interpretation*. Journal of Forensic Sciences. https://onlinelibrary.wiley.com/doi/10.1111/j.1556-4029.2008.00876.x, accessed October 17, 2021.

Dinno, Alexis
2017 Dunn.Test: Dunn's Test of Multiple Comparisons Using Rank Sums. https://CRAN.R-project.org/package=dunn.test.

Dirkmaat, Dennis C., ed.
2012 A Companion to Forensic Anthropology: Dirkmaat/A Companion to Forensic Anthropology. Chichester, UK: John Wiley & Sons, Ltd. http://doi.wiley.com/10.1002/9781118255377, accessed June 2, 2021.

Dovoedo, Yinaze Herve
2011 Contributions to Outlier Detection Methods: Some Theory and Applications. University of Alabama.

Dunn, Olive Jean
1964 Multiple Comparisons Using Rank Sums. Technometrics 6(3): 241–252.

Ejima, S, S Holcombe, P Zhang, et al.
2017 The Effect of Rib Fracture Patterns in the Obese: 9.

Eknoyan, G.
2007 Adolphe Quetelet (1796 1874) the Average Man and Indices of Obesity. Nephrology Dialysis Transplantation 23(1): 47–51.

Elkbuli, Adel, Brad Boserup, Amy Liu, Scott Rowe, and Mark McKenney
2021 The Association of Body Mass Index and Outcomes in Adult Patients with Chest Wall Injuries. Journal of Surgical Research 267: 544–555.

Field, Andy P., Jeremy Miles, and Zoë Field
2012 Discovering Statistics Using R. London ; Thousand Oaks, Calif: Sage.

Frey, William H.
2021 Brookings. Mapping America's Diversity with the 2020 Cencus. https://www.brookings.edu/research/mapping-americas-diversity-with-the-2020-census/.

Galloway, Allison, and Vicki L. Wedel
2013 Chapter 9. The Axial Skeleton. *In* Broken Bones: Anthropological Analysis of Blunt Force Trauma. Second edition. Pp. 161–194. Springfield, Illinois: Charles C. Thomas, Publisher.

Galloway, Allison, Vicki L. Wedel, and Lauren Zephro
2013 Chapter 2. Proccess and Procedures for Trauma Analysis. *In* Broken Bones: Anthropological Analysis of Blunt Force Trauma. Second edition. Pp. 11–27. Springfield, Illinois: Charles C. Thomas, Publisher.

Gamer, Matthias, Jim Lemon, and Ian Fellows
2019 Irr: Various Coefficients of Interrater Reliability and Agreement. https://CRAN.R-project.org/package=irr.

Garvin, Heather M., and Natalie R. Langley, eds.
2020 Case Studies in Forensic Anthropology: Bonified Skeletons. Boca Raton, FL: CRC Press, Taylor & Francis Group.

Gayzik, Francis S., Mao M. Yu, Kerry A. Danelson, Dennis E. Slice, and Joel D. Stitzel
2008 Quantification of Age-Related Shape Change of the Human Rib Cage through Geometric Morphometrics. Journal of Biomechanics 41(7): 1545–1554.

Gennarelli, Thomas A., and Elaine Wodzin
2006 AIS 2005: A Contemporary Injury Scale. Injury 37(12): 1083–1091.

Gere, James M., and Barry J. Goodno
2013 Mechanics of Materials. 8th ed. Stamford, CT: Cengage Learning.

Gibson, Jason
2013 Relative and cumulative frequency distributions. http://proxy.library.carleton.ca/login?url=http://methods.sagepub.com/video/relative-and-cumulative-frequency-distributions, accessed October 30, 2021.

Gisev, Natasa, J. Simon Bell, and Timothy F. Chen
2013 Interrater Agreement and Interrater Reliability: Key Concepts, Approaches, and Applications. Research in Social and Administrative Pharmacy 9(3): 330–338.

Gozna, E.R.
1982 Biomechanics of Long Bone Injuries. *In* Biomechanics of Musculoskeletal Injury. 2. ed. Pp. 1–24. Champaign, IL: Human Kinetics.

Harden, Angela, and Amanda M. Agnew
2018 Classification of Fractures in Human Ribs Subjected to Anterior-Posterior Loading. Poster Presentation presented at the Amaerican Association of Physical Anthropologists.

Harden, Angela, Yun-Seok Kang, and Amanda Agnew

2019 Rib Fractures: Validation of an Interdisciplinary Classification System. Forensic Anthropology 2(3): 158–167.

Harris County Institute of Forensic Sciences 2019 Annual Report
2019. https://ifs.harriscountytx.gov/Documents/2019AnnualReport_FINAL.pdf.

Hastie, Trevor, Robert Tibshirani, and Jerome Friedman
2008 The Elements of Statistical Learning: Data Mining, Inference, and Prediction. Second. Springer.

Herman, Daniel C., James A. Onate, William E. Garrett, Bing Yu, and Darin A. Padua
2007 The Effects of Augmented Feedback With and Without Strength Training on Lower Extremity Biomechanics: 933 June 1 4:45 PM - 5:00 PM. Medicine & Science in Sports & Exercise 39(5): S96.

Hoffman, Donna L., and Jan De Leeuw
1992 Interpreting Multiple Correspondence Analysis as a Multidimensional Scaling Method. Marketing Letters 3(3): 259–272.

Hoffmann, Michael, Rolf Lefering, Michaela Gruber-Rathmann, Johannes Maria Rueger, and Wolfgang Lehmann
2012 The Impact of BMI on Polytrauma Outcome. Injury 43(2): 184–188.

Holcombe, Sven A., Stewart C. Wang, and James B. Grotberg
2016 The Effect of Rib Shape on Stiffness. *In* Pp. 2016-22–0002. https://www.sae.org/content/2016-22-0002/, accessed April 14, 2021.

Holm, Sture
1979 A Simple Sequentially Rejective Multiple Test Procedure. Scandinavian Journal of Statistics 6(2): 65–70.

Hulse, Cortney, Kyra Stull, and Laura Knight
2021 Homicide Fracture Pattern Frequencies by Sex and Geographic Location. Poster Presentation presented at the American Academy of Forensic Sciences, Virtual Conference Proceedings, February.

Hulse, Cortney, Kyra Stull, Laura Knight, and Kyle Bocinsky
2018 Common Skeletal Injury Location Based on Manner of Death. Podium Presentation presented at the American Academy of Forensic Sciences, Baltimore, February.

Hulse, Cortney, Kyra Stull, and Ashley Weaver
2018 Rib Fracture Frequency and Location Using Vehicular Crash Data. Forensic Anthropology 2(1): 1–8.

Husson, François, Julie Josse, Sebastien Le, and Jeremy Mazet

2008 {FactoMineR}: A Package for Multivariate Analysis. Journal of Statistical Software 25(1): 1–18.

Ingram, Deborah, and Sheila J. Franco
2014 NCHS Urban-Rural Classification Scheme for Counties. Maryland: U.S. Department of Health and Human Services, Centers for Disease Controm and Prevention, National Center for Health Statistics.

Jentzsch, Thorsten, Valentin Neuhaus, Burkhardt Seifert, et al.
2020 Are the Rib Fracture Score and Different Computed Tomography Measures of Obesity Predictors for Mortality in Patients with Rib Fractures? A Retrospective Cohort Study. European Journal of Trauma and Emergency Surgery. https://link.springer.com/10.1007/s00068-020-01483-1, accessed November 2, 2021.

Jingwen, HU, Jonathan D Rupp, and Matthew P Reed
2012 Focusing on Vulnerable Populations in Crashes: Recent Advances in Finite Element Human Models for Injury Biomechanics Research 3(4): 13.

Kang, Yun-Seok, Hyun Jung Kwon, Jason Stammen, Kevin Moorhouse, and Amanda M. Agnew
2021 Biomechanical Response Targets of Adult Human Ribs in Frontal Impacts. Annals of Biomedical Engineering 49(2): 900–911.

Karadayi, Sule, Aydin Nadir, Ekber Sahin, et al.
2011 An Analysis of 214 Cases of Rib Fractures. Clinics 66(3): 449–451.

Keaveny, Tony M., Elise F. Morgan, Glen L. Niebur, and Oscar C. Yeh
2001 Biomechanics of Trabecular Bone. Annual Review of Biomedical Engineering 3(1): 307–333.

Kemper, Andrew R., Craig Mcnally, Eric A. Kennedy, et al.
2005 Material Properties of Human Rib Cortical Bone from Dynamic Tension Coupon Testing. *In* Pp. 2005-22–0010. https://www.sae.org/content/2005-22-0010/, accessed April 14, 2021.

Kemper, Andrew R, Craig McNally, Clayton A Pullins, et al.
2007 The Biomechanics of Human Ribs: Material and Structural Properties from Dynamic Tension and Bending Tests. Stapp Car Crash Journal: 40.

Kleinman, P. K., and Alan E. Schlesinger
1997 Mechanical Factors Associated with Posterior Rib Fractures: Laboratory and Case Studies. Pediatric Radiology 27(1): 87–91.

Kraemer, Helena Chmura, and Daniel A. Bloch
1988 Kappa Coefficients in Epidemiology: An Appraisal of a Reappraisal. Journal of Clinical Epidemiology 41(10): 959–968.

Kralj, Eduard, Matej Podbregar, Nataša Kejžar, and Jože Balažic

2015 Frequency and Number of Resuscitation Related Rib and Sternum Fractures Are Higher than Generally Considered. Resuscitation 93: 136–141.

Kriss, Stevan, Angela Thompson, Gina Bertocci, Melissa Currie, and Vesna Martich
2020 Characteristics of Rib Fractures in Young Abused Children. Pediatric Radiology 50(5): 726–733.

Kroman, Anne M, and Steven A. Symes
2013 Investigation of Skeletal Trauma. *In* Research Methods in Human Skeletal Biology. Elizabeth A. DiGangi and Megan K. Moore, eds. Pp. 219–239. Oxford ; Waltham, MA: Academic Press.

Kruskal, William H, and W Allen Wallis
1952 Use of Ranks in One-Criterion Variance Analysis: 40.

Kuhn, Max, and Kjell Johnson
2013 Applied Predictive Modeling. New York: Springer.

L'Abbé, En, Sa Symes, De Raymond, and Dh Ubelaker
2019 The Rorschach Butterfly, Understanding Bone Biomechanics Prior to Using Nomenclature in Bone Trauma Interpretations. Forensic Science International 299: 187–194.

Landis, J. Richard, and Gary G. Koch
1977 The Measurement of Observer Agreement for Categorical Data. Biometrics 33(1): 159.

Larsson, Karl-Johan, Amanda Blennow, Johan Iraeus, Bengt Pipkorn, and Nils Lubbe
2021 Rib Cortical Bone Fracture Risk as a Function of Age and Rib Strain: Updated Injury Prediction Using Finite Element Human Body Models. Frontiers in Bioengineering and Biotechnology 9: 677768.

Leport, Tiphaine, Pascal Baudrit, Pascal Potier, et al.
2011 Study of Rib Fracture Mechanisms Based on the Rib Strain Profiles in Side and Forward Oblique Impact. *In* Pp. 2011-22–0009. https://www.sae.org/content/2011-22-0009/, accessed April 14, 2021.

Lesciotto, Kate M.
2015 The Impact of *Daubert* on the Admissibility of Forensic Anthropology Expert Testimony. Journal of Forensic Sciences 60(3): 549–555.

Leventhal, John M.
1993 Fractures in Young Children: Distinguishing Child Abuse From Unintentional Injuries. American Journal of Diseases of Children 147(1): 87.

Li, Zuoping, Matthew W. Kindig, Jason R. Kerrigan, et al.
2010 Rib Fractures under Anterior–Posterior Dynamic Loads: Experimental and Finite-Element Study. Journal of Biomechanics 43(2): 228–234.

Loe, Louise
2016 Perimortem Trauma. *In* Handbook of Forensic Anthropology and Archaeology. http://www.vlebooks.com/vleweb/product/openreader?id=none&isbn=9781315528939, accessed November 2, 2021.

Louppe, Gilles
2015 Understanding Random Forests: From Theory to Practice. ArXiv:1407.7502 [Stat]. http://arxiv.org/abs/1407.7502, accessed November 3, 2021.

Love, Jennifer C., Sharon M. Derrick, Jason M. Wiersema, et al.
2013 Novel Classification System of Rib Fractures Observed in Infants. Journal of Forensic Sciences 58(2): 330–335.

Love, Jennifer C., and Steve A. Symes
2004 Understanding Rib Fracture Patterns: Incomplete and Buckle Fractures. Journal of Forensic Sciences 49(6): 1–6.

Love, Jennifer C., and Jason M. Wiersema
2016 Skeletal Trauma: An Anthropological Review. Academic Forensic Pathology 6(3): 463–477.

Lynch, Sarah K
2015 Characterization of Rib Cortical Bone Thickness Changes With Age and Sex: 67.

Maggiano, Isabel S, Corey M Maggiano, and David ML Cooper
2021 Osteon Circularity and Longitudinal Morphology: Quantitative and Qualitative Three-Dimensional Perspectives on Human Haversian Systems. Micron 140: 102955.

Magnello, M.E.
2005 Karl Pearson, Paper on the Chi Square Goodness of Fit Test (1900). *In* Landmark Writings in Western Mathematics 1640-1940 Pp. 724–731. Elsevier. https://linkinghub.elsevier.com/retrieve/pii/B9780444508713501376, accessed October 30, 2021.

Majumdar, S., H. K. Genant, S. Grampp, et al.
1997 Correlation of Trabecular Bone Structure with Age, Bone Mineral Density, and Osteoporotic Status: In Vivo Studies in the Distal Radius Using High Resolution Magnetic Resonance Imaging. Journal of Bone and Mineral Research 12(1): 111–118.

Marinho, Luísa, and Hugo F.V. Cardoso
2016 Comparing Known and Reconstructed Circumstances of Death Involving a Blunt Force Trauma Mechanism through a Retrospective Analysis of 21 Skeletonized Individuals. Journal of Forensic Sciences 61(6): 1416–1430.

Marsh, Nick

2014 Forensic Photography: A Practitioner's Guide. Hoboken, New Jersey: John Wiley & Sons Inc.

Matos, Vítor
2009 Broken Ribs: Paleopathological Analysis of Costal Fractures in the Human Identified Skeletal Collection from the Museu Bocage, Lisbon, Portugal (Late 19th to Middle 20th Centuries). American Journal of Physical Anthropology 140(1): 25–38.

Mccreadie, Barbara R., and Steven A. Goldstein
2000 Biomechanics of Fracture: Is Bone Mineral Density Sufficient to Assess Risk? Journal of Bone and Mineral Research 15(12): 2305–2308.

McDonald, John H
2014 Kruskal-Wallis Test and Mann-Whitney U Test. *In* Handbook of Biological Statistics Pp. 165–172. Baltimore: Sparky House Publishing.

McDonnell, Lisa K., Patria A. Hume, and Volker Nolte
2011 Rib Stress Fractures Among Rowers: Definition, Epidemiology, Mechanisms, Risk Facotrs, and Effectiveness of Injury Prevention Strategies. Sports Medicine 41(11): 883–901.

McElhaney, J H
1966 Dynamic Response of Bone and Muscle Tissue. Journal of Applied Physiology 21(4): 1231–1236.

McHugh, Marry L.
2012 Interrater Reliability: The Kappa Statistic. Biochemia Medica: 276–282.

Meinberg, Eg, J Agel, Cs Roberts, Md Karam, and Jf Kellam
2018 Fracture and Dislocation Classification Compendium—2018. Journal of Orthopaedic Trauma 32(1): S1–S10.

Moore, Keith L., Arthur F. Dalley, and A. M. R. Agur
2014 Clinically Oriented Anatomy. 7th ed. Philadelphia: Wolters Kluwer/Lippincott Williams & Wilkins Health.

Morris, Roisin, Padraig MacNeela, Anne Scott, et al.
2008 Ambiguities and Conflicting Results: The Limitations of the Kappa Statistic in Establishing the Interrater Reliability of the Irish Nursing Minimum Data Set for Mental Health: A Discussion Paper. International Journal of Nursing Studies 45(4): 645–647.

National Medicolegal Review Panel
1999 Death Investigation: A Guide for the Scene Investigator: 72.

Newell, Mark A., Michael R. Bard, Claudia E. Goettler, et al.
2007 Body Mass Index and Outcomes in Critically Injured Blunt Trauma Patients: Weighing the Impact. Journal of the American College of Surgeons 204(5): 1056–1061.

Osterhoff, Georg, Elise F. Morgan, Sandra J. Shefelbine, et al.
2016 Bone Mechanical Properties and Changes with Osteoporosis. Injury 47: S11–S20.

Ottochian, Marcus, Ali Salim, Joseph DuBose, et al.
2009 Does Age Matter? The Relationship between Age and Mortality in Penetrating Trauma. Injury 40(4): 354–357.

Park, Chang Un, and Hyun Jung Kim
2015 Measurement of Inter-Rater Reliability in Systematic Review. Hanyang Medical Reviews 35(1): 44.

Passalacqua, Nicholas V., and Christopher W. Rainwater, eds.
2015 Skeletal Trauma Analysis. Hoboken, NJ: John Wiley & Sons Inc.

Poole, Galen V., and Richard T. Myers
1981 Morbidity and Mortality Rates in Major Blunt Trauma to the Upper Chest: Annals of Surgery 193(1): 70–75.

Prahlow, Joseph A., and Roger W. Byard
2012 Atlas of Forensic Pathology. Springer Reference. New York: Springer : Humana Press.

Premaor, Melissa Orlandin, Fabio Vasconcellos Comim, and Juliet E. Compston
2014 Obesity and Fractures. Arquivos Brasileiros de Endocrinologia & Metabologia 58(5): 470–477.

R Core Team
2021a R: A Language and Environment for Statistical Computing. https://www.R-project.org/.
2021b R: A Language and Environment for Statistical Computing. Vienna, Austria: R Foundation for Statistical Computing. https://www.R-project.org/.

Radasch, Robert M.
1999 Biomechanics of Bone and Fractures. Veterinary Clinics of North America: Small Animal Practice 29(5): 1045–1082.

Ritchie, Nichole L., Stewart C. Wang, Mark R. Sochor, and Lawrence W. Schneider
2006 A Method for Documenting Locations of Rib Fractures for Occupants in Real-World Crashes Using Medical Computed Tomography (CT) Scans. *In* Pp. 2006-01–0250. https://www.sae.org/content/2006-01-0250/, accessed October 23, 2021.

Ross, Ann H., and Chelsey A. Juarez
2014 A Brief History of Fatal Child Maltreatment and Neglect. Forensic Science, Medicine, and Pathology 10(3): 413–422.

Roylance, David
2000 Stress in Beams. Massachusetts Institute of Techonology.

https://resources.saylor.org/wwwresources/archived/site/wp-content/uploads/2012/09/ME1023.1.2.pdf.

Rubin, C, and J Rubin
2006 Chapter 6. Biomechanics and Machanobiology of Bone. *In* Primer on the Metabolic Bone Diseases and Disorders of Mineral Metabolism. Second. Pp. 36–42. Trends in Endocrinology & Metabolism. https://linkinghub.elsevier.com/retrieve/pii/1043276094900213, accessed November 3, 2021.

Schafman, Michelle A., Yun-Seok Kang, Kevin Moorhouse, et al.
2016 Age and Sex Alone Are Insufficient to Predict Human Rib Structural Response to Dynamic A-P Loading. Journal of Biomechanics 49(14): 3516–3522.

Scheirs, Sarah, Willeke Langenhorst, Assumpció Malgosa, et al.
2018 Perimortem Fracture Pattern in Ribs by Blunt Force Trauma. International Journal of Legal Medicine 132(4): 1205–1213.

Scott, William A.
1955 Reliability of Content Analysis: The Case of Nominal Scale Coding. Public Opinion Quarterly 19(3): 321.

Sharma, Om P., Michael F. Oswanski, Shashank Jolly, et al.
2008 Perils of Rib Fractures. The American Surgeon 74(4): 310–314.

Shi, Xiangnan, Libo Cao, Matthew P. Reed, et al.
2014 A Statistical Human Rib Cage Geometry Model Accounting for Variations by Age, Sex, Stature and Body Mass Index. Journal of Biomechanics 47(10): 2277–2285.

Smith, O.B. C., and Steve A. Symes
2003 Chapter 15: Look until You See: Identification of Trauma in Skeletal Material. *In* Hard Evidence: Case Studies in Forensic Anthropology. 2nd edition Pp. 138–154. New Jersey: Prentice Hall.

Soto Martinez, Miriam E., Jennifer C. Love, Deborrah C. Pinto, et al.
2019 The Infant Injury Database: A Tool for the Study of Injury Patterns in Medicolegal Investigations of Child Abuse. Journal of Forensic Sciences 64(6): 1622–1632.

Stillion, Judith M., and Eugene E. McDowell
2002 The Early Demise of the “Stronger” Sex: Gender-Related Causes of Sex Differences in Longevity. OMEGA - Journal of Death and Dying 44(4): 301–318.

SWGANTH Trauma
2011. FBI/DoD.
https://www.nist.gov/system/files/documents/2018/03/13/swganth_trauma.pdf.

Symes, Steven A., Ericka N. L’Abbé, Erin Chapman, Ivana Wolff, and Dennis C. Dirkmaat

2012 Interpreting Traumatic Injury to Bone in Medicolegal Investigations. *In* A Companion to Forensic Anthropology: Dirkmaat/A Companion to Forensic Anthropology. Dennis C. Dirkmaat, ed. Pp. 340–389. Chichester, UK: John Wiley & Sons, Ltd. http://doi.wiley.com/10.1002/9781118255377, accessed June 2, 2021.

Symes, Steven A., Ericka N. L'Abbé, Kyra Stull, Marcelle LaCroix, and James T. Pokines
2014 Taphonomy and the Timing of Fractures in Trauma Analysis. *In* Manual of Forensic Taphonomy Pp. 367–402. Boca Raton: CRC Press/Taylor & Francis Group.

Thermo Fisher Software, Amira v.6.5.0
N.d. Amira Software for Biomedical and Life Science Research. ThermoFishier Scientific.

Turner, C. H.
2002 Biomechanics of Bone: Determinants of Skeletal Fragility and Bone Quality. Osteoporosis International 13(2): 97–104.

Vavalle, Nicholas A., Matthew L. Davis, Joel D. Stitzel, and F. Scott Gayzik
2015 Quantitative Validation of a Human Body Finite Element Model Using Rigid Body Impacts. Annals of Biomedical Engineering 43(9): 2163–2174.

Vilensky, Joel A., Marsha Baltes, Laura Weikel, Joseph D. Fortin, and Louis J. Fourie
2001 Serratus Posterior Muscles: Anatomy, Clinical Relevance, and Function. Clinical Anatomy 14(4): 237–241.

Waterman, Richard
2017 Conditional probability. https://dx.doi.org/10.4135/9781473996847, accessed October 30, 2021.

Wedel, Vicki L., ed.
2013 Broken Bones: Anthropological Analysis of Blunt Force Trauma. Second edition. Springfield, Illinois: Charles C. Thomas, Publisher.

Weinstein, R.S., and M.S. Hutson
1987 Decreased Trabecular Width and Increased Trabecular Spacing Contribute to Bone Loss with Aging. Bone 8(3): 137–142.

Wescott, D.J.
2013 Biomechanics of Bone Trauma. *In* Encyclopedia of Forensic Sciences Pp. 83–88. Elsevier. https://linkinghub.elsevier.com/retrieve/pii/B9780123821652000155, accessed November 3, 2021.

Yamada, Hiroshi, and F. Gaynor Evans
1970 Strength of Biological Materials. Baltimore: Williams & Wilkins.

Yang, Kyung-moo, Matthew Lynch, and Chris O'Donnell

2011 “Buckle” Rib Fracture: An Artifact Following Cardio-Pulmonary Resuscitation Detected on Postmortem CT. Legal Medicine 13(5): 233–239.

Zabell, Joseph, Marcus Nashelsky, Timothy Thomsen, et al.
2009 Rural Versus Urban Trauma: Demographic Influences on Autopsy Rates. Journal of Surgical Research 155(1): 132–135.

Zapf, Antonia, Stefanie Castell, Lars Morawietz, and André Karch
2016 Measuring Inter-Rater Reliability for Nominal Data – Which Coefficients and Confidence Intervals Are Appropriate? BMC Medical Research Methodology 16(1): 93.

Appendix 1.1 Fracture Location Statistics

Chi-Square of location -- (variable)

```
set.seed(10)
locationage<-chisq.test(fractures3$location,fractures3$age_group)
p.adjust(locationage$p.value, method= "holm")
```

```
## [1] 8.835386e-16
```

```
set.seed(10)
locationsex<-chisq.test(fractures3$location,fractures3$sex)
p.adjust(locationsex$p.value, method= "holm")
```

```
## [1] 4.095463e-07
```

```
set.seed(10)
locationbmi<-chisq.test(fractures3$location,fractures3$bmi)
p.adjust(locationbmi$p.value, method= "holm")
```

```
## [1] 2.514756e-18
```

```
set.seed(10)
locationnumber<-chisq.test(fractures3$location,fractures3$number)
p.adjust(locationnumber$p.value, method= "holm")
```

```
## [1] 1.949578e-110
```

```
set.seed(10)
locationmod<-chisq.test(fractures3$location,fractures3$mod)
```

```
## Warning in chisq.test(fractures3$location, fractures3$mod): Chi-squared
## approximation may be incorrect
```

```
p.adjust(locationmod$p.value, method= "holm")
```

```
## [1] 2.51923e-33
```

```
set.seed(10)
locationcod<-chisq.test(fractures3$location,fractures3$cod_class)
p.adjust(locationcod$p.value, method= "holm")
```

```
## [1] 6.371958e-39
```

Age group, Sex, BMI, Number, MOD and COD significant

Anterior Fractures

```
set.seed(50)
fractures3$anteriors <- ifelse(fractures3$location == "anterior", "1","0")
fractures3$anteriors <- as.factor(fractures3$anteriors)
anterior-s chi<- dplyr::select(fractures3,"anteriors","ag-e group","sex","co-d class","type","numl
p.anteriors   <-data.frame(lapply(anteriors_chi[,-1], function(x) chisq.test(table(x,anteriors_ch
```

```
## Warning in chisq.test(table(x, anteriors_chi$anteriors), simulate.p.value =
## TRUE): cannot compute simulated p-value with zero marginals
```

```
## Warning in chisq.test(table(x, anteriors_chi$anteriors), simulate.p.value =
## TRUE): Chi-squared approximation may be incorrect
```

```
p.adjust(p.anteriors,"holm")
```

```
##   age_group         sex   cod class        type      number         bmi
## 0.011994003 0.003498251 0.003498251 0.003498251 0.003498251 0.003498251
##      agesex         asw
##         NaN 0.003498251
```

MOD excluded due to zero marginals

Age Category, sex, COD Class, number, BMI, and agesex Significant

Anterolateral Fractures

```
set.seed(50)

fractures3$anterolaterals <-  ifelse(fractures3$location == "anterolateral", "1","0")

fractures3$anterolaterals <- as.factor(fractures3$anterolaterals)

anterolaterals_chi  <-  dplyr::select(fractures3,"anterolaterals", "age_group","sex","cod_class",

p.anterolaterals  <-data.frame(lapply(anterolaterals_chi[,-1], function(x) chisq.test(table(x,an
```

```
## Warning in chisq.test(table(x, anterolaterals_chi$anterolaterals),
## simulate.p.value = TRUE): cannot compute simulated p-value with zero marginals
```

```
## Warning in chisq.test(table(x, anterolaterals_chi$anterolaterals),
## simulate.p.value = TRUE): Chi-squared approximation may be incorrect
```

```
p.adjust(p.anterolaterals,"holm")
```

```
##   age_group         sex   cod class      number        type         bmi
## 0.003498251 0.514742629 0.003498251 0.003498251 0.003498251 0.514742629
##      agesex         asw
##         NaN 0.003498251
```

Age Category, Sex, COD_Class, Number, Type, and Age+Sex, age+sex+weight Significant

Posterolateral Fractures

```
set.seed(50)
fractures3$posterolateral <-  ifelse(fractures3$location == "posterolateral", "1","0")
fractures3$posterolateral <- as.factor(fractures3$posterolateral)
posterolateral_chi  <-  dplyr::select(fractures3,"posterolateral","age_group","sex","cod_class","1
p.posterolateral  <-data.frame(lapply(posterolateral_chi[,-1], function(x) chisq.test(table(x,po:
```

```
## Warning in chisq.test(table(x, posterolateral_chi$posterolateral),
## simulate.p.value = TRUE): cannot compute simulated p-value with zero marginals
```

```
## Warning in chisq.test(table(x, posterolateral_chi$posterolateral),
## simulate.p.value = TRUE): Chi-squared approximation may be incorrect
```

```
p.adjust(p.posterolateral,"holm")
```

```
##   age_group         sex   cod class      number        type         bmi
## 0.003498251 0.841579210 0.003498251 0.003498251 0.003498251 0.003498251
##      agesex         asw
##         NaN 0.003498251
```

MOD excluded due to zero marginals

Age Category, Sex, COD Class, Number, Type, BMI and agesex, agesexweight Significant

Posterior Fractures

```
set.seed(50)
fractures3$posteriors <- ifelse(fractures3$location == "posterior", "1","0")
fractures3$posteriors <- as.factor(fractures3$posteriors)
posteriors_chi  <-  dplyr::select(fractures3,"posteriors","age_group","sex","cod_class","type","ni
p.posteriors  <-data.frame(lapply(posteriors_chi[,-1], function(x) chisq.test(table(x,posteriors
```

```
## Warning in chisq.test(table(x, posteriors_chi$posteriors), simulate.p.value =
##  TRUE): cannot compute simulated p-value with zero marginals
```

```
## Warning in chisq.test(table(x, posteriors_chi$posteriors), simulate.p.value =
## TRUE): Chi-squared approximation may be incorrect
```

```
p.adjust(p.posteriors,"holm")
```

```
##   age_group         sex   cod class        type      number         bmi
## 0.697651174 0.079460270 0.697651174 0.003498251 0.003498251 0.003498251
##      agesex         asw
##         NaN 0.003498251
```

Age category, Rib Number, BMI, and agesex significant

Appendix 1.2 Fracture Type Statistics

Chi-Square

```
set.seed(10)
typeage<-chisq.test(fractures3$type,fractures3$age_group)
p.adjust(typeage$p.value, method= "holm")
```

```
## [1] 7.339089e-09
```

```
set.seed(10)
typesex<-chisq.test(fractures3$type,fractures3$sex)
p.adjust(typesex$p.value, method= "holm")
```

```
## [1] 0.1136379
```

```
set.seed(10)
typebmi<-chisq.test(fractures3$type,fractures3$bmi)
p.adjust(typebmi$p.value, method= "holm")
```

```
## [1] 8.104621e-08
```

```
set.seed(10)
typelocation<-chisq.test(fractures3$type,fractures3$location)
p.adjust(typelocation$p.value, method= "holm")
```

```
## [1] 3.615318e-202
```

```
set.seed(10)
typenumber<-chisq.test(fractures3$type,fractures3$number)
p.adjust(typenumber$p.value, method= "holm")
```

```
## [1] 1.267221e-14
```

```
set.seed(10)
typemod<-chisq.test(fractures3$type,fractures3$mod)
```

```
## Warning in chisq.test(fractures3$type, fractures3$mod): Chi-squared
## approximation may be incorrect
```

```
p.adjust(typemod$p.value, method= "holm")
```

```
## [1] 3.093602e-107
```

```
set.seed(10)
typecod<-chisq.test(fractures3$type,fractures3$cod_class)
```

```
## Warning in chisq.test(fractures3$type, fractures3$cod_class): Chi-squared
## approximation may be incorrect
```

```
p.adjust(typecod$p.value, method= "holm")
```

```
## [1] 9.012008e-106
```

Age group, BMI, Location, Number, and COD significant

Displaced Fractures

```
set.seed(50)
fractures3$displaced_rib <- ifelse(fractures3$type == "Displaced", "1","0")
fractures3$displaced_rib <- as.factor(fractures3$displaced_rib)
displaced_rib_chi <- dplyr::select(fractures3,"displaced_rib","age_group","sex","cod_class","lo,
p.displaced_rib <-data.frame(lapply(displaced_rib_chi[,-1], function(x) chisq.test(table(x,disp:
```

```
## Warning in chisq.test(table(x, displaced_rib_chi$displaced_rib),
## simulate.p.value = TRUE): cannot compute simulated p-value with zero marginals
```

```
## Warning in chisq.test(table(x, displaced_rib_chi$displaced_rib),
## simulate.p.value = TRUE): Chi-squared approximation may be incorrect
```

```
p.adjust(p.displaced_rib,"holm")
```

```
##   age_group         sex   cod class    location      number         bmi
## 0.013993003 0.471764118 0.003498251 0.003498251 0.247376312 0.471764118
##      agesex         asw
##         NaN 0.003498251
```

MOD has zero marginals.

Age, Sex, Cod_Class, Location, Number, BMI, and agesex, asw Significant

Simple Fractures

```
set.seed(50)
fractures3$simple_rib <- ifelse(fractures3$type == "Simple", "1","0")
fractures3$simple_rib <- as.factor(fractures3$simple_rib)
simple_rib_chi <- dplyr::select(fractures3,"simple_rib","age_group","sex","cod_class","location
p.simple_rib <-data.frame(lapply(simple_rib_chi[,-1], function(x) chisq.test(table(x,simple_rib
```

```
## Warning in chisq.test(table(x, simple_rib_chi$simple_rib), simulate.p.value =
## TRUE): cannot compute simulated p-value with zero marginals
```

```
## Warning in chisq.test(table(x, simple_rib_chi$simple_rib), simulate.p.value =
##  TRUE): Chi-squared approximation may be incorrect
```

```
p.adjust(p.simple_rib,"holm")
```

```
##   age_group         sex   cod class    location      number         bmi
## 0.191904048 0.607696152 0.003498251 0.003498251 0.003498251 0.607696152
##      agesex         asw
##         NaN 0.003498251
```

MOD has zero marginals.

Age, Cod_Class, Location, Number, BMI and agesex Significant

Oblique Fractures

```
set.seed(50)
fractures3$obliques <- ifelse(fractures3$type == "Oblique", "1","0")
fractures3$obliques <- as.factor(fractures3$obliques)
obliques_chi <- dplyr::select(fractures3,"obliques","age_group","sex","cod_class","number","loc,
p.obliques  <-data.frame(lapply(obliques_chi[,-1], function(x) chisq.test(table(x,obliques_chi$ol
```

```
## Warning in chisq.test(table(x, obliques_chi$obliques), simulate.p.value = TRUE):
## cannot compute simulated p-value with zero marginals
```

```
## Warning in chisq.test(table(x, obliques_chi$obliques), simulate.p.value = TRUE):
## Chi-squared approximation may be incorrect
```

```
p.adjust(p.obliques,"holm")
```

```
##   age_group         sex   cod class      number    location         bmi
## 0.079960020 1.000000000 0.003498251 1.000000000 0.003498251 0.181409295
##      agesex         asw
##         NaN 0.003498251
```

MOD has zero marginals

Age Category, COD Class, BMI, Location and agesex Significant

Buckle Fractures

```
set.seed(50)
fractures3$buckles <- ifelse(fractures3$type == "Buckle", "1","0")
fractures3$buckles <- as.factor(fractures3$buckles)
buckles-chi<- dplyr::select(fractures3,"buckles","age-group","sex","cod-class","location","bmi
p.buckles   <-data.frame(lapply(buckles_chi[,-1], function(x) chisq.test(table(x,buckles_chi$buck
```

```
## Warning in chisq.test(table(x, buckles_chi$buckles), simulate.p.value = TRUE):
## cannot compute simulated p-value with zero marginals
```

```
## Warning in chisq.test(table(x, buckles_chi$buckles), simulate.p.value = TRUE):
## Chi-squared approximation may be incorrect
```

```
p.adjust(p.buckles,"holm")
```

```
##   age_group         sex   cod class    location         bmi      number
## 0.003498251 0.119940030 0.003498251 0.003498251 0.521239380 0.003498251
##      agesex         asw
##         NaN 0.003498251
```

Age Category, Sex, COD Class, Location, Rib Number, and agesex significant

Multigragmentary Fractures

```
set.seed(50)
fractures3$multifrags <- ifelse(fractures3$type == "Multifragmentary", "1","0")
fractures3$multifrags <- as.factor(fractures3$multifrags)
multifrags_chi  <-  dplyr::select(fractures3,"multifrags","age_group","sex","cod_class","location
p.multifrags   <-data.frame(lapply(multifrags_chi[,-1], function(x) chisq.test(table(x,multifrags
```

```
## Warning in chisq.test(table(x, multifrags_chi$multifrags), simulate.p.value =
## TRUE): cannot compute simulated p-value with zero marginals
```

```
## Warning in chisq.test(table(x, multifrags_chi$multifrags), simulate.p.value =
## TRUE): Chi-squared approximation may be incorrect
```

```
p.adjust(p.multifrags,"holm")
```

```
##   age_group         sex   cod class    location         bmi      number
## 0.019490255 0.059970015 0.003498251 0.003498251 0.003498251 0.059970015
##      agesex         asw
##         NaN 0.003498251
```

Age Category, Sex, COD class, Location, BMI, Number, and agesex all significant

Incomplete Fractures

```
set.seed(50)
fractures3$incomps <- ifelse(fractures3$type == "Incomplete", "1","0")
fractures3$incomps <- as.factor(fractures3$incomps)
incomps- chi<- dplyr::select(fractures3,"incomps","age- group","sex","cod- class","location","bmi
p.incomps  <-data.frame(lapply(incomps_chi[,-1], function(x) chisq.test(table(x,incomps_chi$inco1
```

```
## Warning in chisq.test(table(x, incomps_chi$incomps), simulate.p.value = TRUE):
## cannot compute simulated p-value with zero marginals
```

```
## Warning in chisq.test(table(x, incomps_chi$incomps), simulate.p.value = TRUE):
## Chi-squared approximation may be incorrect
```

```
p.adjust(p.incomps,"holm")
```

```
##   age_group         sex   cod class    location         bmi      number
## 0.019990005 0.917541229 0.019990005 0.003498251 0.003498251 0.108945527
##      agesex         asw
##         NaN 0.003498251
```

Age category, COD class, Location, BMI, Rib Number, and agesex all Significant

Appendix 1.3 Fractures by Rib Number

Chi-Square

```
set.seed(10)
numberage<-chisq.test(fractures3$number,fractures3$age_group)
p.adjust(numberage$p.value, method= "holm")
```

```
## [1] 0.9502959
```

```
set.seed(10)
numbersex<-chisq.test(fractures3$number,fractures3$sex)
p.adjust(numbersex$p.value, method= "holm")
```

```
## [1] 0.8738832
```

```
set.seed(10)
numberbmi<-chisq.test(fractures3$number,fractures3$bmi)
p.adjust(numberbmi$p.value, method= "holm")
```

```
## [1] 0.9993234
```

```
set.seed(10)
numbermod<-chisq.test(fractures3$number,fractures3$mod)
```

```
## Warning in chisq.test(fractures3$number, fractures3$mod): Chi-squared
## approximation may be incorrect
```

```
p.adjust(numbermod$p.value, method= "holm")
```

```
## [1] 0.5855151
```

```
set.seed(10)
numbercod<-chisq.test(fractures3$number,fractures3$cod_class)
```

```
## Warning in chisq.test(fractures3$number, fractures3$cod_class): Chi-squared
## approximation may be incorrect
```

```
p.adjust(numbercod$p.value, method= "holm")
```

```
## [1] 0.0004203263
```

COD significant

First Ribs

```
fractures3  <-  subset(fractures3, type!="Blank")

set.seed(50)
fractures3$firsts <-  ifelse(fractures3$number ==  "1", "1","0")
fractures3$firsts <- as.factor(fractures3$firsts)
firsts_chi  <-  dplyr::select(fractures3,"firsts","age_group","sex","cod_class","type","bmi","age:
p.firsts  <-data.frame(lapply(firsts_chi[,-1], function(x) chisq.test(table(x,firsts_chi$firsts)
```

```
##  Warning in chisq.test(table(x, firsts_chi$firsts), simulate.p.value = TRUE):
##  cannot compute simulated p-value with zero marginals
```

```
##  Warning in chisq.test(table(x, firsts_chi$firsts), simulate.p.value = TRUE):
## Chi-squared approximation may be incorrect
```

```
p.adjust(p.firsts,"holm")
```

```
##   age_group         sex   cod_class        type         bmi      agesex
##  0.466266867 0.377811094 0.244877561 0.002998501 0.922538731         NaN
##         asw
## 0.734632684
```

MOD, and TYPE had zero margins

Location significant

Rib 4

```
set.seed(50)
fractures3$second_rib <- ifelse(fractures3$number == "2", "1","0")
fractures3$second_rib <- as.factor(fractures3$second_rib)
second_rib_chi <- dplyr::select(fractures3,"second_rib","age_group","sex","cod_class","location
p.second_rib  <-data.frame(lapply(second_rib_chi[,-1], function(x) chisq.test(table(x,second_rib
```

```
## Warning in chisq.test(table(x, second_rib_chi$second_rib), simulate.p.value =
##  TRUE): cannot compute simulated p-value with zero marginals
```

```
##  Warning in chisq.test(table(x, second_rib_chi$second_rib), simulate.p.value =
## TRUE): Chi-squared approximation may be incorrect
```

```
p.adjust(p.second_rib,"holm")
```

```
##   age_group        sex   cod class    location        type
     bmi
## 1.000000000 1.000000000 1.000000000 0.003498251 1.000000000
1.000000000
##      agesex        asw
##         NaN 1.000000000
```

MOD has zero marginals. Age, sex, cod_class, BMI, and agesex have no influence

Location, and Type Significant

Rib 5

```
set.seed(50)
fractures3$third_rib <- ifelse(fractures3$number == "3", "1","0")
fractures3$third_rib <- as.factor(fractures3$third_rib)
third_rib_chi <- dplyr::select(fractures3,"third_rib","age_group","sex","cod_class","location",
p.third_rib  <-data.frame(lapply(third_rib_chi[,-1], function(x) chisq.test(table(x,third_rib_ch:
```

```
##  Warning in chisq.test(table(x, third_rib_chi$third_rib), simulate.p.value =
##  TRUE): cannot compute simulated p-value with zero marginals
```

```
##  Warning in chisq.test(table(x, third_rib_chi$third_rib), simulate.p.value =
## TRUE): Chi-squared approximation may be incorrect
```

```
p.adjust(p.third_rib,"holm")
```

```
##   age_group        sex   cod class    location       type
     bmi
## 1.000000000 1.000000000 1.000000000 0.003498251 1.000000000
1.000000000
##      agesex        asw
##         NaN 1.000000000
```

MOD has zero marginals. Everything else have no influence

Location, Significant

Rib 6

```
set.seed(50)
fractures3$fourth_rib <- ifelse(fractures3$number == "4", "1","0")
fractures3$fourth_rib <- as.factor(fractures3$fourth_rib)
fourth_rib_chi <- dplyr::select(fractures3,"fourth_rib","age_group","sex","cod_class","location
p.fourth_rib  <-data.frame(lapply(fourth_rib_chi[,-1], function(x) chisq.test(table(x,fourth_rib
```

```
##  Warning in chisq.test(table(x, fourth_rib_chi$fourth_rib), simulate.p.value =
##  TRUE): cannot compute simulated p-value with zero marginals
```

```
##  Warning in chisq.test(table(x, fourth_rib_chi$fourth_rib), simulate.p.value =
## TRUE): Chi-squared approximation may be incorrect
```

```
p.adjust(p.fourth_rib,"holm")
```

```
##   age_group        sex   cod class    location       type
     bmi
## 1.000000000 1.000000000 0.812593703 0.003498251 1.000000000
1.000000000
##      agesex        asw
##         NaN 1.000000000
```

MOD has zero marginals. Age, Sex, type, BMI, and agesex have no influence

Location is Significant

Rib 7

```
set.seed(50)
fractures3$fifth_rib <- ifelse(fractures3$number == "5", "1","0")
fractures3$fifth_rib <- as.factor(fractures3$fifth_rib)
fifth_rib_chi <- dplyr::select(fractures3,"fifth_rib","age_group","sex","cod_class","location",
p.fifth_rib  <-data.frame(lapply(fifth_rib_chi[,-1], function(x) chisq.test(table(x,fifth_rib_ch:
```

```
##  Warning in chisq.test(table(x, fifth_rib_chi$fifth_rib), simulate.p.value =
##  TRUE): cannot compute simulated p-value with zero marginals
```

```
##  Warning in chisq.test(table(x, fifth_rib_chi$fifth_rib), simulate.p.value =
## TRUE): Chi-squared approximation may be incorrect
```

```
p.adjust(p.fifth_rib,"holm")
```

```
##   age_group        sex   cod class    location       type
     bmi
##  1.000000000 1.000000000 1.000000000 0.003498251 0.422788606
1.000000000
##      agesex        asw
##         NaN 1.000000000
```

MOD has zero marginals. Age, Sex, cod_class, bmi, and agesex have no influence

Rib 8

```
set.seed(50)
fractures3$sixth_rib <- ifelse(fractures3$number == "6", "1","0")
fractures3$sixth_rib <- as.factor(fractures3$sixth_rib)
sixth_rib_chi <- dplyr::select(fractures3,"sixth_rib","age_group","sex","cod_class","location",
p.sixth_rib  <-data.frame(lapply(sixth_rib_chi[,-1], function(x) chisq.test(table(x,sixth_rib_ch:
```

```
##  Warning in chisq.test(table(x, sixth_rib_chi$sixth_rib), simulate.p.value =
##  TRUE): cannot compute simulated p-value with zero marginals
```

```
##  Warning in chisq.test(table(x, sixth_rib_chi$sixth_rib), simulate.p.value =
## TRUE): Chi-squared approximation may be incorrect
```

```
p.adjust(p.sixth_rib,"holm")
```

```
##   age_group        sex   cod class    location       type
     bmi
##  1.000000000 1.000000000 1.000000000 0.003498251 0.308845577
1.000000000
##      agesex        asw
##         NaN 1.000000000
```

MOD has zero marginals. Age, sex, cod_class, BMI, and agesex have no influence

Location Significant

Rib 9

```
set.seed(50)
fractures3$seventh_rib <- ifelse(fractures3$number == "7", "1","0")
fractures3$seventh_rib <- as.factor(fractures3$seventh_rib)
seventh_rib_chi  <-  dplyr::select(fractures3,"seventh_rib","age_group","sex","cod_class","locati1
p.seventh_rib   <-data.frame(lapply(seventh_rib_chi[,-1], function(x) chisq.test(table(x,seventh_
```

```
## Warning in chisq.test(table(x, seventh_rib_chi$seventh_rib), simulate.p.value =
## TRUE): cannot compute simulated p-value with zero marginals
```

```
## Warning in chisq.test(table(x, seventh_rib_chi$seventh_rib), simulate.p.value =
## TRUE): Chi-squared approximation may be incorrect
```

```
p.adjust(p.seventh_rib,"holm")
```

```
##  age_group        sex  cod class   location        type        bmi     agesex
##  1.00000000 1.00000000 1.00000000 0.29085457 0.02448776 1.00000000        NaN
##        asw
##  1.00000000
```

Rib 10

```
set.seed(50)
fractures3$tens <-
ifelse(fractures3$number == "11",
"1","0")fractures3$tens <-
as.factor(fractures3$tens)
tens_chi <-
dplyr::select(fractures3,"tens","age_group","sex","cod_class","
location","bmi","age:p.tens  <-data.frame(lapply(tens_chi[,-1],
function(x) chisq.test(table(x,tens_chi$tens), simula
```

```
## Warning in chisq.test(table(x, tens_chi$tens), simulate.p.value = TRUE): cannot
## compute simulated p-value with zero marginals
```

```
## Warning in chisq.test(table(x, tens_chi$tens), simulate.p.value = TRUE): Chi-
## squared approximation may be incorrect
```

```
p.adjust(p.tens,"holm")
```

```
##   age_group         sex   cod class    location         bmi      agesex
## 1.000000000 1.000000000 0.004997501 0.002998501 1.000000000         NaN
##         asw
## 1.000000000
```

Location and COD Significant

Rib 11

```
set.seed(50)
fractures3$elevens <- ifelse(fractures3$number == "11", "1","0")
fractures3$elevens <- as.factor(fractures3$elevens)
eleven-s chi<- dplyr::select(fractures3,"elevens","ag-e group","sex","co-d class","location","bmi
p.elevens  <-data.frame(lapply(elevens_chi[,-1], function(x) chisq.test(table(x,elevens_chi$elev1
```

```
## Warning in chisq.test(table(x, elevens_chi$elevens), simulate.p.value = TRUE):
## cannot compute simulated p-value with zero marginals
```

```
## Warning in chisq.test(table(x, elevens_chi$elevens), simulate.p.value = TRUE):
## Chi-squared approximation may be incorrect
```

```
p.adjust(p.elevens,"holm")
```

```
##   age_group         sex   cod class    location         bmi      agesex
## 1.000000000 1.000000000 0.004997501 0.002998501 1.000000000         NaN
##         asw
## 1.000000000
```

MOD, and Tyoe had zero margins

COD & Location significant

Rib 12

```
set.seed(50)
fractures3$twelfths <- ifelse(fractures3$number == "12", "1","0")
fractures3$twelfths <- as.factor(fractures3$twelfths)
twelfths_chi<- dplyr::select(fractures3,"twelfths","age_group","sex","cod_class","location","b1
p.twelfths  <-data.frame(lapply(twelfths_chi[,-1], function(x) chisq.test(table(x,twelfths_chi$t,
```

```
## Warning in chisq.test(table(x, twelfths_chi$twelfths), simulate.p.value = TRUE):
## cannot compute simulated p-value with zero marginals
```

```
## Warning in chisq.test(table(x, twelfths_chi$twelfths), simulate.p.value = TRUE):
## Chi-squared approximation may be incorrect
```

```
p.adjust(p.twelfths,"holm")
```

```
##   age_group         sex   cod class    location         bmi
## 1.000000000 1.000000000 0.052473763 0.002998501 1.000000000
##         asw
## 1.000000000
```

MOD, Type had zero margins

COD & Location Significant

Appendix 1.4 Kruskal-Wallis and Dunn's Test Results

Number of Fractures

```
kruskal.test(kw$num_Fxs, kw$location)
```

```
##
##  Kruskal-Wallis rank sum test
##
## data:  kw$num_Fxs and kw$location
## Kruskal-Wallis chi-squared= 114.9, df = 3, p-value < 2.2e-16
```

```
kruskal.test(kw$num_Fxs, kw$type)
```

```
##
##  Kruskal-Wallis rank sum test
##
## data:  kw$num_Fxs and kw$type
## Kruskal-Wallis chi-squared= 938.52, df = 5, p-value < 2.2e-16
```

```
kruskal.test(kw$num_Fxs, kw$number)
```

```
##
##  Kruskal-Wallis rank sum test
##
## data:  kw$num_Fxs and kw$number
## Kruskal-Wallis chi-squared= 145.89, df = 11, p-value < 2.2e-16
```

```
dunn.test(kw$num_Fxs,kw$location)
```

```
##   Kruskal-Wallis rank sum test
##
## data: x and group
## Kruskal-Wallis chi-squared= 114.9021, df = 3, p-value = 0
##
##
##                           Comparison of x by group
##                                (No adjustment)
## Col Mean-I
## Row Mean I   anterior   anterola   posterio
## ---------+----------------------------------
## anterola  -0.383910
##              0.3505
##
## posterio  -7.491205  -10.34974
##             0.0000*   0.0000*
##
## posterol  -2.773137  -4.515284   7.504412
##             0.0028*   0.0000*    0.0000*
##
```

```
##alpha= 0.05
## Reject Ho if p <= alpha/2
```

```
dunn.test(kw$num_Fxs, kw$type)
```

```
## Kruskal-Wallis rank sum test
##
## data: x and group
## Kruskal-Wallis chi-squared= 938.5172, df = 5, p-value = 0
##
##
##                           Comparison of x by group
##                                (No adjustment)
## Col Mean-I
## Row Mean I     Buckle  Displace  Incomple  Multifra   Oblique
## ---------+-------------------------------------------------------
## Displace    -15.76870
##              0.0000*
##
## Incomple    0.899291  14.54731
##               0.1842   0.0000*
##
## Multifra   -13.83863 -1.096911 -13.29134
##              0.0000*    0.1363   0.0000*
##
## Oblique    -1.712988  11.87507 -2.429643  10.85294
##               0.0434   0.0000*   0.0076*   0.0000*
##
##  Simple    -4.965425  22.83083 -5.381866  14.12231 -2.323196
##              0.0000*   0.0000*   0.0000*   0.0000*   0.0101*
```

```
##              0.0013*   0.0000*   0.0000*   0.0000*    0.2446
##
##        4    2.838344  4.580739  7.287174  7.338044  0.469600
##              0.0023*   0.0000*   0.0000*   0.0000*    0.3193
##
##        5    2.282119  4.025977  6.824781  6.962196 -0.173220
##              0.0112*   0.0000*   0.0000*   0.0000*    0.4312
##
##        6    2.402543  4.139831  6.914968  7.037886 -0.023556
##              0.0081*   0.0000*   0.0000*   0.0000*    0.4906
##
##        7    1.120211  2.840699  5.809252  6.141845 -1.460705
##               0.1313   0.0023*   0.0000*   0.0000*    0.0720
##
##        8    0.041211  1.719149  4.813473  5.332418 -2.597692
##               0.4836    0.0428   0.0000*   0.0000*   0.0047*
##
##        9   -0.735138  0.890203  4.038348  4.694955 -3.355866
##               0.2311    0.1867   0.0000*   0.0000*   0.0004*
## Col Mean-
## Row Mean           4          5          6          7          8
## ---------+-------------------------------------------------------
##        5   -0.676919
##               0.2492
##
##        6   -0.516530  0.156539
##               0.3027    0.4378
##
##        7   -2.016028 -1.355141 -1.500845
##              0.0219*    0.0877    0.0667
##
##        8   -3.178900 -2.544452 -2.679011 -1.217611
```

```
##
##alpha= 0.05
## Reject Ho if p <= alpha/2
```

```
dunn.test(kw$num_Fxs,  kw$number)
```

```
##   Kruskal-Wallis rank sum test
##
## data: x and group
## Kruskal-Wallis chi-squared= 145.8924, df = 11, p-value  = 0
##
##
##                            Comparison of x by group
##                                 (No adjustment)
## Col Mean-I
## Row Mean I          1         10         11         12          2          3
## ---------+------------------------------------------------------------------
##       10   -1.532394
##              0.0627
##
##       11   -4.473752  -3.134253
##             0.0000*   0.0009*
##
##       12   -5.065475  -3.935282  -1.185861
##             0.0000*   0.0000*    0.1178
##
##        2    2.349300   4.036188   6.788010   6.952881
##             0.0094*   0.0000*   0.0000*   0.0000*
##
##        3    3.013547   4.743030   7.413902   7.446355   0.691623
```

```
##             0.0007*   0.0055*   0.0037*    0.1117
##
##       9   -3.934568 -3.330415 -3.455831 -2.051638 -0.860388
##             0.0000*   0.0004*   0.0003*   0.0201*    0.1948
##
##alpha= 0.05
## Reject Ho if p <= alpha/2
```

Location

```
set.seed(50)
kruskal.test(kw$age,  kw$location)
```

```
##
## Kruskal-Wallis rank sum test
##
## data:  kw$age and kw$location
## Kruskal-Wallis chi-squared= 82.731, df = 3, p-value < 2.2e-16
```

```
dunn.test(kw$age,kw$location)
```

```
## Kruskal-Wallis rank sum test
##
## data: x and group
## Kruskal-Wallis chi-squared= 82.7306, df = 3, p-value = 0
##
##
```

```
##                              Comparison of x by group
##                                   (No adjustment)
## Col Mean-I
##  Row Mean I    anterior   anterola   posterio
```

```r
set.seed(50)
kruskal.test(kw$weight,  kw$location)
```

```
##
##  Kruskal-Wallis rank sum test
##
## data:  kw$weight and kw$location
##  Kruskal-Wallis chi-squared= 94.369, df = 3, p-value < 2.2e-16
```

```r
dunn.test(kw$weight,  kw$location)
```

```
##   Kruskal-Wallis rank sum test
##
## data: x and group
## Kruskal-Wallis chi-squared= 94.3694, df = 3, p-value = 0
##
##
##                           Comparison of x by group
##                                (No adjustment)
## Col Mean-I
## Row Mean I   anterior   anterola   posterio
## ---------+---------------------------------
## anterola   7.000376
##             0.0000*
##
## posterio   3.091495  -4.199736
##             0.0010*   0.0000*
##
## posterol   8.474157  2.688054   6.014959
##             0.0000*   0.0036*    0.0000*
##
##alpha= 0.05
## Reject Ho if p <= alpha/2
```

```r
set.seed(50)
kruskal.test(kw$height,  kw$location)
```

```
##
## Kruskal-Wallis rank sum test
##
```

```
## data:  kw$height and kw$location
## Kruskal-Wallis chi-squared= 71.209, df = 3, p-value = 2.352e-15
```

```
dunn.test(kw$height, kw$location)
```

```
##   Kruskal-Wallis rank sum test
##
## data: x and group
## Kruskal-Wallis chi-squared= 71.2089, df = 3, p-value = 0
##
##
##                            Comparison of x by group
##                                (No adjustment)
## Col Mean-I
## Row Mean I   anterior   anterola   posterio
## ---------+----------------------------------
## anterola   7.727823
##             0.0000*
##
## posterio   5.593424  -1.485001
##             0.0000*    0.0688
##
## posterol   8.277658  0.929349   2.112971
##             0.0000*    0.1764    0.0173*
##
## alpha= 0.05
## Reject Ho if p <= alpha/2
```

Type

```
kruskal.test(kw$age, kw$type)
```

```
##
##  Kruskal-Wallis rank sum test
##
## data:  kw$age and kw$type
## Kruskal-Wallis chi-squared= 31.224, df = 5, p-value = 8.459e-06
```

```
dunn.test(kw$age,kw$type)
```

```
##   Kruskal-Wallis rank sum test
##
## data: x and group
## Kruskal-Wallis chi-squared= 31.2242, df = 5, p-value = 0
####
##                            Comparison of x by group
##                                (No adjustment)
```

```
## Col Mean-I
## Row Mean I                Buckle  Displace   Incomple  Multifra   Oblique
##            ---------+-------------------------------------------------------
## Displace             -0.699946
##                        0.2420
##
## Incomple              2.560206  3.865986
##                        0.0052*   0.0001*
##
## Multifra             -0.941019 -0.571690  -3.687662

##              0.1733    0.2838   0.0001*
##
## Oblique    1.538480  2.633148 -1.014365  2.595955
##              0.0620   0.0042*    0.1552   0.0047*
##
##   Simple    0.885206  3.505039 -2.407721  2.542155  -1.138711
##              0.1880   0.0002*   0.0080*   0.0055*    0.1274
##
## alpha= 0.05
```

```
kruskal.test(kw$weight, kw$type)
```

```
##
##  Kruskal-Wallis rank sum test
##
## data:  kw$weight and kw$type
## Kruskal-Wallis chi-squared= 11.632, df = 5, p-value = 0.0402
```

```
dunn.test(kw$weight, kw$type)
```

```
##   Kruskal-Wallis rank sum test
##
## data: x and group
## Kruskal-Wallis chi-squared= 11.6318, df = 5, p-value = 0.04
##
##
##                            Comparison of x by group
```

```
## Displace   1.477514
##              0.0698
##
## Incomple   2.376384  1.780979
##            0.0087*    0.0375
##
## Multifra   1.646279  0.662378 -1.185208
##              0.0499    0.2539    0.1180
##
##  Oblique   -0.533515 -2.017991  -2.746336  -2.118828
##              0.2968   0.0218*   0.0030*   0.0171*
##
##   Simple   1.852246  0.986501 -1.348832  -0.048127  2.343195
##              0.0320    0.1619    0.0887    0.4808   0.0096*
##
## alpha= 0.05
```

```
kruskal.test(kw$height, kw$type)
```

```
##
##  Kruskal-Wallis rank sum test
##
## data:  kw$height and kw$type
## Kruskal-Wallis chi-squared= 15.172, df = 5, p-value = 0.009651
```

```r
dunn.test(kw$height, kw$type)
```

```
##   Kruskal-Wallis rank sum test
##
## data: x and group
##  Kruskal-Wallis chi-squared= 15.1722, df = 5, p-value = 0.01
##
##
##                           Comparison of x by group
##                                (No adjustment)
## Col Mean-I
##  Row Mean I     Buckle  Displace  Incomple  Multifra   Oblique
## ---------+-------------------------------------------------------
##  Displace    2.814154
##              0.0024*
##
## Incomple    1.451227  -0.536832
##               0.0734    0.2957
##
## Multifra    1.084516  -2.021420  -0.653496
##               0.1391   0.0216*    0.2567
##
## Oblique    0.445683  -1.936690  -0.967301  -0.500892
##               0.3279    0.0264    0.1667    0.3082
##
##  Simple    2.785953  0.206911  0.598941  1.993703  1.952565
##              0.0027*    0.4180    0.2746   0.0231*    0.0254
##
##  alpha= 0.05
##  Reject Ho if p <= alpha/2
```

Number

```
kruskal.test(kw$age, kw$number)
```

```
##
##  Kruskal-Wallis rank sum test
##
## data:  kw$age and kw$number
## Kruskal-Wallis chi-squared= 9.1528, df = 11, p-value = 0.6078
```

```
dunn.test(kw$age,kw$number)
```

```
##   Kruskal-Wallis rank sum test
##
## data: x and group
## Kruskal-Wallis chi-squared= 9.1528, df = 11, p-value = 0.61
##
##
##                            Comparison of x by group
##                                 (No adjustment)
## Col Mean-I
## Row Mean I          1         10         11         12          2          3
## ---------+----------------------------------------------------------------
##       10   -1.355997
##               0.0875
##
##       11   -1.140365  0.028900
##               0.1271    0.4885
```

```
##
##       12   -1.196833  -0.210062  -0.215785
##               0.1157     0.4168     0.4146
##
##        2   -1.153938   0.369971   0.278060   0.477523
##               0.1243     0.3557     0.3905     0.3165
##
##        3   -1.850740  -0.274098  -0.259364   0.040086  -0.771835
##               0.0321     0.3920     0.3977     0.4840     0.2201
##
##        4   -1.963976  -0.375732  -0.343139  -0.027229  -0.896807  -0.123313
##              0.0248*     0.3536     0.3657     0.4891     0.1849     0.4509
##
##        5   -1.998646  -0.414061  -0.375069  -0.053757  -0.940027  -0.171280
##              0.0228*     0.3394     0.3538     0.4786     0.1736     0.4320
##
##        6   -2.543648  -0.958453  -0.826578  -0.423364  -1.579157  -0.842461
##              0.0055*     0.1689     0.2042     0.3360     0.0572     0.1998
##
##        7   -2.116975  -0.563754  -0.501547  -0.161353  -1.098907  -0.359064
##              0.0171*     0.2865     0.3080     0.4359     0.1359     0.3598
##
##        8   -1.237862   0.258776   0.186626   0.400732  -0.120933   0.625699
##               0.1079     0.3979     0.4260     0.3443     0.4519     0.2658
##
##        9   -1.082233   0.359747   0.275471   0.471655   0.010734   0.724880
##               0.1396     0.3595     0.3915     0.3186     0.4957     0.2343
## Col Mean-
##  Row Mean           4          5          6          7          8
## ---------+-------------------------------------------------------
##        5 |  -0.048923
##          |    0.4805
```

```
##
##        6   -0.727381  -0.676105
##               0.2335    0.2495
##
##        7   -0.242220  -0.194106   0.462284
##               0.4043    0.4230    0.3219
##
##        8    0.745850   0.788489   1.411326   0.948010
##               0.2279    0.2152    0.0791    0.1716
##
##        9    0.839439   0.879766   1.471210   1.030415   0.123341
##               0.2006    0.1895    0.0706    0.1514    0.4509
##
```

```
kruskal.test(kw$weight, kw$number)
```

```
##
##  Kruskal-Wallis rank sum test
##
## data:  kw$weight and kw$number
## Kruskal-Wallis chi-squared= 20.84, df = 11, p-value = 0.03507
```

```
dunn.test(kw$weight, kw$number)
```

```
##   Kruskal-Wallis rank sum test
##
```

```
## data: x and group
## Kruskal-Wallis chi-squared= 20.8398, df = 11, p-value = 0.04
##
##
##                          Comparison of x by group
##                               (No adjustment)
## Col Mean-I
## Row Mean I          1         10         11         12          2          3
## ---------+-------------------------------------------------------------------
##       10    1.528026
##               0.0633
##
##       11    1.576103   0.256841
##               0.0575     0.3987
##
##       12    0.141254  -0.965807  -1.088461
##               0.4438     0.1671     0.1382
##
##        2   -0.595201  -2.294146  -2.198821  -0.555042
##               0.2759    0.0109*    0.0139*     0.2894
##
##        3   -0.886155  -2.632397  -2.467881  -0.745766  -0.318277
##               0.1878    0.0042*    0.0068*     0.2279     0.3751
##
##        4   -1.201638  -2.955958  -2.732427  -0.954916  -0.683075  -0.378379
##               0.1148    0.0016*    0.0031*     0.1698     0.2473     0.3526
##
##        5   -0.885620  -2.638851  -2.471270  -0.744347  -0.315185   0.005093
##               0.1879    0.0042*    0.0067*     0.2283     0.3763     0.4980
##
##        6   -0.625186  -2.375679  -2.254648  -0.570539  -0.013275   0.319080
##               0.2659    0.0088*    0.0121*     0.2842     0.4947     0.3748
##
##        7   -0.490695  -2.212481  -2.125848  -0.482346   0.130222   0.460132
##               0.3118    0.0135*    0.0168*     0.3148     0.4482     0.3227
##
##        8    0.399895  -1.277360  -1.350433   0.127485   1.128879   1.482607
##               0.3446    0.1007     0.0884     0.4493     0.1295     0.0691
##
##        9    0.848210  -0.773494  -0.926291   0.449984   1.601288   1.951929
##               0.1982    0.2196     0.1771     0.3264     0.0547     0.0255
## Col Mean-I
## Row Mean I          ¦          5          6          7          8
```

```
## ---------+-------------------------------------------------------
##         5    0.385882
##                0.3498
##
##         6    0.701174  0.315935
##                0.2416    0.3760
##
##         7    0.833440  0.457839  0.149471
##                0.2023    0.3235    0.4406
##
##         8    1.847510  1.485722  1.187103  1.020865
##                0.0323    0.0687    0.1176    0.1537
##
##         9    2.301330  1.956754  1.671655  1.504785  0.513775
##               0.0107*    0.0252    0.0473    0.0662    0.3037
##
## alpha= 0.05
## Reject Ho if p <= alpha/2
```

```
kruskal.test(kw$height,  kw$number)
```

```
##
##  Kruskal-Wallis rank sum test
##
## data:  kw$height and kw$number
## Kruskal-Wallis chi-squared= 15.351, df = 11, p-value = 0.167
```

```
dunn.test(kw$height, kw$number)
```

```
##   Kruskal-Wallis rank sum test
##
## data: x and group
## Kruskal-Wallis chi-squared= 15.3513, df = 11, p-value = 0.17
####
##                              Comparison of x by group
##                                   (No adjustment)
 Col Mean-I
 Row Mean I          1         10         11         12          2          3
 ---------+-------------------------------------------------------------------
       10     0.908231
                0.1819

       11     0.859088   0.075385
                0.1951     0.4700

       12     0.389733  -0.269523  -0.306635
                0.3484     0.3938     0.3796
```

```
       2   -0.876563  -1.881339  -1.655970  -1.009370
              0.1904     0.0300     0.0489     0.1564

       3   -1.241595  -2.272212  -1.967691  -1.250319  -0.394724
              0.1072    0.0115*    0.0246*     0.1056     0.3465

       4   -1.522594  -2.556946  -2.199818  -1.436341  -0.717133  -0.333332
              0.0639    0.0053*    0.0139*     0.0755     0.2366     0.3694

       5   -1.170037  -2.205484  -1.910298  -1.201312  -0.307405   0.093574
              0.1210    0.0137*     0.0280     0.1148     0.3793     0.4627

       6   -1.087307  -2.120428  -1.841397  -1.146614  -0.213889   0.189453
              0.1385    0.0170*     0.0328     0.1258     0.4153     0.4249

       7   -0.503869  -1.525166  -1.353798  -0.755340   0.445427   0.866659
              0.3072     0.0636     0.0879     0.2250     0.3280     0.1931

       8    0.053211  -0.942003  -0.873385  -0.371443   1.047928   1.472925
              0.4788     0.1731     0.1912     0.3552     0.1473     0.0704

       9   -0.024095  -0.983437  -0.914713  -0.417832   0.913575   1.310728
              0.4904     0.1627     0.1802     0.3380     0.1805     0.0950
Col Mean-
Row Mean           4          5          6          7          8
----------+-------------------------------------------------------
       5    0.429927
              0.3336

       6    0.525143   0.096909
              0.2997     0.4614


##        7    1.199889   0.780436   0.682980
##               0.1151     0.2176     0.2473
##
##        8    1.795824   1.393606   1.298177   0.631369
##               0.0363     0.0817     0.0971     0.2639
##
##        9    1.615354   1.234267   1.144479   0.514197  -0.083713
##               0.0531     0.1086     0.1262     0.3036     0.4666
##
```